
Theses and Dissertations

Summer 2014

Compositional gradients in photopolymer films utilizing kinetic driving forces

Clinton John Cook
University of Iowa

Follow this and additional works at: <https://ir.uiowa.edu/etd>

 Part of the [Chemical Engineering Commons](#)


Copyright 2014 Clinton John Cook

This dissertation is available at Iowa Research Online: <https://ir.uiowa.edu/etd/1308>

Recommended Citation

Cook, Clinton John. "Compositional gradients in photopolymer films utilizing kinetic driving forces." PhD (Doctor of Philosophy) thesis, University of Iowa, 2014.
<https://doi.org/10.17077/etd.ydmmfmzc>

Follow this and additional works at: <https://ir.uiowa.edu/etd>

 Part of the [Chemical Engineering Commons](#)

COMPOSITIONAL GRADIENTS IN PHOTOPOLYMER FILMS UTILIZING
KINETIC DRIVING FORCES

by
Clinton John Cook

A thesis submitted in partial fulfillment
of the requirements for the Doctor of
Philosophy degree in Chemical and Biochemical Engineering
in the Graduate College of
The University of Iowa

August 2014

Thesis Supervisor: Professor C. Allan Guymon

Copyright by
CLINTON JOHN COOK
2014
All Rights Reserved

Graduate College
The University of Iowa
Iowa City, Iowa

CERTIFICATE OF APPROVAL

PH.D. THESIS

This is to certify that the Ph.D. thesis of

Clinton John Cook

has been approved by the Examining Committee
for the thesis requirement for the Doctor of Philosophy
degree in Chemical and Biochemical Engineering at the August 2014
graduation.

Thesis Committee: _____
C. Allan Guymon, Thesis Supervisor

Alec Scranton

Julie Jessop

Gary Aurand

Ned Bowden

To my loving family.

ACKNOWLEDGMENTS

I do not think I will be able to do proper justice to all the people who have helped me along during my graduate career. I truly appreciate it more than this acknowledgments section can do justice.

First and foremost, I would like to thank my research advisor, Dr. C. Allan Guymon. You have taught me many things beyond polymeric materials and how to do research. I have learned far too many lessons than I can fit in this section but it is safe to say that I would not be where I am today without all of your help and guidance. Thank you.

Next, I would like to thank my committee members, Dean Alec Scranton, Dr. Julie Jessop, Dr. Gary Aurand, and Dr. Ned Bowden for their support and guidance. I feel that all of you have contributed in making me a better scientist and have helped guide me through my research experience at the University of Iowa.

I would also like to thank my fellow graduate students, including but not limited to; Dr. Anna Volkert, Dr. Celine Baguenard, Dr. Brian Dillman, Dr. Brad Forney, Dr. Soon Ki Kim, Dr. Kwame Owusu-Adom, Dr. Lucas Sievens-Figueroa, Kristan Worthington, Brad Tuft, Jon Scholte, Todd Thorson, Jacob McLaughlin, Brian Green, Braden Leigh, Dr. Leroy Magwood, Dr. Ho Seop Eom, Binaya Shrestha, and Dr. Michael Ivanov. I truly enjoyed your camaraderie, support, and lively research discussions.

Finally, I would like to thank my friends and family. Specifically, I would like to mention John Cook, Roberta Cook, Britta Cook Bresina, Cole Cook, Jace Bresina, and Dr. Kurt Wiegel. Without your love, guidance, and support I would have never made it through this degree. I truly appreciate everything you all have done for me.

ABSTRACT

Independent control of the surface and bulk properties is advantageous for many applications such as adhesives, release coatings, and antimicrobial films. Traditional methods for achieving independent control typically require multiple processing steps such as wet-on-wet or wet-on-dry coating methods. Independent control over the surface properties can be achieved in a single step utilizing the temporal and spatial control inherent to photopolymerization. Specifically, a co-photopolymerization of monomers with different reactivities in the presence of a light gradient is capable of producing a polymer film with a surface chemistry that differs from the bulk chemistry. The light gradient, produced via the concentration of photoinitiator in the formulation, results in a reaction gradient through the film with the higher rates of reaction occurring in the high light intensity regions of the film. The preferentially reacting monomer adds at a greater rate in the high light intensity regions resulting in non-uniform consumption yielding a concentration gradient. Consequently, diffusion of the preferentially reacting monomer from the bulk to the surface of the film and a counter-diffusion of the other monomer from the surface to the bulk of the film occurs from the non-uniform monomer consumption thus producing a film with a concentration gradient through the depth of the film with the preferentially reacting monomer enriching the high light intensity regions. A variety of kinetic differences capable of producing a stratified film will be presented including inherent monomer reactivity, number of functional groups per monomer, oxygen inhibition, thiol-ene chemistry, and Norrish type two initiation. Additionally, parameters that control the degree of stratification, such as methods of varying polymerization rate and the light gradient, will be examined. Changes in surface properties (such as contact angle, surface hardness, adhesion) and bulk properties (such as mechanical properties measured by dynamic mechanical analysis and polymer swelling) are studied as a function of stratification. Finally, a mathematical model which

describes and predicts the production of stratified films via photopolymerization is presented. Photopolymerization allows for a facile, single step method of generating stratified films with controllable surface chemistries.

TABLE OF CONTENTS

LIST OF TABLES	ix
LIST OF FIGURES	x
CHAPTER 1 INTRODUCTION	1
Radical Photopolymerization.....	3
Initiation	5
Propagation.....	8
Termination	8
Overall Rate of Polymerization	9
Thiol-Ene Radical Step Growth Photopolymerization	10
Radical Kinetic Differences.....	12
Number of Functional Groups per Monomer	13
Inherent Monomer Reactivity.....	14
Oxygen Inhibition.....	16
Thiol-Ene.....	17
Norrish Type Two Photoinitiation.....	18
Diffusion	19
Current Methods for Controlling Surface Chemistry	22
Plasma Surface Modification	23
Surface Grafting	24
Research Summary	25
Notes	27
CHAPTER 2 OBJECTIVES.....	32
CHAPTER 3 MATERIALS AND METHODS	36
Chemicals	36
Photopolymerization Procedure.....	37
Surface Chemical Analysis via Attenuated Total Reflectance – Fourier Transform Infrared Spectroscopy	37
Notes	40
CHAPTER 4 COMPOSITIONAL GRADIENTS IN PHOTOPOLYMERS UTILIZING MONO- AND DIMETHACRYLATES	41
Abstract.....	41
Introduction.....	42
Experimental.....	44
Materials.....	44
Sample Preparation.....	45
Attenuated Total Reflectance – Fourier Transform Infrared Spectroscopy.....	45
Kinetic Analysis	46
Contact Angle.....	46
Pencil Hardness	46
Results and Discussion	47
Conclusions.....	58

Notes	60
CHAPTER 5 PHOTOPOLYMERIZATION REACTION-DIFFUSION MODEL DESCRIBING INDUCED CHEMICAL COMPOSITION GRADIENT.....	62
Abstract.....	62
Introduction.....	63
Model Development	65
Results and Discussion	69
Conclusions.....	78
Notes	80
CHAPTER 6 HIGHLY STRATIFIED POLYMERIC FILMS VIA PHOTOPOLYMERIZATION.....	82
Abstract.....	82
Introduction.....	83
Experimental.....	85
Materials	85
Sample Preparation.....	86
Fourier Transform Infrared Spectroscopy	86
Confocal Raman Microscopy	86
Results and Discussion	87
Conclusions.....	96
Notes	99
CHAPTER 7 INVESTIGATING THE BULK PROPERTIES AND MULTIPLE PATHWAYS FOR PRODUCING COMPOSITION GRADIENTS IN PHOTOPOLYMER FILMS	101
Abstract.....	101
Introduction.....	102
Experimental.....	104
Chemicals	104
Polymer Film Sample Preparation.....	105
Attenuated Total Reflectance – Fourier Transform Spectroscopy	105
X-ray Photoelectron Spectroscopy	106
Adhesion Test.....	106
Dynamic Mechanical Analysis.....	106
Shrinkage Stress Relief via Heating.....	106
Swelling Studies	107
Results and Discussion	107
Conclusions.....	117
Notes	119
CHAPTER 8 CONCLUSIONS AND RECOMMENDATIONS	121
Notes	129
APPENDIX A MATLAB MODEL OF PHOTO-ENFORCED STRATIFICATION FOR MONO- VS DI-ENE SYSTEMS.....	130
Description.....	130
Background Information.....	130

MatLab Code	130
BIBLIOGRAPHY	136

LIST OF TABLES

Table 4.1. Scratch pencil hardness values for the films.....	58
Table 5.1. List of parameters used to model photo-enforced stratification.	69
Table 7.1. Percent surface enrichment of the three different initiation systems in photopolymers. All monomers are at a 1:1 molar ratio.	115

LIST OF FIGURES

Figure 1.1. Pictorial representation of producing a chemical concentration gradient via co-photopolymerization of a formulation containing monomers of unequal reactivity with a light gradient through the depth produced from the photoinitiator resulting in enrichment of the preferentially reacting monomer in the high light intensity regions of the film.	3
Figure 1.2. Chemical structures of (A) 2-hydroxyethyl methacrylate, (B) 2-hydroxyethyl acrylate, (C) 1,6-hexanediol dimethacrylate, (D) 2,2-dimethoxy-2-phenylacetophenone which are representative chemicals utilized in these studies.	4
Figure 1.3. Norrish type one photo-cleavage of 2,2-dimethoxy-2-phenylacetophenone. (A) α -cleavage of 2,2-dimethoxy-2-phenylacetophenone results in the formation of dimethoxy benzyl radical and a benzaldehyde radical. The dimethoxy benzyl radical can further rearranges (B) to methyl benzoate and a methyl radical. The benzaldehyde radical couples (C) with an additional benzaldehyde radical to form benzil or can abstract a hydrogen (D) to form benzaldehyde and a radical on the hydrogen donor. ³¹	6
Figure 1.4. Schematic of thiol-ene radical step growth photopolymerization. ^{38,39}	11
Figure 1.5. Pictorial representation of a macro radical reacting with a di-ene species to form another macro radical and a pendent ene group off of the growing polymer chain. ⁵⁸	14
Figure 1.6. Representation of a radical reacting with an acrylate to form a secondary radical (top) and a radical reacting with a methacrylate to form a tertiary radical (bottom).	16
Figure 1.7. Qualitative ranking of various ene monomers reactivity toward a thiol in a thiol-ene polymerization. ^{38,39}	18
Figure 1.8. Schematic of volume element used to derive Fick's second of diffusion. ⁸¹	21
Figure 3.1. Experimental diagram of attenuated total reflectance – Fourier transform infrared spectroscopy.	38
Figure 4.1. Chemical structures of (A) 1,6-hexanediol dimethacrylate, (B) 2-hydroxyethyl methacrylate, and (C) 2,2-dimethoxy-2-phenylacetophenone.	45
Figure 4.2. Examples of a typical spectra collected using ATR-FTIR. The hydroxyl peak and carbonyl peak are labeled at approximately 3510 and 1720 wavenumbers respectively for the spectrum of the 1) top and (2) bottom of the film.	48

Figure 4.3. Composition ratio of polymers produced as a function of photoinitiator concentrations using a 1:1 molar ratio of HEMA to HDDMA formulation. Composition ratios normalized to the composition ratio of a low light attenuation film. Films were polymerized in a 300 μm laminate mold with 365 nm light at 1 mW/cm^2 . Composition ratios were determined via ATR-FTIR. Error bars represent the standard deviation of a minimum of three replicate measurements.....	49
Figure 4.4. Correlation between fractional attenuation based on photoinitiator concentration and time to reach the maximum rate of polymerization. The fractional attenuation was calculated from the Beer Lambert Law, and the time to reach the maximum rate of polymerization determined from rates measured with real time FTIR.	51
Figure 4.5. Examination of light attenuation effects on photo-enforced stratification. A) Variation of normalized polymer composition ratio as a function of film thickness. B) Comparison of normalized composition ratio when film thickness (\bullet) and DMPA concentration (\square) is varied. The Beer Lambert Law is used to determine the fractional attenuation of light through the film in both cases. Films were polymerized in a laminate mold with 365 nm light at 1 mW/cm^2 . Composition ratios were determined via ATR-FTIR. Error bars represent the standard deviation of a minimum of three replicate measurements.....	52
Figure 4.6. Examination of polymerization rate effects on photo-enforced stratification. A) Normalized composition ratio as a function of the light intensity used to polymerize the film. B) Normalized composition ratio achieved by varying the light intensity (\bullet) and varying the concentration of DMPA (\square) as a function of time to reach the maximum polymerization rate. Real time FTIR spectroscopy was used to determine the time to reach the maximum rate of polymerization in both cases. Films were polymerized in a 300 micron laminate mold with 365 nm light. Error bars represent the standard deviation of a minimum of three replicate measurements.	54
Figure 4.7. Effect of pulsed illumination on stratification. A) Representative photo-DSC trace of pulsed illumination with three seconds of illumination and five seconds with the shutter closed per cycle, 10 times. Post cycling, the light is left on to complete the cure. B) Normalized composition ratio for pulsed (\bullet) and constant (\square) illumination as a function of the fractional attenuation of light. Films were polymerized in a 300 μm laminate mold with 365 nm light at 1 mW/cm^2 . Composition ratios were determined via ATR-FTIR. Error bars represent the standard deviation of a minimum of three replicate measurements.....	55
Figure 4.8. Water contact angle as a function of DMPA concentration. Approximately 200 μm thick films were polymerized on a glass slide in an inert atmosphere with 365 nm light at 1 mW/cm^2 . Error bars represent the standard deviation of a minimum three measurements from at least three samples.....	57
Figure 5.1. Calculated light intensity of 365 nm light as a function of depth through a 300 micrometer thick film with a photoinitiator concentration (DMPA) of 0.04 M, extinction coefficient of 150 $\text{L}/(\text{mol cm})$, and incident light intensity of 1 mW/cm^2	71

Figure 5.2. Modeled rate of polymerization (R_p) of a co-photopolymerization of a mixture of mono-ene and di-ene, with ene concentrations of 8.2 M and 16.4 M respectively (A) as both a function of depth and time and (B) at 0, 150, and 300 micrometers.	72
Figure 5.3. Monomer consumption during co-polymerization. (A) Mono-ene and (B) di-ene consumption in the polymer film as a function of depth and time. (C) Mono-ene and (D) di-ene consumption as a function of depth in the film at 0, 1, 3, and 5 seconds.	73
Figure 5.4. Monomer diffusion in the polymer film during co-polymerization. (A) Mono-ene and (B) di-ene rate of diffusion as a function of depth and time during co-polymerization. Rate of mono-ene and di-ene diffusion at the (C) surface and (D) bottom of the polymer film.	75
Figure 5.5. Polymer film composition as a function of time. (A) Evolution of composition ratio, top(mono-ene/di-ene)/bottom(mono-ene/di-ene) as a function of time. (B) Evolution of polymer film composition as a function of depth and time.	77
Figure 6.1. Chemical structures of monomers and photoinitiators used in this study including: (A) 2-(dimethylamino)ethyl acrylate, (B) 2-hydroxyethyl methacrylate, (C) 2-(dimethylamino)ethyl methacrylate, (D) 2-hydroxyethyl acrylate, (E) 2-methoxyethyl acrylate, (F) 1,6-hexanediol dimethacrylate, (G) 2,4,6-trimethylbenzoyl-diphenyl-phosphineoxide, and (H) 2,2-dimethoxy-2-phenylacetophenone.	85
Figure 6.2. Normalized peak height ratios from the surface of polymers produced with a range of DMPA concentrations for a 1:1 weight ratio of (A) HEMA to DMAEA and (B) HEA to DMAEMA formulations using ATR-FTIR. Peak height ratios were normalized to the ratio determined using transmission FTIR of the same samples. 200 micrometer drawn films were polymerized with 365 nm light at 7 mW/cm ² . Error bars represent the standard deviation of a minimum of three replicate measurements.	89
Figure 6.3. Normalized peak height ratios from the surface of polymers produced with various amounts of (A) TPO in a 1:1 weight ratio of HEMA to DMAEA formulation as determined by ATR-FTIR. (B) Comparison of the normalized peak height ratios observed from TPO (○) and DMPA (●). Peak height ratios were normalized by the C-N/O-H ratio from transmission FTIR of the same samples. 200 micrometer drawn films were polymerized with 365 nm light at 7 mW/cm ² . Error bars represent the standard deviation of a minimum of three replicate measurements.	91
Figure 6.4. Methacrylate to carbonyl peak height ratio from confocal Raman spectroscopy depth profile. Polymer sample was produced from a 1:1 weight ratio of MOA to HEMA with a 1.25 wt% DMPA concentration polymerized in air. 200 micrometer drawn film were polymerized with 365 nm light at 1 mW/cm ²	94

Figure 6.5. Normalized peak height ratio from the surface polymers produced using a 1:1 molar ratio of HDDMA to HEA with various amounts of DMPA using ATR-FTIR. 200 micrometer drawn film were polymerized with 365 nm light at 1 mW/cm ² . Error bars represent the standard deviation of a minimum of three replicate measurements.....	95
Figure 6.6. Normalized peak height ratios from the surface of polymer films of 1:1 molar ratio of HDDMA to HEMA with various amounts of DMPA using ATR-FTIR. 200 micrometer drawn films were polymerized with 365 nm light at 7 mW/cm ² . Error bars represent the standard deviation of a minimum of three replicate measurements.....	96
Figure 7.1. Chemical structures of (A) 2-hydroxyethyl methacrylate, (B) 1,6-hexanediol dimethacrylate, (C) 2,2-dimethoxy-2-phenylacetophenone, (D) 2-methoxyethyl methacrylate, (E) N-hydroxyethyl acrylamide, (F) 2-(dimethylamnio)ethyl methacrylate, (G) methyl methacrylate, (H) 2-methoxyethyl acrylate, (I) 2-hydroxyethyl acrylate, (J) methylene blue, (K) diphenyliodonium chloride, (L) trimethylolpropane diallyl ether, (M) tri(ethylene glycol) divinyl ether, and (N) trimethylpropane tris(2-mercaptoacetate).	104
Figure 7.2. Dynamic mechanical analysis tan delta temperature sweep of neat HEMA (○), neat HDDMA (●), thermally polymerized one to one molar ratio of HEMA to HDDMA (■), and photopolymerized one to one molar ratio of HEMA to HDDMA that exhibits photo-enforced stratification (□). Films were polymerized in a 300 micron laminate mold with 365 nm light at 1 mW/cm ²	109
Figure 7.3. Images of one to one mole ratio 2-methoxyethyl methacrylate and N-hydroxyethyl acrylamide polymerized (A and B) in a laminate mold The high light intensity side of the film is labeled with a t. (C and D) Pulling the laminate mold apart results in the low light intensity side of the film adhering to the glass slide.....	111
Figure 7.4. XPS spectral regions for (A) N 1s and (B) C 1s of polymer composed of a 1:1 mass ratio of methyl methacrylate to 2-(dimethylamino)ethyl acrylate polymerized with (1) 0.1 and (2) 4 wt% photoinitiator.	113
Figure 7.5. Surface composition ratio of thiol-ene films produced from a two to one to one molar ratio of trimethylpropane tris(2-mecaptoacetate) to tri(ethylene glycol) divinyl ether to trimethlpropane diallyl ether as a function of fractional attenuation of light from DMPA. 8 mil thick films were polymerized on a glass slide in an inert atmosphere with 365 nm light at 1 mW/cm ² . Composition ratios were determined via ATR. Error bars represent the standard deviation of a minimum of three replicate measurements.	116

CHAPTER 1 INTRODUCTION

The performance of polymeric materials is strongly dictated by the surface chemistry and surface properties as many applications rely upon the interactions between a polymer its environment.¹ Achieving desired surface chemistry and properties in a single reaction step would be preferable to using multiple synthesis steps and/or post synthesis modification of the polymeric material (vide infra). Not only would single step production result in reducing production time and cost but could also circumvent the negative aspects such as poor control of the surface² or residual chemicals associated with different post polymerization modifications.³ Photopolymerization allows sufficient control of the polymerization for single step production for control of surface chemistry and properties.

The temporal and spatial control inherent to photopolymerization makes it an ideal polymerization technique to produce polymers with control over the localized composition. Photopolymerizations have demonstrated such utility in the production of holographic gratings,⁴ holographic polymer dispersed liquid crystals⁵⁻⁷ (HPDLC), flexible liquid crystal displays,^{8,9} and stratified films.^{10,11} In general, these materials are produced by creating non-uniform polymerization rates and controlling the reaction location via manipulation of the initiating light source. Regions with high and low to no light intensity of the initiating light are developed through the use of multiple lasers to form an interference pattern, photo-masks, or producing a light gradient through the pre-polymer film with a chromophore. Moreover, increasing the light intensity increases the rate of polymerization and therefore control of the light intensity affords non-uniform polymerization. This level of control over the polymerization allows for formulations containing non-reactive species or monomers of unequal reactivity to be spatially resolved with the preferentially reacting monomer enriching the high light intensity

regions of the polymer. Localized control of the chemical composition affords novel properties not attainable with other polymeric materials.

Holographic gratings are materials with periodic holographic index profiles produced with spatially oriented changes in composition, density, or the presence of voids.¹² Production of holographic gratings is achieved by polymerization initiated from multiple laser interference patterns to generate spatially resolved features. Holographic grating can be utilized in numerous applications¹³ such as a data storage media,¹⁴⁻¹⁶ embedded waveguides,^{4,17,18} and prisms.¹² An interesting subset of holographic gratings is HPDLCs which are produced via polymerization initiated from multiple laser interference patterns to spatially resolve polymer from liquid crystal.^{5-7,12} HPDLCs allow for electro-optical holograms resulting in holograms which can change the refractive index profile of the hologram via electrical stimulation.¹² Such modulation is advantageous in many applications^{12,19} including video displays.^{20,21} Additionally, photopolymerization can control the film composition through the depth via light gradient produced from a chromophore to produce a stratified film. For example, an operational liquid crystal display can be produced in a single step.^{8,9} Additionally, stratified films can be produced which can respond to stimulus due to the difference in composition at the different sides of the film.¹¹

The goal of this research is to utilize the spatial and temporal control of radical photopolymerization to produce films with a chemical composition gradient resulting in control over the surface properties in a single reaction step (Figure 1.1). The remainder of this chapter discusses concepts central to understanding the body of work presented in this thesis. Central to this work is radical photopolymerization due to the high degree of control which can be achieved with this polymerization mechanism. As such, a mechanistic and kinetic discussion of radical photopolymerization for both traditional radical chain growth and thiol-ene step growth photopolymerizations. The spatial and temporal control of radical photopolymerization allows for the spatial resolution of

polymer composition in the polymer film by enriching preferentially reacting monomers in a copolymerization in the high light intensity regions of the film. As a result, the kinetic differences utilized to produce a stratified film are discussed. Diffusion of monomer is also discussed as production of a stratified polymer film from an initially homogenous pre-polymer formulation requires diffusion of monomer. Additionally, a few established methods for controlling the surface chemistry are outlined. Finally, a summary of the research presented in this thesis is given at the end of this chapter.

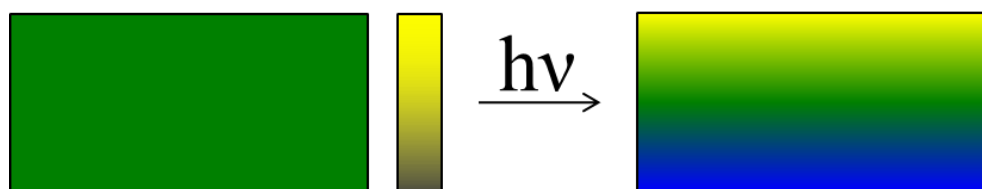


Figure 1.1. Pictorial representation of producing a chemical concentration gradient via co-photopolymerization of a formulation containing monomers of unequal reactivity with a light gradient through the depth produced from the photoinitiator resulting in enrichment of the preferentially reacting monomer in the high light intensity regions of the film.

Radical Photopolymerization

Photopolymerization utilizes light to generate active centers which initiate polymerization.²² Specifically, light is absorbed by photoinitiators to produce the active species which then initiates the polymerization (see Figure 1.2 for an example of a photoinitiator used in these studies). Using light to initiate polymerization has numerous advantages over conventional thermal polymerizations. Specifically, photopolymerization reactions are very rapid reactions resulting in polymer networks which rapidly form at ambient temperatures. Additionally, photo-initiated polymerization processes are typically considered to be green because of significantly lower energy requirement to initiate polymerization as well as requiring little to no volatile organic compounds in the

formulations. A wide range of monomers functionalities, such as acrylate, methacrylate, acrylamide, methacrylamide, vinyl, and thiol-enes, can be photopolymerized to generate polymer networks²³⁻²⁶ (see Figure 1.2 for examples of monomers used in these studies).

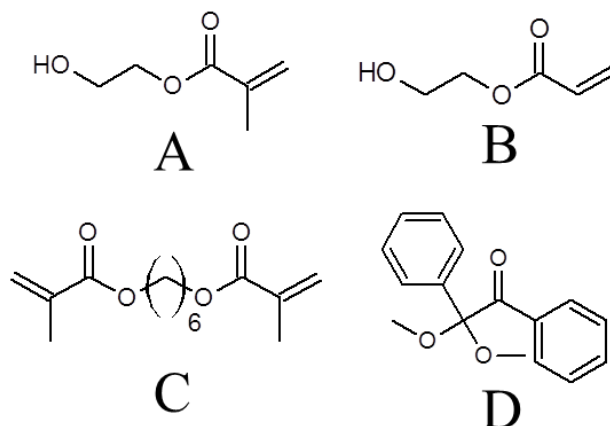


Figure 1.2. Chemical structures of (A) 2-hydroxyethyl methacrylate, (B) 2-hydroxyethyl acrylate, (C) 1,6-hexanediol dimethacrylate, (D) 2,2-dimethoxy-2-phenylacetophenone which are representative chemicals utilized in these studies.

Radical polymerization typically utilizes monomers containing an alkene functional group. With respect to radical chain growth photopolymerization, each alkene group has a functionality of two which results in an alkene being able to form two covalent bonds with alkene groups from other monomers. Monomers must contain a functionality of at least two in order to form a linear polymer. Increasing the functionality of the monomers in the formulation results in crosslinked polymers upon photopolymerization. Furthermore, increasing the ratio of monomer functionality to monomer molecular weight increases the crosslink density of the formed polymer.²² Radical chain photopolymerization proceed via the typical radical reaction pathway of

initiation, propagation, and termination.²⁷ The individual steps of this pathway are described below:

Initiation

The first step in radical chain photopolymerization is the generation of a reactive species with which to start the polymerization.²² For radical photopolymerization the reactive species is generated via absorption of light by a light sensitive compound called a photoinitiator. The radicals generated from the light absorption of the photoinitiator will react with the electron rich double bonds present in the monomer. The photoinitiator absorbance is wavelength dependent and different for different photoinitiators; thus, generation of radicals requires overlap between the emission spectra of the initiating light source and absorption spectra of the photoinitiator.²⁸ Two different processes are used for generating radicals from photoinitiators: Norrish type one and Norrish type two processes. Typically, a Norrish type two process is at least a two component photoinitiation system containing a photoinitiator and a co-initiator.²⁹ The photoinitiator absorbs light resulting in an excited electronic state. From this higher energy state, the photoinitiator can then form an exciplex with the co-initiator resulting in the photoinitiator abstracting a hydrogen atom from the co-initiator thus forming a radical species which can then initiate polymerization. Producing radicals without direct bond cleavage allows lower energy light to be utilized.

In a Norrish type one process, the photoinitiator absorbs UV light and generates radicals through α -cleavage of a carbon-carbon bond.³⁰ An example of a radical generation via Norrish type one is illustrated in Figure 1.3 where the multiple-step photocleavage of 2,2-dimethoxy-2-phenylacetophenone is depicted.³¹ Adsorption of appropriate wavelength of light by 2,2-dimethoxy-2-phenylacetophenone results in α -cleavage forming a dimethoxy benzyl radical and a benzaldehyde radical. The dimethoxy benzyl radical can further rearrange to form methyl benzoate and a methyl radical.

Additionally, the benzaldehyde radical can couple with another benzaldehyde radical to form benzil or can abstract a hydrogen to form benzaldehyde and a radical on the hydrogen donor.

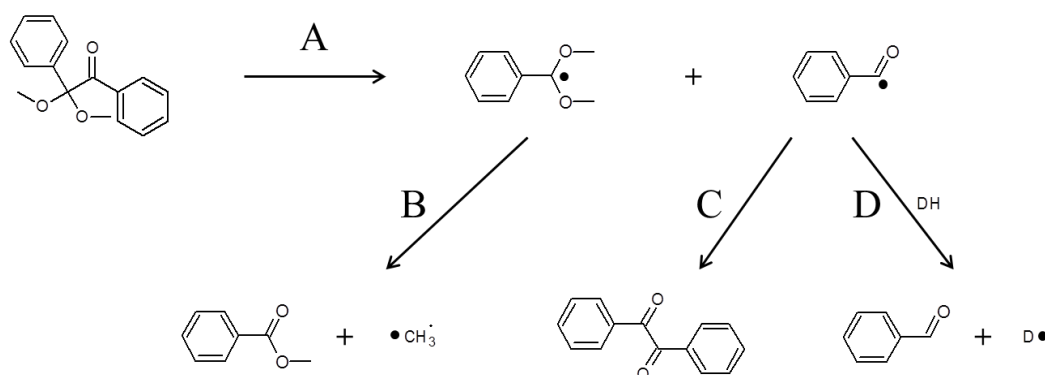


Figure 1.3. Norrish type one photo-cleavage of 2,2-dimethoxy-2-phenylacetophenone. (A) α -cleavage of 2,2-dimethoxy-2-phenylacetophenone results in the formation of dimethoxy benzyl radical and a benzaldehyde radical. The dimethoxy benzyl radical can further rearranges (B) to methyl benzoate and a methyl radical. The benzaldehyde radical couples (C) with an additional benzaldehyde radical to form benzil or can abstract a hydrogen (D) to form benzaldehyde and a radical on the hydrogen donor.³¹

For a Norrish type one photoinitiator, photon absorption and α -cleavage, assuming the production of two reactive radicals, can be expressed with the chemical reaction (Equation 1):



where PI is the photoinitiator, $h\nu$ is the initiating light, and R^* is the radical formed from the photoinitiator bond cleavage. The rate of consumption of the photoinitiator can be described by (Equation 2):

$$R_i = \frac{\epsilon I [PI]}{E} \quad (2)$$

where ϵ is the molar absorptivity of the photoinitiator, I is the light intensity available for initiation, $[PI]$ is the concentration of photoinitiator, and E is the energy per mole of photons which can be determined by (Equation 3):

$$E = N_a h \nu \quad (3)$$

where N_a is Avogadro's number, h is Planck's constant, and ν is the frequency of light. The light available for photoinitiation is not constant throughout the thickness of the polymerizing polymer and needs to be considered.^{32,33} To simplify, only non-photobleaching initiators will be considered such that any light attenuation is approximately constant during the course of the reaction. Thus, calculation of the light intensity available for photoinitiation and is described from the Beer-Lambert law as (Equation 4):

$$I = I_0 10^{(-\epsilon z [PI])} \quad (4)$$

where I is the light intensity at a certain depth in the sample, I_0 is the incident light intensity, and z is the depth in the sample. After the generation of radicals, the second step of initiation is the reaction of the radicals with the alkene in the monomer. This second and final step can be represented with the chemical reaction (Equation 5):



where M is the reactive monomer, k_i is the initiation rate coefficient and P_1^* is the formed monomer radical.

Propagation

After initiation, the monomer radical can then react with an additional monomer which increases the length of the growing polymer chain and results in another radical being produced at the terminal end of the polymer chain. This reaction can be represented with the chemical reaction (Equation 6):



where k_p is the propagation rate coefficient. The generated radical will continue to react with additional monomers resulting in continual increasing of the molecular weight of the growing polymer while also generating a radical which can proceed with propagation. In general, radical propagation can be expressed with the following chemical reaction (Equation 7):



where each propagation step results in increasing the molecular weight of the growing polymer. Thus the rate of polymerization can be determined by (Equation 8):

$$R_p = k_p [R^*] [M] \quad (8)$$

where R^* is a generic radical species.

Termination

The final step in a radical polymerization mechanism is termination where radicals react to form a stable covalent bond. In traditional radical polymerization this results in a stopping the growth of the polymer chain. Combination and disproportionation are the

two basic mechanisms of radical termination in radical photopolymerization which can be represented by (Equations 9 and 10):



where k_{tc} and k_{td} are the rate coefficients for termination by combination and disproportionation, respectively. Additionally, chain transfer reactions to monomers or solvents are possible but not discussed here.³⁴ Rate of termination can be represented by (Equation 11)

$$R_t = k_t [R^*][R^*] \quad (11)$$

where k_t is an overall rate coefficient for termination.

Overall Rate of Polymerization

Determining an overall rate of polymerization is difficult as it is challenging to determine the absolute radical concentration in the system. A typical approach to developing an overall rate of polymerization equation is to make a pseudo steady-state assumption for the concentration of radicals, in essence, stating that the radical concentration during polymerization is constant. This assumption then implies that the rate of generation and consumption of radicals via initiation and termination, respectively, must be equal. Therefore, the concentration of radicals during the polymerization can be solved by setting the rate of initiation equal to the rate of termination. Replacing the radical concentration with this assumption allows for the general expression of the rate of photopolymerization (Equation 12):²²

$$R_p = k_p [M] \left(\frac{R_i}{2k_t} \right)^{1/2} \quad (12)$$

This generalized equation illustrates that the rate of polymerization is directly dependent upon the square root of the light intensity available for photopolymerization. Thus, attenuation of light through the film will result in a higher rate of polymerization in the high light intensity regions of the film.

In considering radical photopolymerization, the rate varies significantly beyond simple disappearance of monomer. During photopolymerization, the viscosity of the formulation increases with conversion causing decreased rates of diffusion.^{35,36} This causes the kinetic coefficients k_p and k_t to vary during the polymerization. At low conversion, and thus low viscosity, the reactive species can readily diffuse resulting allowing for high rates of termination and propagation.²² As conversion increases the viscosity of the formulation also increases resulting in decreased diffusion inducing a decrease in k_p and k_t . However, the decrease in k_t is significantly larger as the radicals are attached to growing polymer chains which further decreases radical diffusion. The non-uniform change in k_p and k_t results in an increase in the rate of polymerization known as autoacceleration.^{36,37} Continued polymerization results in further diffusional limitations resulting in a decrease in the rate of polymerization called autodeceleration.²² This behavior is very different from traditional reactions where a decrease in reagents results in a corresponding decrease in reaction. The onset of autoacceleration is very dependent upon the formulation with high functionality formulations experiencing autoacceleration at lower conversions.²²

Thiol-Ene Radical Step Growth Photopolymerization

Thiol-ene photopolymerization differs from the radical photopolymerization mechanism described above in that the polymerization proceeds via a radical step growth mechanism.^{38,39} This difference in polymerization allows alleviation of some

disadvantages of typically observed in more traditional acrylate-based photopolymerization. Specifically, thiol-ene photopolymerization result in more homogenous network formation which may result in less shrinkage stress.⁴⁰⁻⁴² Additionally, the range of properties which can be achieved via thiol-ene polymerizations is significant due to the large number of ene monomers which will polymerize via this mechanism.⁴¹ In addition, thiol-ene photopolymerizations polymerize readily in air, overcoming oxygen inhibition issues typically observed in radical photopolymerizations.⁴³⁻⁴⁷

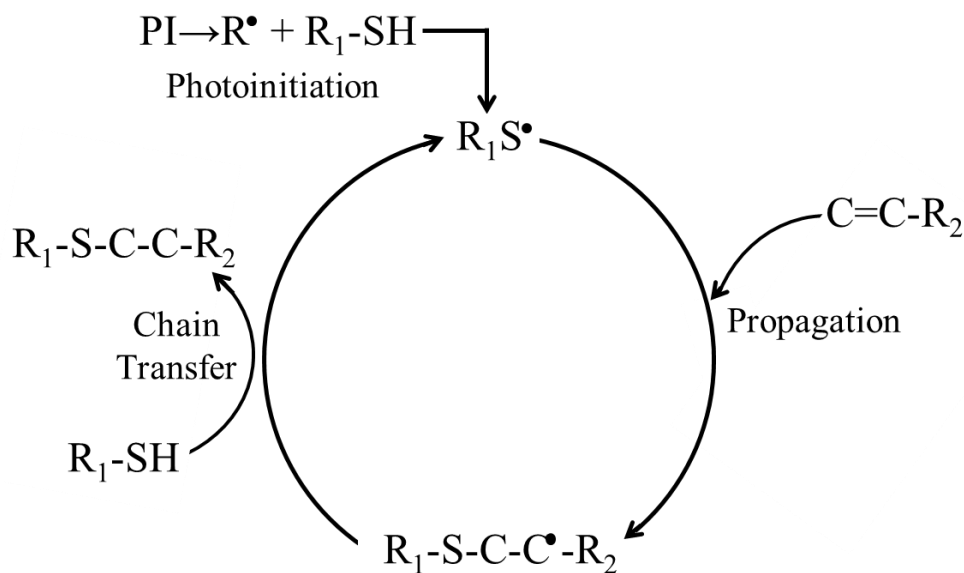


Figure 1.4. Schematic of thiol-ene radical step growth photopolymerization.^{38,39}

The radical, step growth mechanism of thiol-ene photopolymerization starts similarly to radical chain growth mechanism with radicals being produced via absorption of light by the photoinitiator (Figure 1.4).^{38,48} The radical from the initiator fragment abstracts a hydrogen from the thiol group forming a thiyl radical. This radical then

propagates across the ene of the other monomer in the formulation which results in a covalent bond between the thiol and carbon of the ene while forming another radical. The radical formed from this propagation step will then abstract a hydrogen from another thiol to form a thiyl radical via chain transfer. This radical step growth reaction of propagation followed by chain transfer will continue until the radicals terminate. Due to this reaction mechanism, a formulation containing multifunctional thiols and multifunctional ene monomers in stoichiometric balance is required to produce polymer at high conversion. Additionally, the reaction is not inhibited by oxygen because reaction with oxygen creates a peroxy radical which is still capable of abstracting a hydrogen from the thiol to produce a thiyl radical.⁴⁹⁻⁵¹ The step polymerization results in a much slower development of polymer molecular weight, with high molecular weight being achieved only at high conversion, leading to a delay in the gelation of the system and a reduction in the shrinkage stress.^{52,53}

Radical Kinetic Differences

The overall goal of this research is to produce a photopolymer film that has a chemical composition gradient in a single reaction step via photopolymerization. We have utilized the inherent temporal and spatial control of photopolymerization to create regions of higher and lower reactivity via a light gradient. This light gradient creates a gradient in the rate of initiation which then results in a gradient in the rate of polymerization. As a result, the high light intensity regions polymerize at a greater rate than the rest of the polymerizing film. To take advantage of the reaction gradient to produce a film with a chemical concentration gradient via photopolymerization from an initially homogenous pre-polymer formulation, the monomers in the co-polymerization must react at different rates.

A copolymerization is the mixture of two or more monomers to form a copolymer.⁵⁴ The monomers react together to form a polymer containing both monomeric

units. Thus, a copolymer is not a mixture of two homogenous polymers but rather a mixture of monomers in the polymer. The addition of monomers to the growing polymer depends on the concentration and reactivity of the monomers. The polymer formed at the beginning of a polymerization could be composed of a different monomer ratio than the polymer formed toward the end of the polymerization because of changing concentration and diffusional affects. Additionally, the rate at which monomers add to the polymer are not necessarily indicative of the monomers homopolymerization rate.^{22,55} Therefore, it is necessary to understand basic monomer reactivities in copolymerizations which directly depends on the other monomer(s) in the copolymerization.

Monomers reactivity in a co-photopolymerization determines how monomers will add to the growing polymer.⁵⁶ Coupling reactivity differences with non-uniform photopolymerization in the presence of a light gradient will allow design of formulations which will stratify during photopolymerization and result in enrichment of the preferentially reacting monomer in the high light intensity regions of the film. The kinetic differences of functional group number, inherent reactivity, oxygen inhibition, thiol-ene, and Norrish type two photoinitiation that have been utilized to produce stratified films in these studies are outlined below.

Number of Functional Groups per Monomer

Polymerization of monomers with a single ene functional group results in the addition of the monomer to a linear growing polymer chain and the formation of a radical. This reaction also occurs when monomers with more than one ene functional group polymerize.⁵⁷ However, when a monomer with two ene functional groups polymerizes, when one group reacts a pendent reactive group ene group remains⁵⁸ (Figure 1.5). The pendent group is in close proximity to other propagating radicals thus increasing the observed reactivity of the pendent group.⁵⁹ Additionally, crosslinking monomers result in rapid decrease in diffusion due to network formation resulting in

autoacceleration occurring very early in the polymerization.⁶⁰ These affects result in a di-ene monomer polymerizing at a much greater rate than an analogous mono-ene monomer.⁶¹

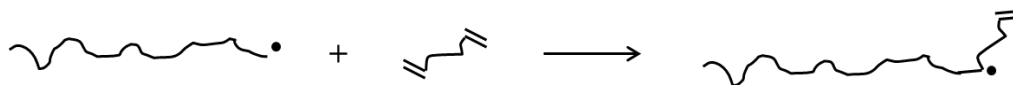


Figure 1.5. Pictorial representation of a macro radical reacting with a di-ene species to form another macro radical and a pendent ene group off of the growing polymer chain.⁵⁸

The differences in the rate of polymerization between a mono- and di-ene monomer can be utilized to produce films with a chemical composition gradient via photopolymerization. Specifically, the crosslinking monomer would add to the growing polymer network at a greater rate than the mono-ene enriching the crosslinking monomer in the high light intensity regions of the film.

Inherent Monomer Reactivity

The reactivity of an alkene toward radical chain polymerization can be greatly affected by the chemical structure of the monomer.⁶² For example, acrylates and methacrylates have very similar structures yet a homopolymerization of acrylate is considerably faster than that of methacrylate.²² One reason for the difference in homopolymerization rate is due to the radical intermediate formed upon propagation through the alkene (Figure 1.6).²⁷ Polymerization of an acrylate produces a secondary radical where as a methacrylate produces a tertiary radical. The secondary radical is less stable and thus more reactive leading to increased rate of polymerization observed in acrylates.

Differences in chemical structure can influence copolymerizations as well which is not obvious based on the homopolymerization rates. For example, a copolymerization of acrylate and methacrylate results in the preferential reaction of the methacrylate monomer. Thus, examination and understanding of copolymerization is critical in designing formulations which will stratify upon photopolymerization. Methacrylate preferentially reacts in a copolymerization with an acrylate because the radical intermediate formed is more stable. Reactivity ratios are the ratio of the homopolymerization rate constant divided by the copolymerization rate constant giving a simple quantity to examine copolymerization reactivity.^{63,64} Moreover, reactivity ratios illustrate which monomer in a copolymerization will preferentially react, the strength of reaction preference, and the behavior of the copolymerization.²² For instance, the reactivity ratios for a copolymerization of methyl methacrylate and methyl acrylate are 2.2 and 0.4, respectively. These values indicate that the methyl methacrylate is the preferentially reacting monomer in the copolymerization for both methacrylate and acrylate terminated radicals. Additionally, the reactivity ratios indicate that the copolymerization behaves as an ideal copolymerization as the product of the reactivity ratios being approximately equal to one.²² For an ideal copolymerization, both monomers react with the same likelihood with both radical species. Therefore, for the methacrylate/acrylate polymerization, the methacrylate reacts to both radicals at a rate over 2 times that of the acrylate.

The reactivity ratios of numerous copolymerizations have been determined, thus facilitating prediction of the preferentially reacting monomer in a copolymerization to be determined and for calculation of the instantaneous copolymer composition.²² Thus, copolymerization formulations can be designed with different monomer types and the surface enrichment can be predicted utilizing reactivity ratios for the given copolymerization.

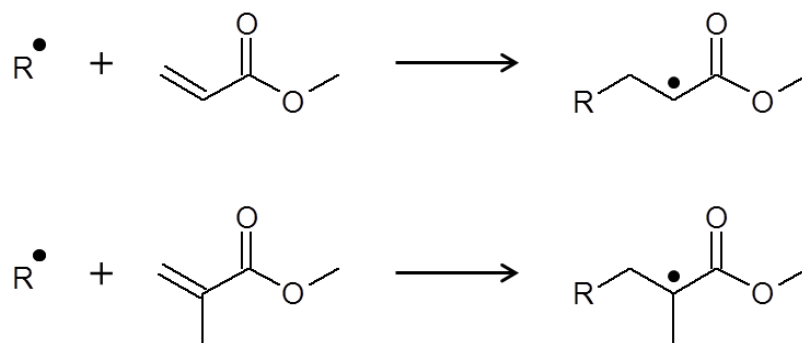
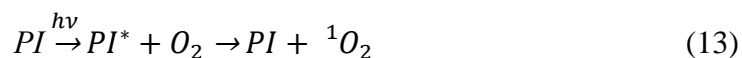


Figure 1.6. Representation of a radical reacting with an acrylate to form a secondary radical (top) and a radical reacting with a methacrylate to form a tertiary radical (bottom).

Oxygen Inhibition

Atmospheric oxygen is in the triplet state at its ground state meaning oxygen has two unpaired electrons. As a result, oxygen can have rather detrimental effects on many steps of radical photopolymerization.^{65,66} Oxygen can quench the excited state of photoinitiators resulting in lower quantum yields of radical production,⁶⁰ represented by Equation 13:



where PI^* is the excited state of the photoinitiator and 1O_2 is singlet oxygen.

Additionally, oxygen can react with radicals to form a peroxy radical,⁶⁰ represented by Equation 14:



Peroxy radicals are not reactive enough to react with an alkene in a propagation reaction.⁶⁰ As a result, oxygen prevents polymerization until all of the oxygen is reacted

in the system. During polymerization oxygen can continue to diffuse into the polymerizing polymer resulting in an oxygen inhibited layer.^{67,68} Within this layer, high conversion of monomer to polymer is not achieved, leading to poor property development and tacky surfaces. The thickness of this layer is determined by the rate of polymerization and the rate at which additional oxygen can diffuse into the film. Many methods to mitigate oxygen inhibition are used including high photoinitiator concentration, high light intensity, high viscosity formulations,⁶⁹ and blanketing with an inert gas such as nitrogen.

While oxygen is detrimental to radical photopolymerization, differences in oxygen reactivity with radicals exist. For example, acrylates experience greater degrees of oxygen inhibition than methacrylates.^{70,71} Presumably the more stable ternary radical intermediate of the methacrylate compared to the more reactive secondary radical intermediate of the acrylate results in the decreased degree of oxygen inhibition of the methacrylate relative to the acrylate. Thus, oxygen inhibition also changes monomer reactivity to produce stratification from a co-photopolymerization of a methacrylate and acrylate. Additionally, methacrylates preferentially react in a co-polymerization with acrylates resulting in increased preference for methacrylate reaction in the high light intensity region at the surface of the film as discussed previously. These factors could be combined to allow for increased methacrylate surface enrichment.

Thiol-Ene

Thiol-ene polymerizations, as discussed earlier, are formed via a radical, step growth mechanism which requires at least a thiol and an ene monomer to produce a polymer. Thus, producing thiol-ene formulations which stratify upon photopolymerization would require formulations containing at minimum two thiols and one ene or two enes and one thiol. Due to the higher number of ene monomers available for thiol-ene polymerization, formulations containing two ene monomers and a thiol

monomer have been examined. Additionally, a wide range of reactivity of ene monomers with thiols exists making varying the ene monomer a strategic choice for producing stratified films.³⁸⁻⁴⁰

Ene reactivity with thiol can vary from rapid to slow polymerization to not polymerizing with thiol and reacting almost exclusively via homopolymerization rather than via thiol-ene polymerization. In general, ene reactivity increases with increasing electron density of ene (Figure 1.7). Thus, production of a stratified film from thiol-ene photopolymerization would result in an enrichment of the faster reacting ene monomer at the surface.

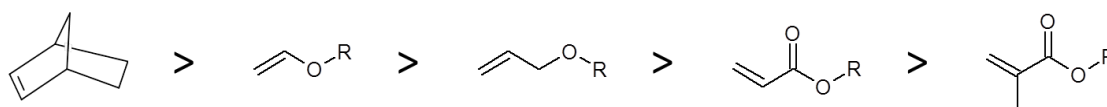


Figure 1.7. Qualitative ranking of various ene monomers reactivity toward a thiol in a thiol-ene polymerization.^{38,39}

Norrish Type Two Photoinitiation

Previous kinetic differences discussed were primarily observed in during the propagation step of the polymerization. Conversely, type two photopolymerization could utilize differences in monomer reactivity in the initiation step. Specifically, type two photoinitiation requires the use of a co-initiator which has an easily abstractable hydrogen to create a radical for initiation. Rather than add a separate co-initiator to the formulation, a monomer could be added to the pre-polymer formulation which could also react as a co-initiator.⁷² Utilizing a light gradient to produce a stratified film results in higher rates of initiation in the high light intensity regions of the film increases the consumption of the co-initiator in the high light intensity regions. Thus, formulations could be developed

which result in stratified films with the co-initiator monomer being enriched in the high light intensity regions of the film utilizing the same monomer reactive group.

Diffusion

Production of stratified films via photopolymerization is possible via non-uniform polymerization of a formulation containing monomers of unequal reactivity. Non-uniform polymerization is achieved with the production of a light gradient through the film resulting from the photoinitiator. Thus, the high light intensity regions of the film results in higher rates of polymerization and the preferentially reacting monomer is consumed at a greater rate than the other monomer in the co-photopolymerization. As a result, a chemical concentration gradient is produced through the film inducing monomer diffusion and ultimately produce a polymer film with a composition gradient with preferentially reacting monomer enriched in the high light intensity regions of the film.

The kinetics important in this process have been described in previous sections of this chapter. This section examines the aspects of diffusion that produce a stratified film. Determining and understanding monomer diffusion during polymerization is important for applications where localized control of the polymer composition is desired.⁷³⁻⁸⁰

Diffusion is random molecular motion which results in the transport of matter within a system.⁸¹ Interestingly, even though the motion is random with no preferred direction, the net result of the random motion is that matter moves from an area of higher concentration to an area of lower concentration. Thus, movement from diffusion can be defined relative to the concentration gradient present in the system. Specifically, the movement of matter across a two dimensional plane can be described by the rate of material transfer per unit area, also known as the flux, which is defined to be (Equation 15):

$$F = -D(\partial C/\partial x) \quad (15)$$

where F is the flux of matter, D is the diffusion coefficient, C is the concentration of the matter of interest, and x is the direction of the flux. The diffusion coefficient is defined in units of length squared per time and determines that rate at which matter moves in the system. The negative sign results as diffusion results in matter transport in the opposite direction of increasing concentration.

However, the above equation is defined at steady state and as such does not have any time dependence. Oftentimes, concentration varies with time. To understand this effect, Figure 1.8 shows a hypothetical cube with side lengths of $2dx$, $2dy$, and $2dz$ which is a subset of the larger system surrounding the cube.⁸¹ The concentration of the material of interest is defined to be C with the labeled faces of $abcd$ and $a'b'c'd'$ perpendicular to the x axis. Finally, the flux through the center point is defined to be F . Thus, to determine the change in concentration in the cube at point $p(x,y,z)$, the amount of material entering and leaving the cube would be determined.⁸¹ Figure 1.8 shows flux along the x axis where matter could enter by crossing face $abcd$ in the plane of $x-dx$ would be given by Equation 16 and the rate leaving the cube by crossing face $a'b'c'd'$ in the plane of $x+dx$ would be given by Equation 17:

$$4dydz\left(F_x - \frac{\partial F_x}{\partial x} dx\right) \quad (16)$$

$$4dydz\left(F_x + \frac{\partial F_x}{\partial x} dx\right) \quad (17)$$

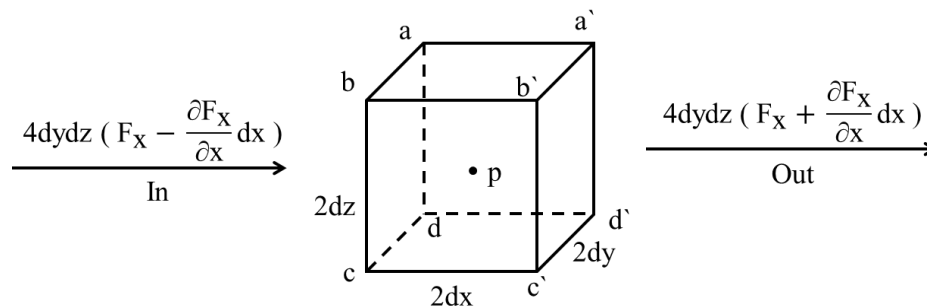


Figure 1.8. Schematic of volume element used to derive Fick's second of diffusion.⁸¹

These expressions are simply the flux multiplied by the area the material is passing through. Thus, the net change would be the matter entering less the matter leaving as expressed by Equation 18.

$$4dydzF_x - 4dydz \frac{\partial F_x}{\partial x} dx - 4dydzF_x - 4dydz \frac{\partial F_x}{\partial x} dx = -8dydz \frac{\partial F_x}{\partial x} dx \quad (18)$$

Similar arguments can be made for fluxes in the y and z directions to yield Equation 19 and Equation 20, respectively.

$$-8dydzdx \frac{\partial F_y}{\partial y} \quad (19)$$

$$-8dydzdx \frac{\partial F_z}{\partial z} \quad (20)$$

Additionally, the change in concentration could be examined by examining the volume element and monitoring the changing in concentration with respect to time directly as shown in Equation 21:

$$8dx dy dz \frac{\partial C}{\partial t} \quad (21)$$

Utilizing a simple mass balance, it is apparent that the change in concentration with time must be equal to the flux of matter in the x, y, and z directions expressed by Equation 22 which simplifies to Equation 23.

$$8dx dy dz \frac{\partial C}{\partial t} = -8dx dy dz \left(\frac{\partial F_x}{\partial x} + \frac{\partial F_y}{\partial y} + \frac{\partial F_z}{\partial z} \right) \quad (22)$$

$$\frac{\partial C}{\partial t} = D \left(\frac{\partial F_x}{\partial x} + \frac{\partial F_y}{\partial y} + \frac{\partial F_z}{\partial z} \right) \quad (23)$$

Finally, substituting Equation 15 into Equation 23 and assuming a constant diffusion coefficient yields Equation 24 which is better known as Fick's Second Law of Diffusion.

$$\frac{\partial C}{\partial t} = D \left(\frac{\partial^2 C}{\partial x^2} + \frac{\partial^2 C}{\partial y^2} + \frac{\partial^2 C}{\partial z^2} \right) \quad (24)$$

Fick's second law facilitates examination of concentration variation with time in a system given an initial condition. If a gradient in concentration is only present in one direction, for example in the x direction, Fick's second law can be simplified to Equation 25 as the derivatives of the concentration profiles are zero in the absence of a concentration gradient in the y and z directions.

$$\frac{\partial C}{\partial t} = D \frac{\partial^2 C}{\partial x^2} \quad (25)$$

Current Methods for Controlling Surface Chemistry

The ability to control surface and bulk chemistry in polymer films could provide significant advantages for many applications including antifouling systems,^{82,83}

antimicrobial films,⁸⁴⁻⁸⁶ and adhesives.^{87,88} Different surface chemistry could allow tailoring of numerous surface properties including hardness,^{89,90} contact angle,⁹¹ adhesion,^{87,88} and biological response^{92,93} thereby facilitating advanced applications not accessible with homogenous polymers. Currently, polymeric materials with different surface and bulk properties are generally obtained by multiple step processes, including changing or modifying the substrate,⁹⁴ precipitation of one component during polymerization,⁹⁴⁻⁹⁶ casting multiple films,^{97,98} surface grafting,⁹⁹⁻¹⁰¹ or plasma modification.^{102,103} Although each of these methods allows control of surface chemistry of the polymer film; these methods require additional production time, are not well controlled, and/or deleteriously affect final film properties. Plasma modification and surface grafting are active areas of research and post synthesis, polymeric surface modification methods and are described below.

Plasma Surface Modification

Plasma is the result of ionization of a gas using high energy radiation, electric fields, or high temperatures to form a gaseous mixture of oppositely charged particles.² Plasmas are very high in energy and highly reactive with organic and inorganic substances. When plasma reacts with an organic material, such as a polymer, the material will typically undergo thermal degradation and fragment.² The high energy plasma quickly loses energy to the surrounding environment thereby requiring a continuous supply of energy to maintain the plasma. The most common, man-made plasma is produced from electric discharge.

The high reactivity of plasma makes it a good candidate for post synthesis modification of a polymer surface. There are three main methods for modifying surfaces with plasma. Plasma can be used for plasma-enhanced synthesis to add a thin layer of polymeric material to the surface. This is accomplished by plasma dislocation of the original polymer surface and either depositing or grafting new polymeric material to the

surface via plasmonic polymerization. Another method is to utilize plasma to functionalize the surface of a polymer. In this case non-polymerizing plasma is utilized. The original polymer surface is still dislocated but active molecular fragments from the plasma covalently bind to the polymer. This method allows for even very inert polymers to be functionalized due to the high reactivity of plasma.¹⁰⁴ Finally, plasma can be utilized to etch the polymer surface which allows for the development of specific surface morphologies by selective ablation.²

Post synthesis modification of polymer surfaces with plasma also has limitations.¹⁰⁵ Specifically, plasma modification post polymerization requires additional equipment and time. Furthermore, the additional equipment required for plasma treatment is rather expensive with plasma generation typically requiring vacuum¹⁰⁵ but there are some examples of atmospheric plasma generation.² In addition to increased manufacturing costs, plasma processes are extremely complicated and system dependent which results in difficulty both in trying to scale up to production and in precisely controlling the changes in functional group formation that occur on the surface. Therefore, while plasma modification of polymer surfaces has many applications, the practical implementation of this method industrially is difficult and expensive.

Surface Grafting

Grafting is a process in which polymer chains are covalently attached to a polymer surface as a means of functionalizing and changing the polymer surface properties.¹ Grafting is generally characterized by grafting-from or grafting-to methods. For grafting-from, active centers required to produce the covalent bond between the surface and the grafted material are formed on the surface. Thus, the surface is utilized to initiate polymerization from the surface of the grafted material. The other method is grafting-to for which preformed polymers contain the reactive group which will form the

covalent bond with the surface. However, grafting-to methods have been difficult to scale for industrial uses.¹

Grafting is an advantageous method of changing polymer surface properties because addition of the grafted polymer can be well controlled and added to the surface in high density. Grafting results in long term chemical stability of the grafted polymer and avoids delamination due to the presence of the covalent bonds between the grafted material and the original polymer surface. Additionally, grafting attaches polymer to the surface allowing for control and modification of the surface properties while preserving the bulk polymer properties. However, grafting requires multiple processing steps and may add significant cost. Additionally, residual chemicals utilized for grafting and/or residual active moieties for grafting maybe difficult to remove and remain in the final material.

Research Summary

The goal of this work is to develop a processing technique and formulations which will produce a polymer film with a chemical concentration gradient through the film. Significant research has examined how to gain control over the localized polymer composition with most requiring multiple processing steps. This work aims at utilizing the inherent temporal and spatial control of photopolymerization to produce a film with a chemical concentration gradient yielding control of the surface properties in a single reaction step. Specifically, this research works to establish an understanding of the monomer kinetic differences required to produce a stratified film, the effect of processing conditions on film stratification, surface properties resulting from stratification, and development of a model which can describe the process of generating a chemical composition gradient in a film via photopolymerization.

To this end, this work entails extensive studies of the kinetics and diffusion required to produce a chemical concentration gradient via photopolymerization. Chapter

4 examines the kinetic difference between a mono- and di-ene as a means of producing a stratified film as well as studying the effect on stratification of various processing conditions such as light intensity and film thickness. Additionally, surface property differences are examined as a function of stratification. A mathematical model is generated in Chapter 5 based on photopolymerization kinetics and monomer diffusion to describe the production of a stratified film from a co-photopolymerization of the mono- and di-ene formulation previously explored in Chapter 4. Chapter 6 details several kinetic differences for producing a stratified film as well as combining multiple kinetic differences in a single formulation as a means of increasing final stratification in the film. Other properties, analytical techniques, and kinetic differences are relevant to the production of a stratified film with photopolymerization. Chapter 7 describes investigation of issues which could be of interest in future research. In summary, photopolymerization is a promising method of generating in a single reaction step a photopolymer film with chemical concentration gradient through the film resulting in control over the surface properties.

Notes

1. Kato, K., et al., Progress in Polymer Science (2003) 28, 209
2. Denes, F. S., and Manolache, S., Progress in Polymer Science (2004) 29, 815
3. Li, X., et al., Langmuir (2012) 29 (4), 1122
4. Straub, M., et al., Optical Materials (2004) 27 (3), 359
5. White, T. J., et al., Macromolecules (2007) 40 (4), 1121
6. White, T. J., et al., Polymer (2007) 48 (20), 5979
7. White, T. J., et al., Polymer (2006) 47 (7), 2289
8. Penterman, R., et al., Nature (2002) 417 (6884), 55
9. Vorflusev, V., and Kumar, S., Science (1999) 283 (5409), 1903
10. Cook, C. J., and Guymon, C. A., Photo-enforced stratification of polymeric materials. The University of Iowa Research Foundation, USA, (2011)
11. van Oosten, C. L., et al., Macromolecules (2008) 41 (22), 8592
12. Bunning, T. J., et al., Annual Review of Materials Science (2000) 30 (1), 83
13. Gleeson, M. R., and Sheridan, J. T., Journal of Optics A: Pure and Applied Optics (2009) 11, 024008
14. Sheridan, J. T., et al., Journal of Optics A: Pure and Applied Optics (2006) 8 (3), 236
15. Barachevskii, V. A., High Energy Chem (2006) 40 (3), 131
16. Lee, S.-H., et al., Journal of Optics (2011) 13 (5), 055403
17. Maruo, S., et al., Opt. Lett. (1997) 22 (2), 132
18. Sullivan, A. C., et al., Appl. Opt. (2007) 46 (3), 295
19. Smith, D. M., et al., Journal of Polymer Science Part B: Polymer Physics (2014) 52 (3), 232
20. Sutherland, R. L., et al., Chemistry of Materials (1993) 5 (10), 1533
21. Zhang, J., and Sponsler, M. B., Journal of the American Chemical Society (1992) 114 (4), 1506
22. Odian, G., Principles of Polymerization. 4 ed.; John Wiley & Sons: Hoboken, New Jersey, 2004
23. Brandrup, J., et al., Polymer Handbook. Fourth ed.; John Wiley & Sons, Hoboken, NJ, (1999)

24. Rosen, S. L., *Fundamental Principles of Polymeric Materials*. Second ed.; John Wiley & Sons, Inc.: New York, New York, 1993
25. Stevens, M. P., *Polymer Chemistry: An Introduction*. Third ed.; Oxford University Press: New York, New York, 1999
26. Allcock, H. R., et al., *Contemporary Polymer Chemistry*. Third ed.; Pearson Education, Inc.: Upper Saddle River, New Jersey, 2003
27. Brown, W. H., and Foote, C. S., *Organic Chemistry*. 2nd ed.; Fort Worth: Saunders College Pub: 1998
28. Kenning, N. S., et al., *Polymer International* (2008) 57 (10), 1134
29. Padon, K. S., and Scranton, A. B., *J. Polym. Sci. A Polym. Chem.* (2000) 38 (11), 2057
30. Ikemura, K., and Endo, T., *Dental Materials Journal* (2010) 29 (5), 481
31. Fouassier, J.-P., *Photoinitiation, Photopolymerization, and Photocuring*. Ludwig Auer GmbH, Donauwörth: Munchen, Germany, 1995
32. Goodner, M. D., and Bowman, C. N., *Modeling and Experimental Investigation of Light Intensity and Initiator Effects on Solvent-Free Photopolymerizations*. In *Solvent-Free Polymerizations and Processes*, 713 SV - 713 DO - doi:10.1021/bk-1998-0713.ch014 ed.; American Chemical Society(1999), pp 220
33. O'Brien, A. K., and Bowman, C. N., *Macromolecules* (2003) 36 (20), 7777
34. Qie, L., and Dubé, M. A., *European Polymer Journal* (2010) 46 (6), 1225
35. Goodner, M. D., and Bowman, C. N., *Macromolecules* (1999) 32 (20), 6552
36. Goodner, M. D., and Bowman, C. N., *Chemical Engineering Science* (2002) 57 (5), 887
37. Goodner, M. D., et al., *Industrial & Engineering Chemistry Research* (1997) 36 (4), 1247
38. Hoyle, C. E., and Bowman, C. N., *Angew. Chem.-Int. Edit.* (2010) 49 (9), 1540
39. Hoyle, C. E., et al., *Chem. Soc. Rev.* (2010) 39 (4), 1355
40. Hoyle, C. E., et al., *J. Polym. Sci. A Polym. Chem.* (2004) 42 (21), 5301
41. Cramer, N. B., et al., *Macromolecules* (2002) 35 (14), 5361
42. Carioscia, J. A., et al., *Dental Materials* (2005) 21 (12), 1137
43. Owusu-Adom, K., et al., *Macromolecules* (2009) 42 (9), 3275
44. Wei, H., et al., *Macromolecules* (2007) 40 (24), 8788
45. Cramer, N. B., et al., *J. Polym. Sci. A Polym. Chem.* (2004) 42 (7), 1752
46. Kim, S. K., and Guymon, C. A., *J. Polym. Sci. A Polym. Chem.* (2011) 49 (2), 465

47. Lee, T. Y., et al., *Macromolecules* (2007) 40 (5), 1466
48. Chan, J. W., et al., *Chemistry of Materials* (2009) 21 (8), 1579
49. Decker, C., and Jenkins, A. D., *Macromolecules* (1985) 18 (6), 1241
50. Cramer, N. B., and Bowman, C. N., *J. Polym. Sci. A Polym. Chem.* (2001) 39 (19), 3311
51. O'Brien, A. K., et al., *J. Polym. Sci. A Polym. Chem.* (2006) 44 (6), 2007
52. Reddy, S. K., et al., *Australian Journal of Chemistry* (2006) 59 (8), 586
53. Lu, H., et al., *Dental Materials* (2005) 21 (12), 1129
54. Tummers, P. H. G., et al., *Vibrational Spectroscopy* (2007) 43 (1), 116
55. Staudinger, H., and Schneiders, J., *Ann. Chim.* (1939) 541 (151)
56. Skeist, I., *Journal of the American Chemical Society*
J. Am. Chem. Soc. (1946) 68 (9), 1781
57. Lovestead, T. M., et al., *Journal of Photochemistry and Photobiology A: Chemistry* (2003) 159 (2), 135
58. Elliott, J. E., et al., *Dental Materials* (2001) 17 (3), 221
59. Berchtold, K. A., et al., *Macromolecules* (2005) 38 (16), 6954
60. Andrzejewska, E., *Progress in Polymer Science* (2001) 26 (4), 605
61. Anseth, K. S., et al., *Macromol. Chem. Phys.* (1996) 197 (3), 833
62. Jansen, J. F. G. A., et al., *Macromolecules* (2003) 36 (11), 3861
63. Jansen, J. F. G. A., et al., *Macromolecules* (2004) 37 (6), 2275
64. Hinkelmann, F., et al., *Macromol. Rapid Commun.* (2008) 29 (9), 695
65. Gou, L., et al., *Recent Research Developments in Polymer Science* (2004), 125
66. Gou, L., et al., *Photochemistry and UV Curing: New Trends* (2006), 301
67. O'Brien, A. K., and Bowman, C. N., *Macromolecules* (2006) 39 (7), 2501
68. O'Brien, A. K., and Bowman, C. N., *Macromol. Theory Simul.* (2006) 15 (2), 176
69. Herlihy, S., *RadTech Europe 99 Conference Proceedings*, 8-10 November 1999 (1999), 489
70. Kloosterboer, J. G., et al., *Polym Mat: Sci Eng Proc ACS Div Polym Mater: Sci Eng* (1989) 60, 122
71. Lee, T. Y., et al., *Polymer* (2004) 45 (18), 6155

72. Corrales, T., et al., *J. Photochem. Photobiol. A-Chem.* (2003) 159 (2), 103
73. Leewis, C. M., et al., *Journal of Applied Physics* (2004) 95 (12), 8352
74. Leewis, C. M., et al., *Journal of Applied Physics* (2004) 95 (8), 4125
75. Leewis, C. M., et al., *Journal of Applied Physics* (2004) 95 (8), 4125
76. Leewis, C. M., et al., *Journal of Chemical Physics* (2004) 120 (4), 1820
77. Leewis, C. M., et al., *Nuclear Instruments and Methods in Physics Research Section B: Beam Interactions with Materials and Atoms 7th International Conference on Nuclear Microprobe Technology and Applications* (2001) 181 (1-4), 367
78. Leewis, C. M., et al., *Nuclear Instruments and Methods in Physics Research Section B: Beam Interactions with Materials and Atoms* (2000) 161-163, 651
79. van der Zande, B. M. I., et al., *Journal of Applied Physics* (2005) 97 (12), 123519
80. van Nostrum, C. F., et al., *Chemistry of Materials* (1998) 10 (1), 135
81. Crank, J., *The Mathematics of Diffusion*. Oxford University Press: New York, 1975
82. Wavhal, D. S., and Fisher, E. R., *Langmuir* (2002) 19 (1), 79
83. Statz, A. R., et al., *Journal of the American Chemical Society* (2005) 127 (22), 7972
84. Huang, J., et al., *Biomacromolecules* (2007) 8 (5), 1396
85. Cen, L., et al., *Langmuir* (2003) 19 (24), 10295
86. Zhang, W., et al., *Biomaterials* (2006) 27 (1), 44
87. Noeske, M., et al., *International Journal of Adhesion and Adhesives* (2004) 24 (2), 171
88. Liston, E. M., et al., *Journal of Adhesion Science and Technology* (1993) 7 (10), 1091
89. Sangermano, M., et al., *Polymer* (2009) 50 (24), 5647
90. Nowicki, M., et al., *Polymer* (2003) 44 (21), 6599
91. Okouchi, M., et al., *Macromolecules* (2006) 39 (3), 1156
92. Goddard, J. M., and Hotchkiss, J. H., *Progress in Polymer Science* (2007) 32 (7), 698
93. Ma, Z., et al., *Colloids and Surfaces B: Biointerfaces* (2007) 60 (2), 137
94. Walheim, S., et al., *Macromolecules* (1997) 30 (17), 4995
95. Chen, J., and Gardella, J. A., *Macromolecules* (1998) 31 (26), 9328
96. Ikejima, T., and Inoue, Y., *Macromol. Chem. Phys.* (2000) 201 (14), 1598

97. Le Minez, J.-J., and Schmitt, B., Wet-on-wet coating process. Peintures Corona S.A., United States, (1983)
98. Chen, W., and McCarthy, T. J., *Macromolecules* (1997) 30 (1), 78
99. Kubota, H., *J. Appl. Polym. Sci.* (1992) 46 (3), 383
100. Pan, B., et al., *J. Polym. Sci. A Polym. Chem.* (2004) 42 (8), 1953
101. Zhu, J., et al., *Macromol. Chem. Phys.* (2006) 207 (1), 75
102. Inagaki, N., et al., *Journal of Polymer Science Part B: Polymer Physics* (2004) 42 (20), 3727
103. Vesel, A., et al., *Surface and Interface Analysis* (2008) 40 (11), 1444
104. Alvarez-Blanco, S., et al., *Polym Bull* (2001) 47, 329
105. Chan, C.-M., et al., *Surface Science Reports* (1996) 24, 1

CHAPTER 2 OBJECTIVES

Utilizing the inherent spatial and temporal control of photopolymerization to produce a compositional gradient through the depth of a polymer film is a promising method to control polymeric surface chemistry and properties. In turn, single step control of the surface properties allows for novel property development in numerous applications that are not accessible through traditional production methods utilized to control the surface chemistry. This study employs co-photopolymerization of formulations containing monomers with kinetic differences and a light gradient to produce polymers with a compositional gradient where the preferentially reacting monomer is enriched in the high light intensity regions of the polymer. While other work has illustrated the ability for photopolymerization to control the local polymer composition, an in-depth study of the impact of monomer kinetics and processing conditions is needed to control this promising process. Characterization of key formulations and processing parameters for the production of a polymer with a compositional gradient from photopolymerization will not only elucidate the relationship between polymerization kinetics and diffusion, but will also serve to demonstrate the degree of control over the surface chemistry and properties that are attainable with photo-enforced stratification.

The overall goal of this work is to develop photocurable coatings that will stratify yielding controllable surface chemistry and properties. Specifically, non-uniform polymerization will be realized by inducing a light gradient through the polymerizing film via photoinitiator light absorption and sufficient loading of the photoinitiator. A co-photopolymerization of monomers of unequal reactivity can then be used to facilitate stratification through the depth of the film as a result of the differences in polymerization rate. The preferentially reacting monomer will add to the growing polymer at an increased rate compared to the other monomer(s) in the co-photopolymer. Additionally, the high light intensity regions at the surface of the film will polymerize at a greater rate

than in the bulk of the film. The combination of non-uniform polymerization and unequal monomer reactivity forms a concentration gradient resulting in the preferentially reacting monomer diffusing from the bulk to the surface of the film and equimolar counter-diffusion of the other monomer from the surface to the bulk of the film. The diffusion and counter-diffusion during the polymerization results in the formation of a chemical composition gradient through the depth of the film where the concentration of the preferentially reacting monomer is enriched at the surface of the polymer film. To attain the overall goal of producing films which stratify upon photopolymerization, the objectives of this work include:

1. Utilize the inherent temporal and spatial control of photopolymerization in conjunction with monomer kinetic differences, arising from differences in the number of reactive groups, in the pre-polymer formulation to produce films with a compositional gradient affording control and modulation of the surface chemistry and properties.
2. Generate a mathematical model from the first principles of diffusion and photopolymerization kinetics to describe the production of films with a compositional gradient created via photo-enforced stratification.
3. Investigate other kinetic differences within Norrish type one photoinitiated radical chain growth photopolymerization and combination of multiple kinetic differences in the same pre-polymer formulation producing large monomer surface enrichments and strong compositional gradients in the polymer.
4. Examine alternative reaction mechanisms to radical chain photopolymerization for producing a stratified polymer via photopolymerization as well as probe changes in bulk properties as a result of stratification.

The first objective (Chapter 4) introduces the concept of utilizing the temporal and spatial control of photopolymerization to produce a polymer film with a compositional gradient through the depth of the film via photo-enforced stratification. It is demonstrated that the combination of a preferentially reacting monomer (di-ene vs. mono-ene) and a reaction gradient yields enrichment of the preferentially reacting monomer in the high light intensity regions of the film. The amount of monomer enrichment achieved from various processing techniques are tested and illustrate that production of stratified films requires a balance of kinetic differences being present while still allowing sufficient time for monomer diffusion to create a stratified film. Additionally, the surface energy and surface hardness are shown to vary with the amount of monomer enrichment.

Completion of the second objective (Chapter 5) has demonstrated that production of a stratified film via photopolymerization can be successfully modeled as a reaction-diffusion model from first principles. The reaction component of the model is based on kinetics of photopolymerization while the diffusion component is based on Fick's second law of diffusion. The produced model is shown to accurately describe the production of a stratified film from photopolymerization.

The third objective (Chapter 6) explores other kinetic differences within Norrish type one photoinitiated radical chain growth photopolymerization to produce a film with a composition gradient. Specifically, inherent differences in monomer reactivity between methacrylate and acrylates were shown to be a sufficient kinetic difference for stratification. Additionally, combinations of kinetic differences, such as inherent monomer reactivity and oxygen inhibition, result in increasing the enrichment of the preferentially reacting monomer in the high light intensity regions of the film.

Finally, the fourth objective (Chapter 7) briefly explores various aspects of photopolymer films with a compositional gradient. Specifically, bulk properties are shown to have only small variations with the degree of stratification. Stratified films were

produced which illustrated different adhesive properties on the top and bottom of the film. Additionally, polymer surface composition is determined using x-ray photoelectron spectroscopy. Norrish type two photoinitiation and thiol-ene chemistry are shown to be additional reaction mechanisms capable of producing a stratified film.

Through the completion of the above objectives, a greater understanding of inducing compositional gradients with photopolymerization has been achieved. This understanding will allow for production of stratified polymer films with controllable surface chemistry and properties, allowing novel property development not possible with tradition methods for surface chemistry and property control. Characterization of stratified films has identified the key components and processing conditions that will lead to the successful production and eventual industrial use of stratified photopolymers. Overall, the demonstration of control of the surface chemistry and properties with photopolymerization has provided a basis for future work and advancements in producing polymer films with independent control over the localized composition.

CHAPTER 3 MATERIALS AND METHODS

This chapter will briefly outline some common materials and materials from the research chapters. Specifically, the chemicals used in these studies, the photopolymerization procedure used to produce polymer samples, and methods to determine local polymer composition at the surface of the produced polymer films will be covered in this chapter. Infrared spectroscopy was the primary method utilized to analyze the surface composition of polymer films warranting the increased level of detail on the technique described in this chapter.

Chemicals

The chemicals utilized for these studies were primarily monomers and photoinitiators. Monomers utilized include 1,6-hexanediol dimethacrylate (HDDMA), 2-hydroxyethyl methacrylate (HEMA), 2-hydroxyethyl acrylate (HEA), 2-methoxyethyl acrylate (MOA), 2-(dimethylamino)ethyl acrylate (DMAEA), 2-(dimethylamino)ethyl methacrylate (DMAEMA), 2-methoxyethyl methacrylate (MOMA), N-hydroxyethyl acrylamide (HEAA), methyl methacrylate (MMA), trimethylolpropane diallyl ether, tri(ethylene glycol) divinyl ether, and trimethylolpropane tris(2-mercaptoacetate) (see Chapters 4 – 7 for chemical structures). 2,2-dimethoxy-2-phenylacetophenone (DMPA) and 2,4,6-trimethylbenzoyl-diphenyl-phosphineoxide (TPO) were the photoinitiators utilized for these studies (see Chapters 4 – 7 for chemical structures). The monomers were purchased from Sigma-Aldrich and the photoinitiators were provided by CIBA. All chemicals were used as received without further purification.

Monomers were chosen for these studies primarily based on differences in reactivity in order to allow for the production of a stratified film via photopolymerization. Additionally, the monomers required sufficient chemical structural differences so that the chemical composition could be determined spectroscopically. Finally, the molecular weight of the monomers was kept low to minimize diffusional limitations. The primary

photoinitiator used in these studies was 2,2-dimethoxy-2-phenylacetophenone because it is an efficient, non-photobleaching photoinitiator. 2,4,6-trimethylbenzoyl-diphenyl-phosphineoxide was also used to study a photobleaching photoinitiator.

Photopolymerization Procedure

Photopolymerization was utilized to produce polymer films to test if a chemical composition gradient was produced. Films were produced as either a drawn film or in a laminate mold. The thickness of the film was controlled by either the height of the drawdown bar or the thickness of the spacers used in the laminate mold. Polymerization was initiated with UV light filtered to 365 nm. The light was filtered in order to better characterize and calculate the light gradient through the film. Glass microscope slides treated with Rain-X were used in the laminate systems. In general, drawn films were polymerized under an inert atmosphere and the laminate films were polymerized in the atmosphere as oxygen inhibition is not a concern in a laminate mold.

Surface Chemical Analysis via Attenuated Total

Reflectance – Fourier Transform Infrared Spectroscopy

The primary method utilized to analyze the surface of the polymer films was attenuated total reflectance – Fourier transform infrared spectroscopy (ATR) which facilitates the determination of the near surface region IR spectra of the polymer films. ATR works by passing the IR beam through an ATR crystal which has a high index of refraction.¹ The IR beam enters the crystal at an angle and is internally reflected through the ATR crystal (Figure 1). At each bounce point of the IR beam within the crystal a small evanescent wave leaves the ATR crystal. The evanescent wave can interact with matter directly adjacent to the ATR crystal. If the material is IR active² then some of the evanescent wave will be absorbed. As with other IR techniques, the functional groups

present in the material absorb IR light which is then detected.³ As such, the concentration of functional groups present in the material adjacent to the ATR crystal can be determined. The penetration depth of the evanescent wave is determined by:⁴

$$d_p = \frac{\lambda}{2\pi n_1 \sqrt{(\sin^2 \theta - (n_2/n_1)^2)}} \quad (1)$$

where d_p is the penetration depth, λ is the wavelength of light, n_1 is the refractive index of the ATR crystal, n_2 is the refractive index of the matter directly adjacent to the ATR crystal (polymer for these studies), and θ is the angle of incidence of the IR beam. Examination of equation 1 illustrates that the IR spectrum obtained from ATR is indeed sampling the near surface region of the polymer film. The penetration depth is wavelength and polymer sample dependent but is on the order of approximately one micrometer for the equipment used in this research.

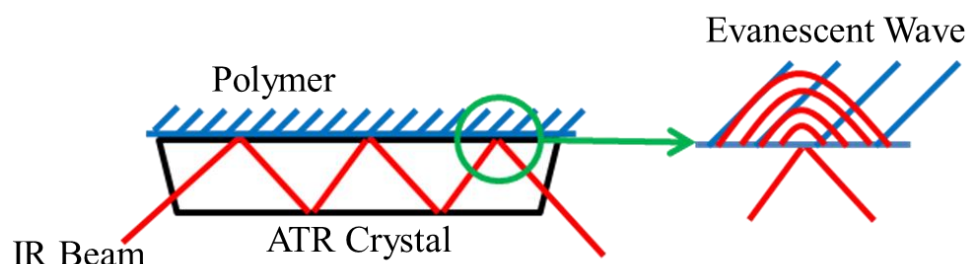


Figure 3.1. Experimental diagram of attenuated total reflectance – Fourier transform infrared spectroscopy.

Specifically, a polymer sample is placed on top of the ATR crystal. Pressure is then applied to the polymer sample via accessory plunger to increase contact with the ATR crystal. Polymer samples do not have to cover the entire ATR crystal and in most cases covering the entire ATR crystal results in poor spectra with absorbance values

outside of the linear regime of the Beer Lambert Law. It is most important to have the polymer sample in contact with the crystal at the location of the first few bounce points. The peak height ratios of the resulting IR spectra were used to quantify the chemical composition of the sample. Specifically, the peak height ratio was determined by dividing the peak height that corresponds to a unique functional group from one monomer in the co-polymerization by the height of a peak that corresponds to either a unique functional group on the other monomer in the co-polymerization or a common functional group to both monomers in the co-polymerization. Peak heights were determined using Omnic. For example, in the mono- and di-ene monomer system the peak height at 3510 cm^{-1} (hydroxyl OH) was divided by the peak height at 1720 cm^{-1} (carbonyl OH). Therefore, the identity of the enriched monomer can be determined from the change in the peak height ratio. The peak heights ratios were further used to determine the surface and homogeneous composition of the polymer films.

If a stratified film is produced, the surface composition will be different from the other side of the polymer film and will differ from the homogenous composition. Stratification of the polymers produced via laminate mold was determined via ATR of the bottom of the polymer film as well. Drawn films required a comparison of the surface composition to the homogenous composition. The homogeneous composition was examined using transmission IR of the polymerized formulation between salt plates. Deviation of the surface composition from either the bottom or homogenous composition indicates surface enrichment of a monomer and illustrates that photopolymerization resulted in films with a chemical concentration gradient.

Notes

1. McQuillan, A. J., *Adv. Mater.* (2001) **13** (12-13), 1034
2. Atkins, P., and De Paula, J., *Atkins' Physical Chemistry*. 8th ed.; W. H. Freeman and Company: New York, NY, 2006
3. Brown, W. H., and Foote, C. S., *Organic Chemistry*. 2nd ed.; Fort Worth: Saunders College Pub: 1998
4. Elabd, Y. A., *et al.*, *Journal of Polymer Science Part B: Polymer Physics* (2003) **41** (22), 2794

CHAPTER 4 COMPOSITIONAL GRADIENTS IN PHOTOPOLYMERS UTILIZING MONO- AND DIMETHACRYLATES

Abstract

The ability to control and modulate polymeric surface properties independently from the bulk polymeric properties allows for the generation of materials that can be tuned for specific applications. Currently, there are methods for generating polymers with different surface and bulk properties but most of these methods require multiple processing steps or are limited to certain chemistries to produce the desired film thus limiting the scope of application. Photopolymerization and different monomer reactivity should allow for the generation of polymer films with controllable surface chemistry and thus surface properties in a single reaction step. In this study, a co-photopolymerization of 1,6-hexanediol dimethacrylate (HDDMA) and 2-hydroxyethyl methacrylate (HEMA) occurs in the presence of a light gradient generated from the photoinitiator which creates a reaction gradient through the depth of the film producing films exhibiting HDDMA surface enrichment ranging from approximately 15 to 20 percent. The effects of rate of reaction and light gradient strength on stratification are examined by varying light intensity and film thickness illustrating a negative and positive effect on the stratification obtained, respectively. Polymeric surface properties of water contact angle and hardness are examined with respect to stratification. HDDMA surface enrichment allowed for an increase in the water contact of approximately 5 degrees and resulted in a harder surface. These results illustrate that a co-photopolymerization of monomers with different reactivities is a robust procedure for producing stratified films and achieving properties not accessible with homogenous polymers.

Introduction

The ability to control surface and bulk chemistry in polymer films could provide significant advantages for many applications including antifouling systems,^{1,2} antimicrobial films,³⁻⁵ and adhesives.^{6,7} Different surface chemistry could allow tailoring of numerous surface properties including hardness,^{8,9} contact angle,¹⁰ adhesion,^{6,7} and biological response¹¹⁻¹³ thereby allowing for advanced applications not accessible with homogenous polymers. Currently, polymeric materials with different surface and bulk properties are generally obtained by multiple step processes, including changing or modifying the substrate,¹⁴ precipitation of one component during polymerization,¹⁴⁻¹⁶ casting multiple films,^{17,18} surface grafting,¹⁹⁻²¹ or plasma modification.^{22,23} Although each of these methods allows control of surface chemistry of the polymer film; these methods require additional production time, are not well controlled, and/or deleteriously affect final film properties.

The temporal and spatial control inherent to photopolymerization has been utilized to control the localized polymer composition to produce holographic polymer dispersed liquid crystals²⁴⁻²⁶ (HPDLC), flexible liquid crystal displays^{27,28} (LCD), and holographic gratings.²⁹ For example, HPDLCs²⁴⁻²⁶ are created by initiating polymerization of a pre-polymer formulation containing monomer and an unreactive liquid crystal using interference patterns from multiple laser sources. The interference creates alternating regions of high and low light intensity. Thereby, the reacting monomer is polymerized more quickly in the high intensity regions. Monomer depletion from reaction in these regions results in a concentration gradient, leading to diffusion of monomer from the dark regions and a counter-diffusion of the liquid crystal molecules to the dark regions. Thus, this process generates alternating polymer rich and liquid crystal rich regions for potential use in dynamic light gratings.

Similarly, a process to obtain flexible polymer encapsulated liquid crystal for LCDs utilizing similar principles has been reported.^{27,28} In this case, a chromophore is

added to produce a gradient of the initiating light through the film. The illuminated side of the film is exposed to the highest light intensity with the light attenuating through the film. Because the rate of radical photopolymerization with bimolecular termination is proportional to the square root of the light intensity, the high light intensity surface of the film exhibits higher rates of reaction than the rest of the film. As with HPDLCs, the reactive monomer is polymerized at greater rates with higher light intensity inducing diffusion of the reacting monomer to the surface of the film, with the non-reactive liquid crystal counter-diffusing to the opposite surface thereby producing polymer encapsulated LCDs.

These systems utilize the spatial control of photopolymerization to separate a reactive monomer from a non-reactive liquid crystal molecule. Similar techniques may also be useful to create differences in composition using different reactive monomers. Materials have been produced in which preferentially reacting monomer diffuses to areas with higher light intensity with counter-diffusion of the lower reactivity species.³⁰ Holographic gratings²⁹ and stimuli responsive polymers³⁰ have been produced in this manner with the preferentially reacting monomer in the copolymerization being enriched in the high light intensity regions. Additionally thin films with compositional gradients could be produced utilizing similar techniques and principles. One such kinetic driving force that has been utilized to create films with a composition gradient is the inherent difference in polymerization rate between a mono-ene and a di-ene³⁰. The di-ene reacts about ten times faster than an analogous mono-ene³¹ which allows the di-ene to diffuse to regions with higher light intensity.

At the surface of the film, where the light intensity is the greatest, the preferentially reacting monomer should add to the growing network at a greater rate than in the bulk of the film, which results in a concentration gradient through the depth of the film. Consequently, the preferentially reacting monomer diffuses from the bulk to the surface of the film and the other monomer counter-diffuses from the surface to the bulk

of the film. The resulting film could thereby exhibit an enriched surface concentration of the preferentially monomer. The aim of this study is to control the surface chemistry of a polymer film utilizing the inherent spatial and temporal control of photopolymerization. For this work the pre-polymer formulation consists of monomers with different inherent reactivity and sufficient photoinitiator to create a light gradient through the polymerizing film. Specifically, formulations containing a 1:1 molar ratio of 1,6-hexanediol dimethacrylate to 2-hydroxyethyl methacrylate with varying concentrations of the photoinitiator, 2,2-dimethoxy-2-phenylacetophenone, were utilized to study the if the difference in reaction rate between di- and mono-enes could be utilized to produce a stratified film. To determine if stratification occurs, the chemical composition of the top and bottom of the film is calculated from data obtained with attenuated total reflectance – Fourier transform infrared spectroscopy (ATR-FTIR). The possible impact of the light gradient and the time allowed for monomer diffusion on the stratification is examined through various processing techniques including varying the film thickness, changing the initiating light intensity, and utilizing pulsed illumination. In addition, the potential influence of stratification on the surface properties of contact angle and hardness will be examined. These investigations illustrate a straightforward, single-step method to produce films with differing chemistries and properties between the surface and bulk, which could lead to numerous applications.

Experimental

Materials

Monomers used for these studies include 1,6-hexanediol dimethacrylate (HDDMA, Sigma-Aldrich) and 2-hydroxyethyl methacrylate (HEMA, Sigma-Aldrich). Systems were photoinitiated with 2,2-dimethoxy-2-phenylacetophenone (DMPA, BASF, see Figure 1 for chemical structures). Monomers and photoinitiator were used as received

without further purification. The photoinitiator is also utilized as the chromophore for the formulations.

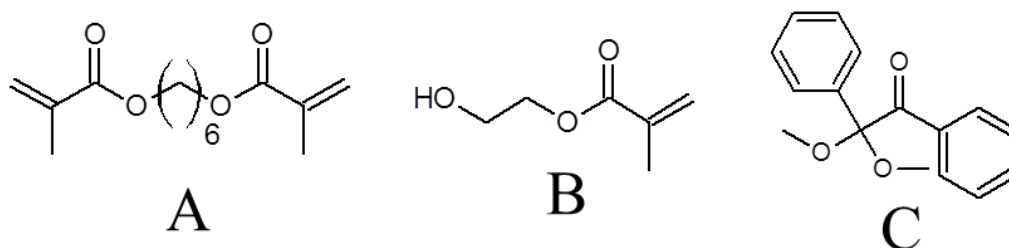


Figure 4.1. Chemical structures of (A) 1,6-hexanediol dimethacrylate, (B) 2-hydroxyethyl methacrylate, and (C) 2,2-dimethoxy-2-phenylacetophenone.

Sample Preparation

Polymerization was initiated in a laminate mold, consisting of two glass slides separated by spacers between 150 and 600 micrometers thick. The laminate mold allows production of polymer films for which both the top and bottom of the film can be chemically analyzed. Unless otherwise stated, the polymer films were 300 micrometers thick and were polymerized with an OmniCure Series 1500 lamp with a collimating lens and 365 nm filter adjusted to a light intensity of 1 mW/cm².

Attenuated Total Reflectance – Fourier Transform Infrared

Spectroscopy

Chemical composition of the polymer surface was analyzed using a Thermo Fisher Nexus 670 Fourier Transform Infrared Spectrometer (FTIR) with a Horizontal Attenuated Total Reflector (ATR) attachment containing a ZeSn crystal with a 45° angle of incidence. The ATR attachment allows for the collection of an IR surface spectrum of

both sides of the film (Figure 2). The ratio of hydroxyl (OH) and the carbonyl (CO) peak height at approximately 3510 cm^{-1} and 1720 cm^{-1} , respectively was calculated. The ratio from the high light intensity side is divided by the low light intensity side to allow direct comparison between samples.

Kinetic Analysis

Real time kinetic evaluation of the polymerization was conducted with FTIR and photo-differential scanning calorimetry (photo-DSC). The polymerization was initiated using an Efos Acticure lamp with a 365 nm band pass filter. The ene peak at approximately 810 cm^{-1} was monitored to track the conversion of the reaction. Additionally, photo-DSC was utilized to further examine to monitor real time reaction kinetics by monitoring the heat released by polymerization from an approximate 3 mg sample. Polymerization was initiated with a medium pressure Hg vapor lamp.

Contact Angle

An approximately 200 micrometer coating of reactive mixture was drawn on an untreated glass slide and then polymerized under an inert atmosphere until a tack free surface was achieved. Contact angle of water was measured with a goniometer (ramehart, inc. NRL C.A. Goniometer model number 100-00) using a light (ACE I light, Fostec Schott-Fostec, LLC) for contrast and an Eppendorf pump for water drop placement. At least three replicate measurements of advancing contact angle from three samples were taken for a minimum of nine measurements in total.

Pencil Hardness

Surface hardness was evaluated by pencil hardness testing in accordance to ASTM standards.³² Briefly, a pencil was used to scratch the surface of a cured polymer film. Testing began with a pencil assumed to be too soft to scratch the surface and the hardness was systematically increased until a visible scratch occurred on the polymer

film surface. The first pencil able to scratch the surface was the reported surface hardness value for the film tested.

Results and Discussion

Control of polymer surface properties by tuning the surface chemistry may be possible by exploiting the inherent spatial and temporal control of photopolymerization. Generation of such films has the potential to be achieved via co-photopolymerization of monomers with inherently different reaction rates. To facilitate stratification, the co-photopolymerization would occur in the presence of a light gradient resulting in a gradient in the rate of polymerization. Consequently, the preferentially reacting monomer in the co-photopolymerization would be depleted at the film surface faster than in the bulk. In this study, the large polymerization rate difference between a mono- and di-ene is explored as a possible method to create stratified films. When one double bond of a di-ene reacts during polymerization the un-reacted ene becomes a pendent ene species. Pendent enes are more likely to react due to their proximity to other radicals in the growing polymer network, resulting in di-enes polymerizing approximately ten times faster than the analogous mono-ene.³¹ The disparity in consumption creates a concentration gradient, which results in possible diffusion of the preferentially reacting monomer to the surface of the film and a counter-diffusion of the other monomer to the bulk. With sufficient diffusion and counter-diffusion it may be possible to generate a polymer exhibiting a composition gradient as a function of depth with the preferentially reacting monomer enriched at the surface of the film. Therefore, a co-photopolymerization of a mono-ene with a di-ene could result in an enrichment of di-ene at the surface of the polymerized film.

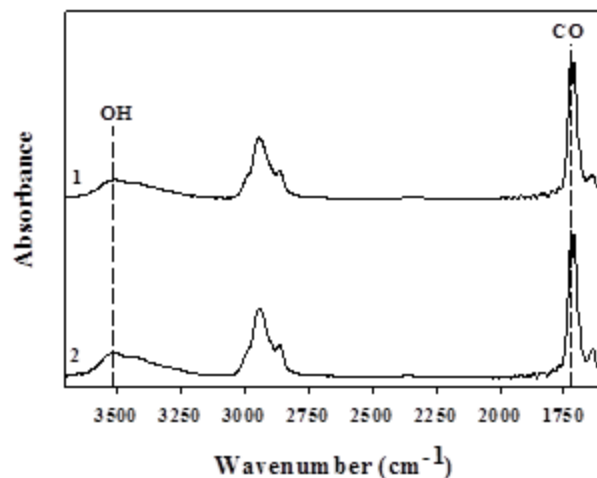


Figure 4.2. Examples of a typical spectra collected using ATR-FTIR. The hydroxyl peak and carbonyl peak are labeled at approximately 3510 and 1720 wavenumbers respectively for the spectrum of the 1) top and (2) bottom of the film.

As a means of testing the capability to produce a stratified film employing the kinetic difference between mono- and di-enes, polymer films were produced with an equimolar ratio of di-ene (HDDMA) to mono-ene (HEMA) with varying concentrations of photoinitiator/chromophore (DMPA) to vary the overall light gradient and rate. The monomers were selected because of their low molecular weight, minimizing diffusion limitations. Additionally, the hydroxyl group of HEMA allows for differentiation of the monomers via infrared spectroscopy. Polymerized films were analyzed with ATR-FTIR to determine the surface composition. This was determined by taking the ratio of the hydroxyl (from HEMA) to carbonyl peak height ratio (from both monomers) from the high light intensity side divided by the hydroxyl to carbonyl peak height ratio from the low light intensity side (Figure 4.2). Composition ratios of unity indicate that both sides of the film have the same chemical composition. Ratios above and below unity indicate mono-ene and di-ene enrichment, respectively, on the high light intensity side of the film. The composition ratios are then plotted as a function of weight percent DMPA (Figure 4.3). All formulations shown have composition ratios that are less than one indicating

that significant HDDMA surface enrichment is observed and a stratified film has been produced. The lowest concentration of photoinitiator results in the largest deviation from one with a composition ratio of approximately 0.8, indicating approximately 20 percent enrichment of HDDMA at the surface of the polymer. As the photoinitiator concentration is increased, the amount of stratification systematically decreases with the highest DMPA concentration yielding an approximate composition ratio of 0.85 or about 15 percent surface enrichment of HDDMA. This enrichment of HDDMA illustrates that the reactivity difference between HEMA and HDDMA is sufficient to generate stratification.

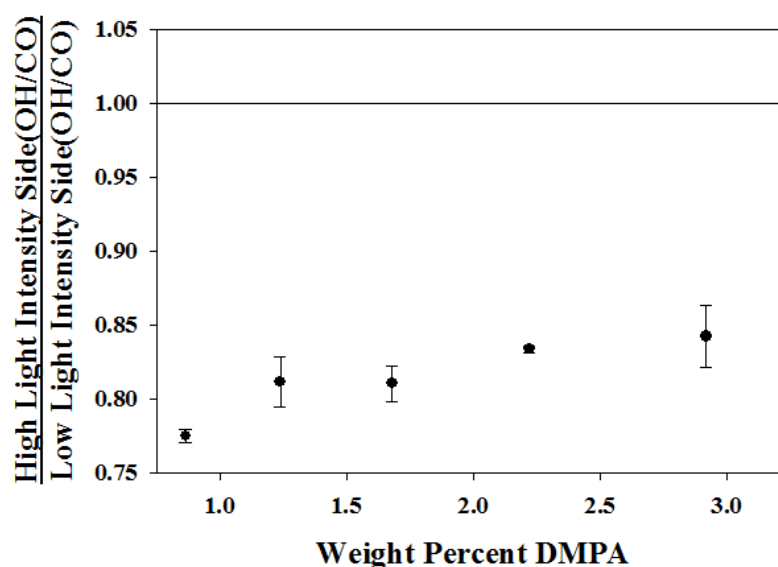


Figure 4.3. Composition ratio of polymers produced as a function of photoinitiator concentrations using a 1:1 molar ratio of HEMA to HDDMA formulation. Composition ratios normalized to the composition ratio of a low light attenuation film. Films were polymerized in a 300 μm laminate mold with 365 nm light at 1 mW/cm^2 . Composition ratios were determined via ATR-FTIR. Error bars represent the standard deviation of a minimum of three replicate measurements.

Increasing the DMPA concentration slightly decreases the composition ratio and overall stratification. Higher concentrations of DMPA increase the gradient which should enhance the concentration gradient. At the same time, increasing the concentration of DMPA also increases the rate of polymerization which may limit the diffusion time. To understand the balance between diffusion time and the magnitude of the light gradient, the fractional attenuation, or the fraction of light that is throughout the sample, was calculated via the Beer Lambert Law. The calculated intensity using the film surface opposite the UV lamp is used to determine the fractional transmission or the fraction of the initial light intensity at the bottom of the film. Fractional attenuation, or the fraction of light absorbed by the film, is equal to one minus the fractional transmission. Additionally, the reaction of double bonds during polymerization of these formulations was evaluated with FTIR. The derivative of the resulting conversion profile of these formulations yields the rate of polymerization. The time required to reach the maximum rate of polymerization was determined as a relative measure of the time monomers have for diffusion. While the rates of reaction and diffusion are not equivalent, the faster the reaction rates will lead to faster vitrification and thus less time for monomer diffusion that leads to stratification. The impact of DMPA concentration on the light gradient and reaction rate was examined by plotting the time to reach the maximum rate of polymerization versus the fractional attenuation (Figure 4.4). As the attenuation increase with increased photoinitiation, the time to reach the maximum rate of polymerization decreases significantly as would be expected. For example, the 0.9 wt% DMPA sample, corresponding to a fractional attenuation of 0.3, requires 0.86 minutes to achieve the maximum rate of polymerization, whereas the 3 wt% DMPA sample (fractional attenuation of 0.7) requires almost half that time to reach the maximum rate of polymerization. The more significant light gradient results in a much greater polymerization rate decreases as a function of depth as leading to larger differences in monomer consumption. In absence of diffusional limitations, this should lead to greater

monomer diffusion and stratification. However, increases in polymerization rate with photoinitiator concentration decreases the amount of time before the system vitrifies, resulting in less time for monomer diffusion. Since the diffusion time of monomers is reduced, the composition gradient of the final material is also reduced leading to decreased stratification with increasing DMPA concentration.

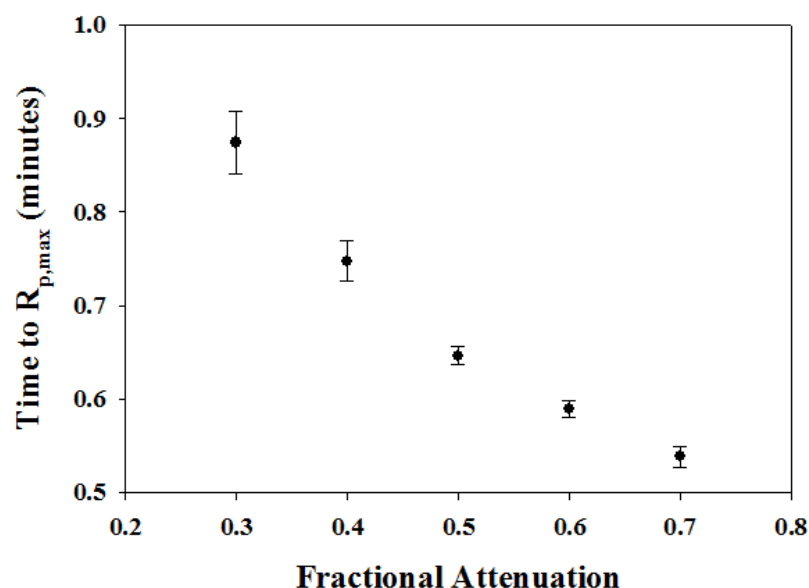


Figure 4.4. Correlation between fractional attenuation based on photoinitiator concentration and time to reach the maximum rate of polymerization. The fractional attenuation was calculated from the Beer Lambert Law, and the time to reach the maximum rate of polymerization determined from rates measured with real time FTIR.

An alternative method that increases the light attenuation through the sample is to vary the film thickness while holding the concentration of DMPA constant. The same concentration of DMPA produces a relatively constant maximum rate of polymerization at the film surface but will increase overall light absorption as the film thickness increases. Therefore, to determine the effect of film thickness on stratification with the composition ratio was determined via ATR-FTIR as a function of film thickness (Figure

4.5A). Increasing the light gradient with increasing film thickness results in increased degrees of stratification. For instance, the 150 micron film showed the lowest degree of stratification with a composition ratio of approximately 0.8. Greater stratification is obtained with a 600 micrometer film, resulting in a composition ratio of approximately 0.75. While this change in thickness results in only about a 5 percent increase in HDDA at the surface, these results indicate an increase in light gradient does result in greater stratification if the light gradient does not reduce the time to vitrification resulting in monomer diffusional limitations.

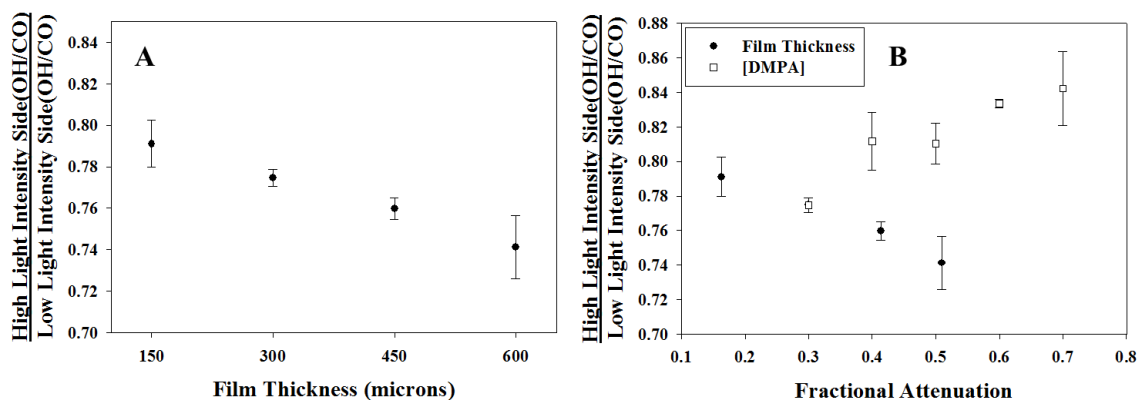


Figure 4.5. Examination of light attenuation effects on photo-enforced stratification. A) Variation of normalized polymer composition ratio as a function of film thickness. B) Comparison of normalized composition ratio when film thickness (●) and DMPA concentration (□) is varied. The Beer Lambert Law is used to determine the fractional attenuation of light through the film in both cases. Films were polymerized in a laminate mold with 365 nm light at 1 mW/cm². Composition ratios were determined via ATR-FTIR. Error bars represent the standard deviation of a minimum of three replicate measurements.

Plotting the composition ratio as a function of fractional attenuation allows direct comparison of the effects of changing film thickness and DMPA concentration (Figure 4.5B). As noted earlier, increasing the attenuation with the photoinitiator results in a

gradual, steady increase in the composition ratio and thus a decrease of stratification. In contrast, increasing the fractional attenuation by increasing the film thickness leads to gradual decrease in the composition ratio and thus increased stratification. For thicknesses with half the light reaching the bottom surface a composition ratio of approximately 0.75 is observed. The stratification for the thickness sample with a 0.5 fractional attenuation is more than 30 percent that observed for the same of that fractional attenuation films from DMPA concentration.

To further examine the role of increased rates of polymerization associated with increased DMPA concentration the rate of polymerization and light gradient was modified with initiating light intensity. Polymers polymerized with a constant DMPA concentration and various light intensities allow for a constant fractional attenuation while allowing for control in the rate of polymerization permitting examination of the rate of polymerization independently from the light gradient. Films were polymerized at various light intensities and the composition ratio was determined as a function of light intensity (Figure 4.6A). Films polymerized with 1 mW/cm^2 showed the highest degree of stratification with a composition ratio of less than 0.8 and also exhibit the highest degree of control over the stratification, as evident by the small error bars. While small decreases in stratification are observed upon increasing the light intensity to 9 mW/cm^2 these changes are quite small and not significantly different. A critical rate of polymerization appears to be between 9 and 12 mW/cm^2 , where the observed stratification is greatly reduced as indicated by a composition ratio increase to above 0.9. Further increases in light intensity have little further effect on the stratification. Additionally, films produced near this critical rate of polymerization exhibited less control over the stratification, resulting in larger variation. By increasing the light intensity, higher polymerization rates are achieved. This increase in rate lowers the diffusion time of monomers reducing the degree of stratification achieved.

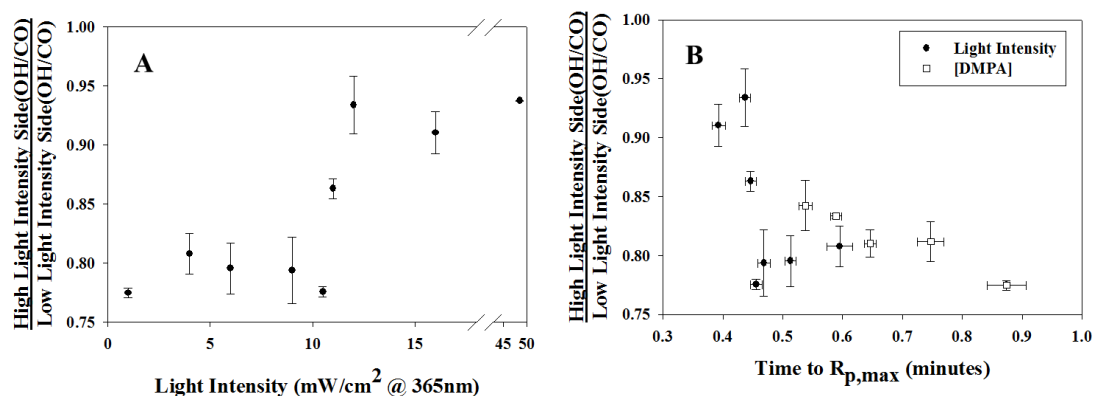


Figure 4.6. Examination of polymerization rate effects on photo-enforced stratification. A) Normalized composition ratio as a function of the light intensity used to polymerize the film. B) Normalized composition ratio achieved by varying the light intensity (●) and varying the concentration of DMPA (□) as a function of time to reach the maximum polymerization rate. Real time FTIR spectroscopy was used to determine the time to reach the maximum rate of polymerization in both cases. Films were polymerized in a 300 micron laminate mold with 365 nm light. Error bars represent the standard deviation of a minimum of three replicate measurements.

A direct comparison between the stratification obtained from changing the rate of polymerization with light intensity versus the concentration of DMPA can be made by examining reaction rate for both systems. To this end, real time kinetic evaluation of the polymerization with increasing light intensity was conducted using real time FTIR. The composition ratios from the light intensity study and the DMPA concentration study were plotted as a function of time to reach the maximum rate of polymerization (Figure 4.6B). With both initiator concentration and light intensity, the longest times to reach the maximum rate of polymerization result in the greatest stratification. On the other hand, when the time to reach the maximum rate of polymerization is lower, less stratification is observed. The sample prepared with increasing initiation concentration never polymerized fast enough to experience the drastic reduction in stratification observed with changes in light intensity. Thus a substantial loss of stratification appears to occur when the maximum rate of polymerization occurs before 0.5 minutes. The correlation

between increasing the polymerization rate with DMPA and light intensity illustrates stratification is achieved with a balance between sufficient driving force for diffusion produced through the light gradient and the time for diffusion. Without sufficient diffusion time, significantly lower degrees of stratification are reached.

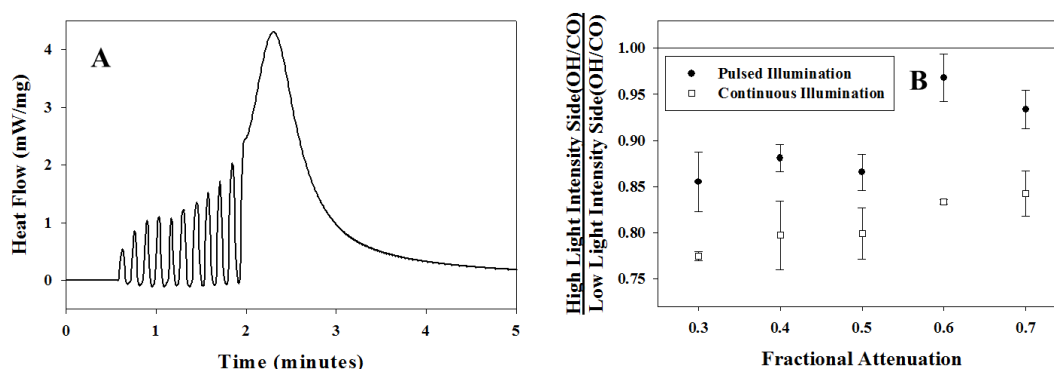


Figure 4.7. Effect of pulsed illumination on stratification. A) Representative photo-DSC trace of pulsed illumination with three seconds of illumination and five seconds with the shutter closed per cycle, 10 times. Post cycling, the light is left on to complete the cure. B) Normalized composition ratio for pulsed (●) and constant (□) illumination as a function of the fractional attenuation of light. Films were polymerized in a 300 μm laminate mold with 365 nm light at 1 mW/cm^2 . Composition ratios were determined via ATR-FTIR. Error bars represent the standard deviation of a minimum of three replicate measurements.

The effect of monomer diffusion can be further examined by utilizing pulsed illumination in which the sample is exposed to light at regular intervals. Shuttering the light stops initiation and allows diffusion to occur in the absence of extensive polymerization. The polymerization rate is tracked readily measuring heat flow using a photo-DSC (Figure 4.7A). Samples were cycled through illumination periods of three seconds and dark periods of five seconds. At the start of illumination a rapid rise is observed in the heat flow which sharply drops as soon as the light is shuttered. After ten pulse cycles, the polymer is then fully cured under constant illumination and analyzed

with ATR-FTIR. The composition ratio for the pulsed and normal illumination studies were plotted as a function of fractional attenuation (Figure 4.7B). Interestingly, the pulsed illumination samples result in an approximate ten percent reduction in the composition ratio or more than a 30 percent decrease in the degree of stratification compared to the continual illumination analogs. Pulsed illumination would affect the monomer diffusion in two ways. During dark periods diffusion occurs in the absence of additional initiation, thereby allowing for free diffusion of monomer without differential consumption and decreasing monomer concentration gradient. Second, pulsed illumination allows for a longer total time for monomer diffusion to occur before vitrification occurs. With the additional time for monomer diffusion in the absence of the reaction a more homogenous final film is produced.

If stratified films are produced, the final film surface properties should change accordingly. Generation of inhomogeneous stratified films should lead to unique and controllable surface property development. To this end, surface properties have been evaluated to examine the effect of stratification. Water contact angle is an effective method to measure differences in surface energy and composition. Increasing the concentration of HDDMA should make the film surface more hydrophobic resulting in higher contact angles whereas lower degrees of stratification indicates that hydrophilic hydroxyl groups from HEMA are more prevalent at the surface resulting in lower contact angle. Films drawn on glass slides and polymerized under nitrogen were used for measurements. The contact angle was plotted as a function of attenuation as shown in Figure 4.8. The solid line represents the contact angle for a low light gradient film used as the control. The low light gradient film exhibits a contact angle of approximately 64 degrees. The film with the highest degree of stratification at more than 20 percent enrichment of HDDMA (Figure 4.3), exhibits a significantly higher contact angle of approximately 69 degrees. Films produced from higher DMPA concentrations that correspond to lower degrees of stratification result in lower contact angle as would be

expected with a lower surface concentration of HDDMA that approaches the angles for the control film. These results verify that HDDMA is enriched at the surface and illustrates that stratification allows control over the surface chemistry.

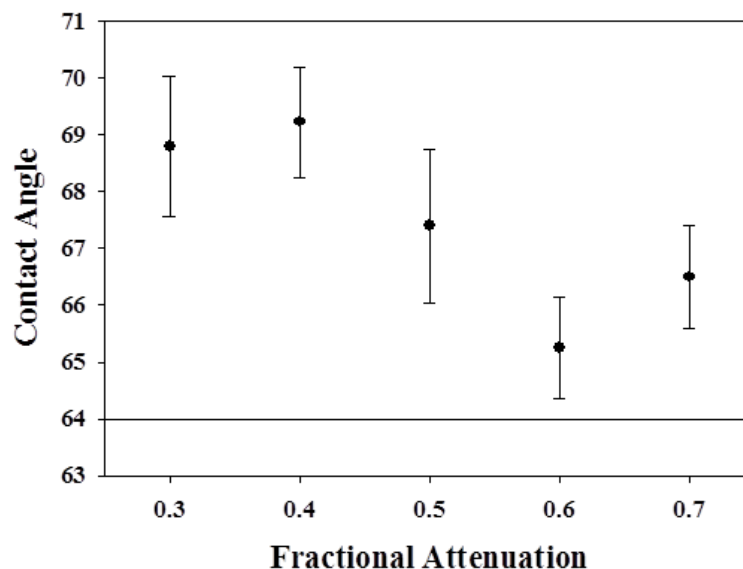


Figure 4.8. Water contact angle as a function of DMPA concentration. Approximately 200 μm thick films were polymerized on a glass slide in an inert atmosphere with 365 nm light at 1 mW/cm^2 . Error bars represent the standard deviation of a minimum three measurements from at least three samples.

The surface hardness should also vary constantly with the surface composition. Pencil hardness³² was tested to evaluate any changes in chemistry (Table 2.1). Surface enrichment of HDDMA and thus higher cross-link density should result in a film with a harder surface. The low light gradient film with minimal stratification exhibits a scratch pencil hardness value of 2H. The stratified samples produced with photoinitiator of 0.86 and 2.9 weight percent DMPA had scratch pencil hardness values of 4H and 3H, respectively indicating a significantly harder surface. The highest degree of HDDMA enrichment, according the ATR-FTIR analysis, was the same 0.86 weight percent DMPA films which requires the hardest pencils to scratch the surface. The 2.9 weight percent

DMPA films exhibited HDDMA enrichment as well, yielding an intermediate hardness value. The modulation of hardness and the correlation with the ATR-FTIR surface analysis illustrate the ability to control surface properties with stratification in a single reaction step.

Table 4.1. Scratch pencil hardness values for the films.

Formula Fractional Attenuation	% HDDMA Enrichment	Pencil Hardness
~0	0	2H
0.7	16	3H
0.3	23	4H

Note: Approximately 200 μm thick films were polymerized on a glass slide in an inert atmosphere with 365 nm light at 1 mW/cm^2 .

Conclusions

This research illustrates that co-photopolymerization in the presence of a light gradient utilizing monomers of different reactivity can be used to produce a composition gradient with controllable surface chemistry. Specifically, reactivity differences between mono- and di-enes were examined via co-photopolymerization of HEMA and HDDMA with sufficient photoinitiator to create a light gradient through the depth of the film. The increased reaction rate of HDDMA allows HDDMA enrichment at the surface of the film. Production of a stratified film requires a light gradient with sufficient time for monomer diffusion. Increasing the light gradient using thicker films results increased enrichment of HDDMA. Conversely, time for monomer diffusion is inversely related to stratification. Polymerizing films with increasing light intensity and faster polymerization

rates results in less stratification. Significant stratification is only achieved when sufficient diffusion of monomer occurs during polymerization in the presence of a light gradient. If pulsed illumination is used which allows more time for monomer diffusion, but in the absence of reaction, then a significant a decrease in stratification is observed. Stratified films with HDDMA enriched surfaces results in the water contact angle being reduced as much as 5 degrees while the pencil hardness increases. The ability to control the surface properties independent from the bulk properties in a polymer film in a single reaction step is highly valuable as it allows for the production of polymeric materials with novel properties not accessible with homogenous polymers. Additionally, the stratification method presented has the potential to be applied to numerous co-photopolymerization formulations increasing the utility of the process.

Notes

1. Wavhal, D. S., and Fisher, E. R., *Langmuir* (2002) **19** (1), 79
2. Statz, A. R., *et al.*, *Journal of the American Chemical Society* (2005) **127** (22), 7972
3. Huang, J., *et al.*, *Biomacromolecules* (2007) **8** (5), 1396
4. Cen, L., *et al.*, *Langmuir* (2003) **19** (24), 10295
5. Zhang, W., *et al.*, *Biomaterials* (2006) **27** (1), 44
6. Noeske, M., *et al.*, *International Journal of Adhesion and Adhesives* (2004) **24** (2), 171
7. Liston, E. M., *et al.*, *Journal of Adhesion Science and Technology* (1993) **7** (10), 1091
8. Sangermano, M., *et al.*, *Polymer* (2009) **50** (24), 5647
9. Nowicki, M., *et al.*, *Polymer* (2003) **44** (21), 6599
10. Okouchi, M., *et al.*, *Macromolecules* (2006) **39** (3), 1156
11. Goddard, J. M., and Hotchkiss, J. H., *Progress in Polymer Science* (2007) **32** (7), 698
12. Ma, Z., *et al.*, *Colloids and Surfaces B: Biointerfaces* (2007) **60** (2), 137
13. Clapper, J. D., *et al.*, *Biomacromolecules* (2008) **9** (4), 1188
14. Walheim, S., *et al.*, *Macromolecules* (1997) **30** (17), 4995
15. Chen, J., and Gardella, J. A., *Macromolecules* (1998) **31** (26), 9328
16. Ikejima, T., and Inoue, Y., *Macromol. Chem. Phys.* (2000) **201** (14), 1598
17. Le Minez, J.-J., and Schmitt, B., Wet-on-wet coating process. Peintures Corona S.A., United States, (1983)
18. Chen, W., and McCarthy, T. J., *Macromolecules* (1997) **30** (1), 78
19. Kubota, H., *J. Appl. Polym. Sci.* (1992) **46** (3), 383
20. Pan, B., *et al.*, *J. Polym. Sci. A Polym. Chem.* (2004) **42** (8), 1953
21. Zhu, J., *et al.*, *Macromol. Chem. Phys.* (2006) **207** (1), 75
22. Inagaki, N., *et al.*, *Journal of Polymer Science Part B: Polymer Physics* (2004) **42** (20), 3727
23. Vesel, A., *et al.*, *Surface and Interface Analysis* (2008) **40** (11), 1444
24. White, T. J., *et al.*, *Macromolecules* (2007) **40** (4), 1121

25. White, T. J., *et al.*, *Polymer* (2007) **48** (20), 5979
26. White, T. J., *et al.*, *Polymer* (2006) **47** (7), 2289
27. Penterman, R., *et al.*, *Nature* (2002) **417** (6884), 55
28. Vorflusev, V., and Kumar, S., *Science* (1999) **283** (5409), 1903
29. Tomlinson, W. J., *et al.*, *Appl. Opt.* (1976) **15** (2), 534
30. van Oosten, C. L., *et al.*, *Macromolecules* (2008) **41** (22), 8592
31. Andrzejewska, E., *Progress in Polymer Science* (2001) **26** (4), 605
32. Standard, A., ASTM Standard D3363. In *Standard Test Method for Film Hardness by Pencil Test*, ASTM International, West Conshohocken, PA, (2005 (2011))

CHAPTER 5 PHOTOPOLYMERIZATION REACTION-DIFFUSION
MODEL DESCRIBING INDUCED CHEMICAL COMPOSITION
GRADIENT

Abstract

Understanding the production of polymer films with a chemical concentration gradient would be greatly enhanced via the development of a reaction and diffusion model. Herein, a model is developed from first principles of kinetics and diffusion to help describe and predict the production of a chemical concentration gradient through a polymer film from co-photopolymerization. Specifically, the co-photopolymerization of a 1:1 molar ratio of 1,6-hexanediol dimethacrylate (HDDMA) to 2-hydroxyethyl methacrylate (HEMA) in the presence of a light gradient is modeled by solving coupled differential equations for the kinetics with those for diffusion using a modified Euler method. The model qualitatively predicts a gradient in the rate of polymerization as a result of the light gradient. Consequently, the reaction gradient and the difference in rate of polymerization between HDDMA and HEMA results in a concentration gradient being predicted from an initially homogenous pre-polymer film. The coupling of Fick's second law of diffusion results in successfully modeling equimolar counter-diffusion of monomers and predicts a polymer film with approximately 10 percent surface enrichment of the faster reacting monomer, HDDMA. The presented model adequately describes the production of a chemical gradient in a photopolymer film from co-photopolymerization of monomers with different polymerization rates in the presence of a light gradient.

Introduction

Photopolymerization is inherently environmentally friendly because of the relatively low energy input required compared to other polymerization techniques and because the pre-polymer formulations require little to no volatile organic compounds as solvents.¹ Additionally, photopolymerizations are very rapid reactions allowing for high throughput. The benefits associated with photopolymerization have lent themselves to numerous applications including hydrogels,²⁻⁴ drug/protein delivery systems,⁵⁻⁸ molecular imprinted polymers,⁹⁻¹¹ and biomaterials.¹²⁻¹⁵

With its inherent temporal and spatial control, photopolymerization can control the localized composition. Materials produced with this degree of control via photopolymerization include holographic polymer dispersed liquid crystals¹⁶⁻¹⁸ (HPDLC), flexible liquid crystal displays^{19,20} (LCD), stimuli responsive polymers,²¹ and holographic gratings.^{22,23} These systems take advantage of the spatial control of photopolymerization to create areas of high reactivity with light, which in turn allows for the enrichment of desired species in the high light intensity regions. Utilizing similar principles, photopolymer films have been produced with a compositional gradient yielding controllable surface chemistries and properties (Chapter 4). Such films were produced from a co-photopolymerization of monomer with different reactivity, mono- and di-ene monomers, in the presence of a light gradient. Moreover, the preferentially reacting monomer is enriched in the higher light intensity regions of the film.

Models have been developed to help describe and predict the production materials with localized concentration control such as the production of LCD^{24,25} and holographic gratings.^{23,26,27} Models specific to the production of stratified films from a co-photopolymerization of mono- and di-ene monomers are lacking. A general model for producing a stratified film would incorporate equations from principles of the kinetics and diffusion. Many other models for radical photopolymerization exist which describe and predicted aspects of the reaction such as reaction kinetics,^{28,29} monomer diffusion,³⁰

oxygen inhibition,^{31,32} radical termination,³³ thermal effects³⁴ and even thiol-ene polymerization.^{35,36}

As stated previously, the production of a stratified film can be modeled based on photopolymerization kinetics and diffusion first principles. Specifically, the copolymerization of monomers of unequal reactivity, such as mono- and di-ene monomers, in the presence of a light gradient can be modeled. Herein, a model predicting photo-enforced stratification is described. Light gradients results in decreasing the rate of initiation through the film thus the rate of polymerization also changes with the higher rates of polymerization occurring in the high light intensity regions at the surface of the film. The increased rates of polymerization lead to quicker monomer consumption in these regions. Additionally, the formulations have monomers of unequal reactivity which when coupled with the non-uniform monomer consumption leads to different gradients in monomer concentration. Specifically, the di-ene reacts at a greater rate than the mono-ene producing the concentration gradient (Chapter 4). The ability for the model to predict the non-uniformity in polymerization rate and monomer consumption is examined. Successful prediction of this behavior allows for the modeling of equimolar counter diffusion of monomer in the system utilizing Fick's second law of diffusion. Monomer diffusion and counter-diffusion affords the ability to model the change in film composition and thus predicts the production of a polymer film with a compositional gradient where the faster reacting di-ene monomer is enriched in the high light intensity regions of the film. The presented model is the ground work for a model with could be used to predict and/or optimize the production of a composition gradient in polymer films. This level of predictive power would assist in the ability to scale up the production of stratified films to the industrial level.

Model Development

The development of stratification during photopolymerization was modeled using the kinetic equations describing photopolymerization and Fick's second law of diffusion. Moreover, the modeled system is a co-polymerization of mono- and di-ene polymerized in the presence of a light gradient. The classical radical reactions of initiation (Equations 1 and 2), propagation (Equation 3), and termination (Equations 4 and 5) are shown below as shown below:³⁰

Initiation



Propagation



Termination



Initiation for a Norrish Type I photoinitiator occurs when the photoinitiator (PI) absorbs light ($h\nu$) which results in the cleavage of the photoinitiator to generate radicals (R^*) (Equation 1). The radical reacts with a monomer (M), either a mono-ene or a di-ene

monomer, to form a monomer radical and the start of a polymer chain (P_1^*) and the reaction rate is dictated by the rate coefficient, k_i (Equation 2). Propagation is the reaction of a growing polymer radical with another monomer resulting in increasing the chain length of the polymer and with the radical propagating across a double bond. The rate of propagation is dictated by the rate coefficient (k_p) (Equation 3). Termination results in the loss of radicals and occurs when radicals react in either electron-electron coupling (Equation 4) or hydrogen atom abstraction (Equation 5). For this, the rate of termination is modeled to be only dependent upon radical concentration thus allowing for Equations 4 and 5 to be combined into a single equation governed by a single kinetic coefficient, k_t .

To model the generation of stratified films, the light gradient generated from the absorption of light from the photoinitiator needs to be estimated which results in the rate of initiation varying as a function of depth.³⁰

$$R_i = \frac{\epsilon I [PI]}{E} \quad (6)$$

$$E' = N_a h \nu \quad (7)$$

$$I = I_0 10^{(-\epsilon z [PI])} \quad (8)$$

As a result, the rate of initiation (R_i , Equation 6), which is normalized to the energy per mole photons (E' , Equation 7), can be modified using the Beer-Lambert Law (Equation 8) to describe the light intensity (I) available for initiation where I_0 is the initial light intensity, ϵ is the molar absorptivity of the photoinitiator, $[PI]$ is the concentration of photoinitiator, N_a is Avogadro's number, h is Planck's constant, ν is the frequency of light, and z is the depth in the film being modeled. The rate of initiation, and in turn the rate of propagation, now varies as a function of depth in the polymer film allowing for differential monomer consumption resulting in monomer diffusion.

The use of di-enes and mono-enes in the formulations requires an additional step to model the propagation.³⁷



When one double bond of di-ene (Di) reacts with any radical species (X^*) it forms another radical species and a pendent group (Pen) which is in close proximity to many propagating radical centers. This proximity results in increased reaction of the pendent group which is dictated by the kinetic coefficient k_{pen} (Equation 9).³⁸

Utilizing Equations 1 through 9 allows for the modeling of the photopolymerization reactions as well as the generation of a concentration gradient with depth inducing monomer diffusion.

$$\frac{dC_i}{dt} = D_i \frac{d^2 C_i}{dz^2} \quad (10)$$

$$\frac{dC_i}{dz} = 0 \text{ at } z=0 \text{ and } z=z_{max} \quad (11)$$

Monomer diffusion was modeled using Fick's Second Law (Equation 10) where D_i is the diffusion coefficient and C_i is the concentration of species i . The diffusion and counter-diffusion was modeled using the boundary condition that monomers cannot diffuse across the boundary of the film (Equation 11).

$$\frac{dC_i}{dt} = D_i \frac{d^2 C_i}{dz^2} + R_i \quad (12)$$

Combining the diffusion and the reaction (R_i) allows for the determination of the mass balance for each species in the formulation (Equation 12).³⁰

Specifically, the mass balance equation was solved for all reactive species in the polymerizing system utilizing a modified Euler method. The initial concentrations of the reactive species are used to solve both the reaction and diffusion equations at all depths for the initial time step. Using the mass balance the resulting change in concentrations is determined. The new concentrations are used as the initial conditions for the next time step. This process continues for the desired length of illumination. These calculation loops are executed with MatLab resulting in matrices with concentrations and solutions to reaction, diffusion, and mass balance equations as a function of depth and time.

Other assumptions made in modeling the generation of stratified films from photopolymerization³⁰ include: 1) Photoinitiator cleavage produces two radicals of equal reactivity. 2) The initiating light source is monochromatic. 3) The kinetic reactions that describe photopolymerization are independent of polymer chain length. 4) All radicals in system were assumed equivalent reactivities. 5) Shrinkage is ignored allowing for the volume of each modeled layer, and thus the system, to remain constant. 6) Polymer chains and radical species do not undergo diffusion.³⁰ The constants used in the model equations are for a co-photopolymerization of 1,6-hexanediol dimethacrylate and 2-hydroxyethyl methacrylate using the photoinitiator 2,2-dimethoxy-2-phenylacetophenone (Table 1). Experimental results indicate this formulation will produce a stratified film upon photopolymerization (Chapter 4).

Table 5.1. List of parameters used to model photo-enforced stratification.

Parameter	Value	Units
Δt	0.01	s
Δz	0.0005	cm
$k_{p,mono-ene}$ ^{30,38} , $k_{p,di-ene}$ ^{28,30}	18	L/(mol s)
$k_{p,pendent}$ ³⁸	180	L/(mol s)
k_t ^{28,30}	415	L/(mol s)
ϵ ²⁸	150	L/(mol cm)
I_o	1	mW/cm ²
λ	365	nm
$D_{mono-ene}$ ^{28,39} , D_{di-ene} ^{28,39}	4.5 x 10 ⁻⁶	cm ² /s
$[ene]_o$ from mono-ene ²⁸	4.1	mol/L
$[ene]_o$ from di-ene	8.2	mol/L
$[pendent]_o$	0	mol/L
$[PI]_o$	0.04	mol/L

Results and Discussion

Photo-enforced stratification is dictated by reaction and diffusion processes. Models for both photopolymerization kinetics and diffusion have been developed that are directly applicable for photo-enforced stratification.^{33,37} Two criteria must be fulfilled for photo-enforced stratification to occur. First, a light gradient throughout the film must be established with sufficient loading of a chromophore (typically a photoinitiator). A light gradient results in a gradient in the rate of initiation and thus the rate of polymerization leading to a non-uniform consumption of monomer throughout the depth of the film. Second, monomers in the formulation must have different reactivity rates to promote concentration gradients that result in diffusion and counter-diffusion of the two monomer species with the preferentially reacting monomer diffusing to the surface of the film. By

combining and applying these elements in a model, photo-enforced stratification may be predicted. Explicitly, a co-photopolymerization of 1,6-hexanediol dimethacrylate (di-ene) and 2-hydroxyethyl methacrylate (mono-ene) using the photoinitiator 2,2-dimethoxy-2-phenylacetophenone will be modeled were experimental results with this formulation resulted in enrichment of the di-ene in the high light intensity regions of the film. The results of the model presented below explore various aspects regarding the production of a stratified film and all results are from the completed reaction-diffusion model.

As stated previously, the first step in producing a stratified film is establishing a light gradient through the film which can be calculated using the Beer-Lambert law. Figure 5.1 shows the light intensity as a function of depth through a 300 micrometer thick polymer film using a photoinitiator concentration of 0.04 M, an incident light intensity of 1 mW/cm^2 . The surface of the film (i.e. side closest to the initiating light source) has the full initiating light intensity of 1 mW/cm^2 . The light intensity available for photoinitiation through the film continues to decrease until reaching the side of the film, furthest from the initiating light source which under these conditions has approximately 65 percent of the initial light intensity available for initiation.

This light gradient results in decreasing rates of initiation, and thus a gradient in the rate of polymerization, through the depth of the film. Examination of the rate of polymerization through the film depth and time can be examined with great detail using a 3D contour map (Figure 5.2A). Specifically, the polymerization rate 3D contour map plots colors representing the rate of polymerization as a function of depth in micrometers (y axis) and illumination time in seconds (x axis). At a constant depth both autoacceleration and autodeceleration are observed as a function of illumination time. The rate of polymerization at a constant time while examining different depths illustrates a continuous decrease in the rate of polymerization with increasing film depth. The 3D contour map demonstrates the ability to track the photopolymerization and highlights differences in polymerization rate as a function of depth and time.

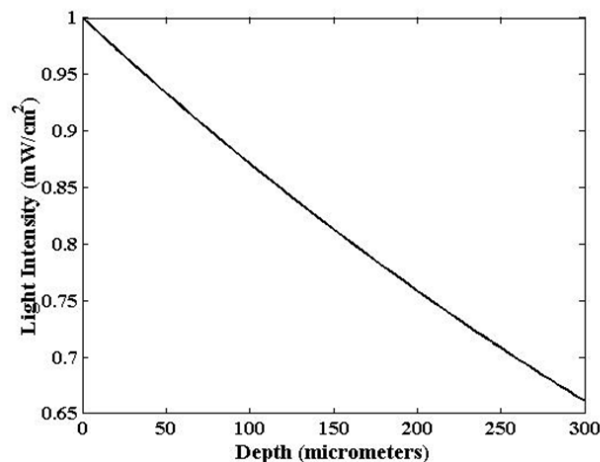


Figure 5.1. Calculated light intensity of 365 nm light as a function of depth through a 300 micrometer thick film with a photoinitiator concentration (DMPA) of 0.04 M, extinction coefficient of 150 L/(mol cm), and incident light intensity of 1 mW/cm².

The change in rate with depth can be further highlighted by examining the rate of polymerization (R_p) as a function of time at the surface (0 micrometers), midway (150 micrometers), and at the bottom (300 micrometers) of the film based on model predictions (Figure 5.2B). The rate of polymerization increases rapidly then decreases for all three film depths which is indicative of autoacceleration and autodeceleration, respectively. Decreasing light intensity with respect to film depth results in higher rates of polymerization at the surface of the film than in the bulk throughout the modeled illumination time. These differences in rates are most apparent in the maximum rates of polymerization, occurring after roughly 40 seconds of illumination, with a decrease in overall rate of almost 25 percent through the film.

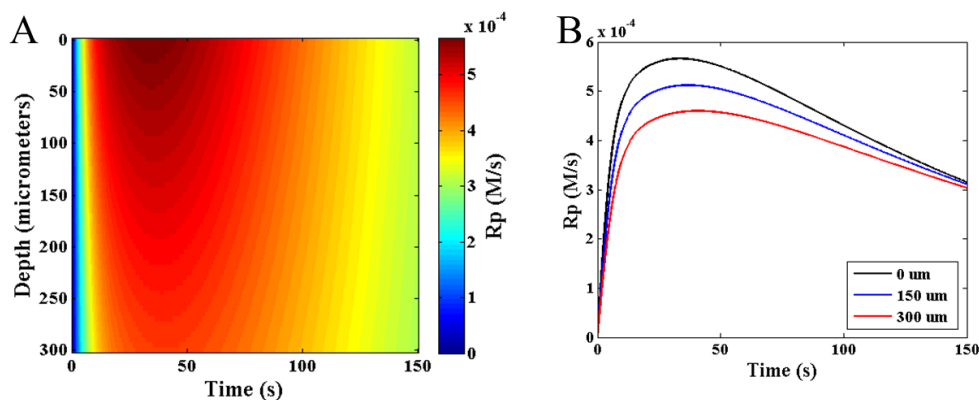


Figure 5.2. Modeled rate of polymerization (R_p) of a co-photopolymerization of a mixture of mono-ene and di-ene, with ene concentrations of 8.2 M and 16.4 M respectively (A) as both a function of depth and time and (B) at 0, 150, and 300 micrometers.

The observed gradient with depth in the rate of polymerization results in differential monomer consumption through the depth of the film. Examining the evolution of the concentration gradient with depth and time in a 3D contour map illustrates a smooth transition from homogenous concentration to gradients in concentration. Specifically, color represents the mono-ene (Figure 5.3A) and di-ene (Figure 5.3B) concentration as a function of depth in micrometers (y axis) and illumination time in seconds (x axis). At the start of the polymerization the mono-ene and di-ene have homogeneous concentration profiles. With increasing illumination time a monomer concentration gradient occurs with less monomer at the surface than in the bulk of the film. With continued illumination, the concentration gradient increases and persists throughout the modeled illumination time as illustrated by the increased difference between the film surface and bottom concentrations for both the mono- and di-ene. The

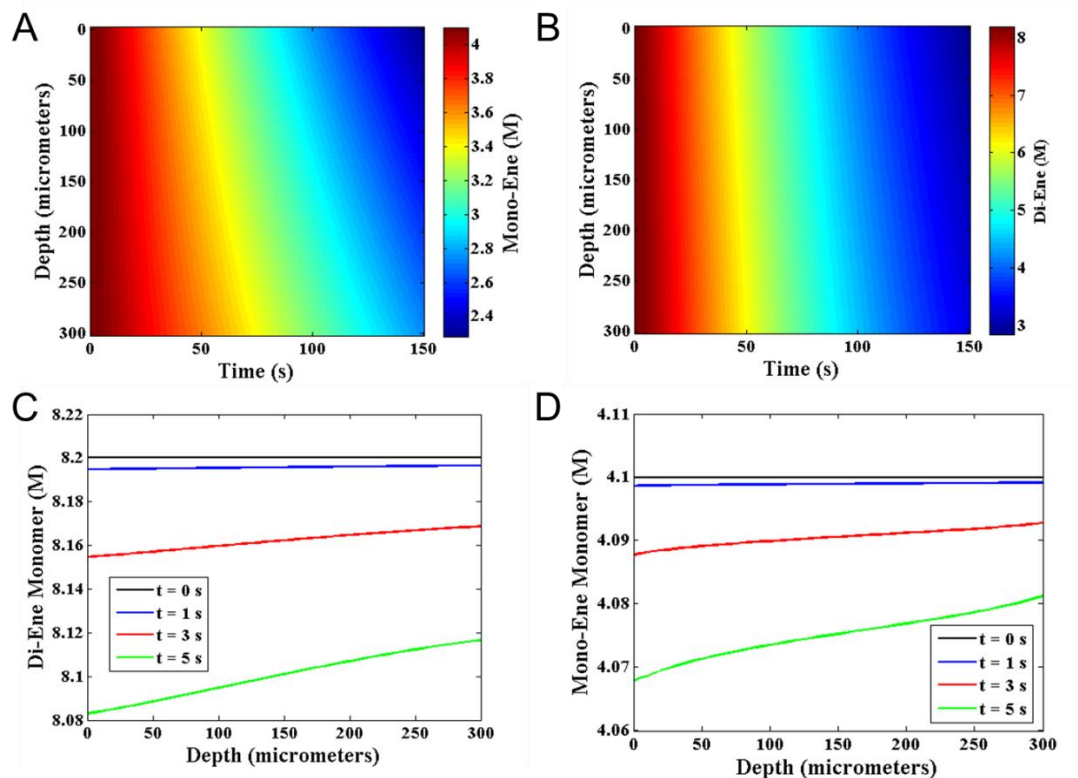


Figure 5.3. Monomer consumption during co-polymerization. (A) Mono-ene and (B) di-ene consumption in the polymer film as a function of depth and time. (C) Mono-ene and (D) di-ene consumption as a function of depth in the film at 0, 1, 3, and 5 seconds.

concentration gradients shown in the 3D contour maps are a direct result of the increased rates of polymerization observed in the higher light intensity regions of the modeled film. Increased polymerization rates result in increased monomer consumption and thus a gradient in polymerization rate results in a monomer concentration gradient.

The evolution of the concentration gradient can be highlighted by examining the concentration profiles at early stages of the polymerization. Figures 5.3C-D show the monomer concentration profile through the depth of the film for 0, 1, 3, and 5 seconds for the mono- (Figure 5.3C) and di-ene (Figure 5.3D). Initially, the mono and di-ene have a flat concentration profiles indicating a homogenous film. After 1 second of illumination a

very slight decrease in the concentration throughout the film depth is observed while still maintaining an approximately homogenous concentration profile for both the mono and di-ene monomers. After 3 seconds of illumination a noticeable concentration gradient is present in both monomers with an approximate percent difference between the top and bottom concentrations of 0.1 and 0.2 for the mono-ene and di-ene, respectively. As the illumination time increases to 5 seconds, the concentration gradient approximately doubles from the 3 second concentration gradient. Figure 5.3C-D clearly illustrates the generation of a concentration gradient from differential monomer consumption through the depth for both monomers from an initially homogenous pre-polymer film. These results indicate that the reaction-diffusion model does meet the first criteria for accurately describing photo-enforced stratification.

The second criterion for modeling photo-enforced stratification includes monomer diffusion in order to produce a chemical composition gradient. Monomers in the copolymerization have unequal rates of polymerization resulting in the di-ene having a larger gradient in concentration (Figure 5.3). Fick's second law of diffusion and equimolar counter-diffusion can be applied to the monomer concentration gradient predicted from the model to incorporate monomer diffusion. Thus, the diffusion can be examined throughout the film as a function of time and depth utilizing a 3D contour map (Figure 4A-B). Specifically, the rate of diffusion is plotted with colors as a function of depth (y axis) and time (x axis) for mono-ene (Figure 5.4A) and di-ene (Figure 5.4B) diffusion. At the start of illumination (time = 0 seconds) the rate of net diffusion is assumed to be zero since the film is homogenous. Continued illumination results in increasing the rate of diffusion followed by a decrease. The speed of this increase in the absolute rate of diffusion and the absolute magnitude in the rate achieved is maximized at the edges of the film and decreases approaching the center. The center of the film experiences zero net diffusion. Comparing the mono-ene and di-ene diffusion rate illustrates that equimolar counter-diffusion is observed at all points in the film at any time

during illumination as evident by colors corresponding to equal magnitude but opposite signs for the rate of diffusion.

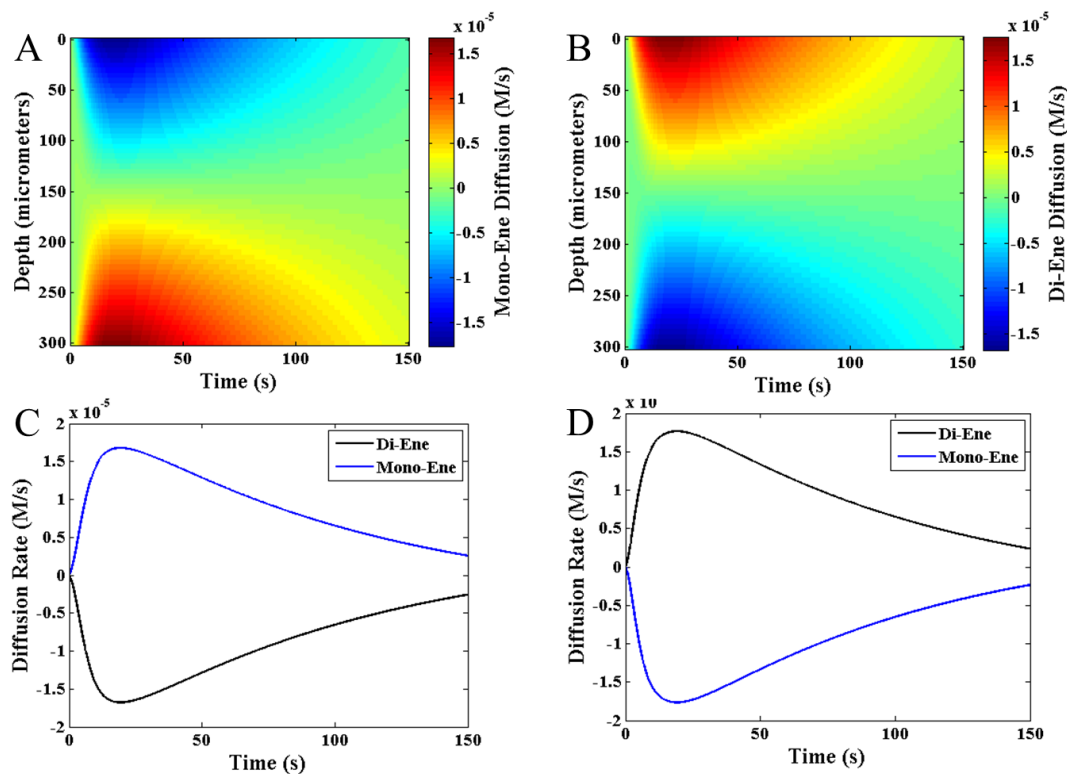


Figure 5.4. Monomer diffusion in the polymer film during co-polymerization. (A) Mono-ene and (B) di-ene rate of diffusion as a function of depth and time during co-polymerization. Rate of mono-ene and di-ene diffusion at the (C) surface and (D) bottom of the polymer film.

Equimolar counter-diffusion can be readily observed by examining the rate of diffusion as a function of time for the di-ene and mono-ene monomers at the surface (Figure 5.4C) and bottom (Figure 5.4D) of the film can be determined. Initially, at the surface the film is homogenous resulting in no net diffusion. Illumination results in monomer diffusion due to the generated a concentration gradient. Based on the model, the absolute rates of diffusion increase and then subsequently decrease and approach

zero. Increases in the absolute rates of diffusion are linked to autoacceleration rapidly generating a concentration gradient and decreases are a result of decreased mobile species available for diffusion. Rates of diffusion of the monomers are of equal magnitude and opposite sign indicating equimolar counter-diffusion. Additionally, the di-ene rate of diffusion has a positive sign which, when coupled with the equimolar counter-diffusion, results in surface enrichment of the di-ene monomer. Trends similar to those observed at the surface are also observed for the bottom of the film. Specifically, equimolar counter-diffusion is observed with a positive diffusion rate for the mono-ene indicating enrichment of mono-ene. Equimolar counter-diffusion at the surface and bottom of the film indicates conservation of mass as expected. Coupling equimolar counter-diffusion with the direction of diffusion (dictated by the sign associated with the rate of diffusion) results in an enrichment of di-ene monomer in the top half of the film and mono-ene enrichment in the bottom half of the film.

The model describing monomer diffusion behavior in the presence of reaction allows a foundation to predict photo-enforced stratification. The moles of mono-ene and di-ene as both monomer and polymer were calculated as a function of depth and time. The composition is examined using a species ratio calculated by dividing the moles of mono-ene and di-ene at a certain depth. The formulation starts as a 1 to 2 mole ratio of mono-ene to di-ene resulting in a composition ratio of 0.5. Increasing and decreasing the composition ratio indicates enrichment of mono-ene and di-ene species, respectively. Colors representing the species ratio are plotted as a function of depth (micrometers, y axis) and illumination time (seconds, x axis) to examine the modeled film composition (Figure 5.5A). Initially, the film is homogenous with a species ratio equaling 0.5. A species ratio of the final film is predicted at approximately 0.475 and 0.525 at the surface and bottom of the film, respectively, while the center of the film maintains the 0.5 species ratio. The modeled species ratios indicate surface enrichment of the di-ene species and

bottom enrichment of the mono-ene species; thus, predicting the production of a polymer film with a chemical composition gradient via photopolymerization.

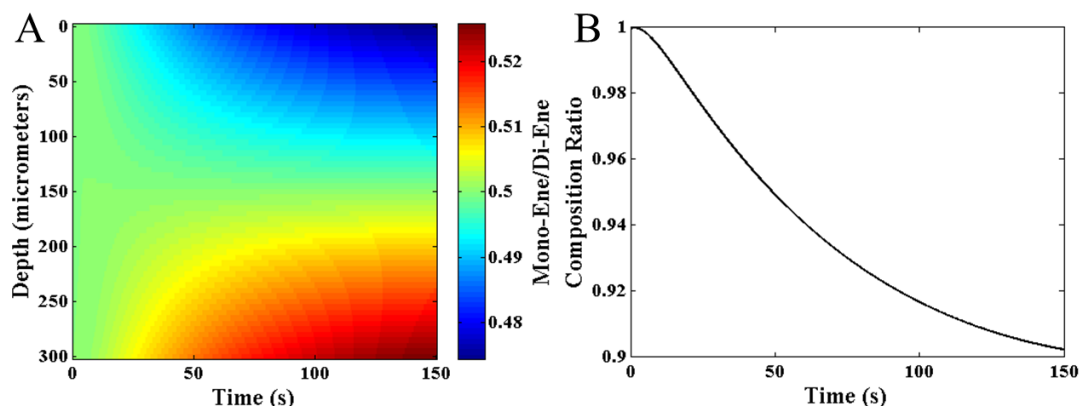


Figure 5.5. Polymer film composition as a function of time. (A) Evolution of composition ratio, top(mono-ene/di-ene)/bottom(mono-ene/di-ene) as a function of time. (B) Evolution of polymer film composition as a function of depth and time.

An alternative method for examining the stratified film is to divide the surface species ratio by the bottom species ratio to calculate the overall composition ratio. The evolution of the composition ratio with illumination time can be examined with the model (Figure 5.5B). The pre-polymer film is initially homogenous which is indicated by a composition ratio of 1 (no stratification present). Upon illumination, the composition ratio quickly decreases for approximately the first 50 seconds and then continues to decrease at a slightly slower rate for the rest of the modeled photopolymerization. The final composition ratio is approximately 0.9. Thus, the initially homogenous pre-polymer film rapidly exhibits surface enrichment of the di-ene species and the surface enrichment continues to increase during the course of the photopolymerization. The resulting polymer exhibits an approximate 10 percent surface enrichment of the di-ene species.

This prediction verifies that the model does predict general trends observed experimentally in photo-enforced stratification.

Previous work (Chapter 4) used composition ratios, calculated via attenuated total reflectance – Fourier transform infrared spectroscopy (ATR-FTIR) of the surface and bottom of the film, to determine the degree of photo-enforced stratification from formulations containing a one to one mole ratio 2-hydroxyethyl methacrylate and 1,6-hexanediol dimethacrylate with the initiator 2,2-dimethoxy-2-phenylacetophenone. Films produced from formulations which closely match the modeled formulation exhibited approximately 20 percent surface enrichment of the dimethacrylate species. While the current model predicts less surface enrichment than observed experimentally, the overall prediction capacity is powerful and shows accurate and reasonable trends when compared to approximately equivalent experimental systems. Deviations between experimental results and theoretical calculation could be due to assumption of constant propagation, termination, and diffusion coefficients used in the model. It is well understood and documented that these coefficients are not constant but rather vary as a function of conversion. Continued model development will account for the changes present in these coefficients. These changes can be modeled via calculation the heat of polymerization as well as the fractional free volume of the polymer as a function of conversion. The ability to model variation in the propagation, termination, and diffusion coefficients will affect both the kinetic and diffusion portions of the current model allowing for more realistic behavior to be predicted and described.

Conclusions

The temporal and spatial control inherent to radical photopolymerization allows for the production of a film with a chemical concentration gradient in a single reaction step via co-polymerization of monomers with different reactivity in the presence of a light gradient. A model has been developed from first principles of photopolymerization

kinetics and diffusion to describe the production of a stratified photo polymer film. Specifically, a co-photopolymerization of monomers with different reactivity in the presence of a light gradient was described. The light gradient from added photoinitiator results in a gradual loss of light with increasing depth in the film. A modeled 300 micrometer film with a 0.04 M concentration of photoinitiator resulted in approximately 65 percent of the initial light intensity reaching the bottom of the film. This light gradient results in a gradient in the rate of initiation and thus the rate of polymerization. Modeling the rate of polymerization shows higher rates of polymerization at the surface of the film compared to the bottom of the film. Varying the rate of polymerization through the depth results in differential monomer consumption for both the mono-ene and di-ene monomers. Thus, an initially homogenous film develops a concentration gradient during photopolymerization. As a result, directed diffusion of monomers occurs in the modeled system. The diffusion is modeled utilizing Fick's second law and equimolar counter-diffusion. Due to its higher reactivity in the formulation, the concentration gradient is larger for the di-ene than for the mono-ene resulting in a net positive diffusion rate of the di-ene at the surface of the film and a net positive diffusion rate of the mono-ene at the bottom of the film. Thus, diffusion and counter-diffusion results in the production of a polymer film with the surface composition enriched in the di-ene species and the bottom of the film enriched in the mono-ene species. This model considering both reaction and diffusion affects results in an approximately 10 percent surface enrichment of the di-ene species. The model presented in this work successfully describes and predicts the production of a polymer film with a chemical composition gradient via photopolymerization. The model described will allow for greater understanding of photopolymerization kinetics and property development in photopolymerized materials and implementation of advanced processes at an industrial scale.

Notes

1. Odian, G., *Principles of Polymerization*. 4 ed.; John Wiley & Sons: Hoboken, New Jersey, 2004
2. Kubota, H., and Fukuda, A., *J. Appl. Polym. Sci.* (1997) **65** (7), 1313
3. Adrus, N., and Ulbricht, M., *React. Funct. Polym.* (2013) **73** (1), 141
4. Forney, B. S., *et al.*, *Chemistry of Materials* (2013) **25** (15), 2950
5. Lee, E., *et al.*, *Drug Deliv.* (2010) **17** (8), 573
6. Bal, T., *et al.*, *Journal of Biomedical Materials Research Part A* (2014) **102** (2), 487
7. Aimetti, A. A., *et al.*, *Biomaterials* (2009) **30** (30), 6048
8. An, Y. J., and Hubbell, J. A., *J. Control. Release* (2000) **64** (1-3), 205
9. Volkert, A. A., and Haes, A. J., *Analyst* (2014) **139** (1), 21
10. Clapper, J. D., *et al.*, *Chemistry of Materials* (2008) **20** (3), 768
11. Oral, E., and Peppas, N. A., *Polymer* (2004) **45** (18), 6163
12. Nguyen, K. T., and West, J. L., *Biomaterials* (2002) **23** (22), 4307
13. Sawhney, A. S., *et al.*, *Macromolecules* (1993) **26** (4), 581
14. Mann, B. K., *et al.*, *Biomaterials* (2001) **22** (22), 3045
15. Bryant, S. J., and Anseth, K. S., *J. Biomed. Mater. Res.* (2002) **59** (1), 63
16. White, T. J., *et al.*, *Macromolecules* (2007) **40** (4), 1121
17. White, T. J., *et al.*, *Polymer* (2007) **48** (20), 5979
18. White, T. J., *et al.*, *Polymer* (2006) **47** (7), 2289
19. Penterman, R., *et al.*, *Nature* (2002) **417** (6884), 55
20. Vorflusev, V., and Kumar, S., *Science* (1999) **283** (5409), 1903
21. van Oosten, C. L., *et al.*, *Macromolecules* (2008) **41** (22), 8592
22. Tomlinson, W. J., *et al.*, *Appl. Opt.* (1976) **15** (2), 534
23. van Nostrum, C. F., *et al.*, *Chemistry of Materials* (1998) **10** (1), 135
24. Qian, T. Z., *et al.*, *Phys. Rev. E* **61** (4), 4007
25. Yu, Y. K., *et al.*, *Journal of Chemical Physics* (1996) **104** (7), 2725

26. Leewis, C. M., *et al.*, *Journal of Applied Physics* (2004) **95** (12), 8352
27. Leewis, C. M., *et al.*, *Journal of Applied Physics* (2004) **95** (8), 4125
28. Goodner, M. D., *et al.*, *Industrial & Engineering Chemistry Research* (1997) **36** (4), 1247
29. Lovestead, T. M., *et al.*, *Journal of Photochemistry and Photobiology A: Chemistry* (2003) **159** (2), 135
30. Goodner, M. D., and Bowman, C. N., *Chemical Engineering Science* (2002) **57** (5), 887
31. O'Brien, A. K., and Bowman, C. N., *Macromolecules* (2006) **39** (7), 2501
32. O'Brien, A. K., and Bowman, C. N., *Macromol. Theory Simul.* (2006) **15** (2), 176
33. Goodner, M. D., and Bowman, C. N., *Macromolecules* (1999) **32** (20), 6552
34. O'Brien, A. K., and Bowman, C. N., *Macromolecules* (2003) **36** (20), 7777
35. Reddy, S. K., *et al.*, *Australian Journal of Chemistry* (2006) **59** (8), 586
36. Cramer, N. B., *et al.*, *Macromolecules* (2003) **36** (12), 4631
37. Elliott, J. E., *et al.*, *Dental Materials* (2001) **17** (3), 221
38. Andrzejewska, E., *Progress in Polymer Science* (2001) **26** (4), 605
39. Leewis, C. M., *et al.*, *Journal of Chemical Physics* (2004) **120** (4), 1820

CHAPTER 6 HIGHLY STRATIFIED POLYMERIC FILMS VIA PHOTOPOLYMERIZATION

Abstract

The ability to control surface chemistry of polymer films has been researched extensively to provide controlled surface properties. The inherent temporal and spatial control of photopolymerization allows significant control of reaction rate through the use of different light intensity, initiator concentration, or monomer chemistry. Herein, the photopolymerization of monomers with different reactivity in the presence of a light gradient is examined to produce polymer films with a composition gradient. The inherent reactivity variation between methacrylate and acrylate monomers produces stratified films with up to 50 percent surface enrichment of methacrylate in the final polymer film. Generating a light gradient with both photobleaching and non-photobleaching photoinitiator is effective in producing significant degrees of stratification. Finally, utilization of various kinetic differences were explored using combinations of with inherent monomer reactivity with oxygen inhibition and number of reactive functional groups. These combinations result in up to a 150 percent increase in surface monomer enrichment. Controlling the surface chemistry in a single reaction step utilizing photopolymerization will allow for the generation of novel polymer films not accessible with current techniques.

Introduction

Controlling the surface chemistry of polymers allows for the modification of many surface properties such as hardness,^{1,2} contact angle,³ adhesion,^{4,5} and biological response.⁶⁻⁸ Increased control of the surface and bulk chemistries could allow for significant improvements which are not accessible with homogenous polymers in advanced applications including antifouling systems,^{9,10} antimicrobial films,¹¹⁻¹³ and adhesives.^{4,5} Presently, independent modification of surface and bulk chemistries typically requires multiple step processes such as changing or modifying the substrate,¹⁴ precipitation of one component during polymerization,¹⁴⁻¹⁶ casting multiple films,^{17,18} surface grafting,¹⁹⁻²¹ or plasma modification.^{22,23} While these methods allow for control of polymer surface chemistry, they are limited by additional production steps and/or potential adverse effects on final film properties.

Control of the localized polymer composition via the inherent temporal and spatial control of photopolymerization has afforded the production of holographic polymer dispersed liquid crystals²⁴⁻²⁶ (HPDLC), flexible liquid crystal displays^{27,28} (LCD), stimuli responsive polymers,²⁹ and holographic gratings.³⁰ The pre-polymer formulations for these applications were either a reactive monomer and a non-reactive liquid crystal component²⁴⁻²⁸ or a co-photopolymerization of monomers of unequal reactivity.^{29,30} These applications utilize areas of high light intensity via interference,²⁴⁻²⁶ chromophore,²⁷⁻²⁹ or photomask³⁰ in the polymerizing film and resulted in enrichment of the reactive monomer or preferentially reactive monomer in the high light intensity regions of the film. Diffusion of one species to the higher intensity regions of the polymerizing film resulted in counter-diffusion of the other monomer or non-reactive species.²⁷ The different reaction rates coupled with the diffusion/counter-diffusion affords spatial control of the polymer composition.

Several reactivity differences have been explored to control composition. For example, di-enes react approximately ten times faster than an analogous mono-ene.³¹

Additionally, different double bonds inherent exhibit different reactivity in photopolymerization producing systems quantified utilizing reactivity ratios to determine which monomer preferentially reacts in a co-photopolymerization.³²⁻³⁴ While these differences in reactivity allow for the production of polymers with localized control of the polymer composition, other kinetic differences may also result in such control. For example, monomers can exhibit varying degrees of oxygen inhibition.^{35,36} Additionally, factors that affect monomer reactivity can be combined to tailor monomer kinetics³⁷ and thus increase control of the localized polymer composition.

Photopolymerization of formulations containing monomers of unequal reactivity along with a chromophore results in a light gradient in the polymerizing films, which has shown the production of polymer films with controllable surface chemistries (Chapter 4). Specifically, the preferentially reacting monomer is enriched in the high light intensity regions of the film. Herein, the production of a compositional gradient in polymer film via photopolymerization is described. The inherent reactivity difference between a methacrylate and an acrylate is examined to produce polymer film with a compositional gradient (attenuated total reflectance – Fourier transform infrared spectroscopy (ATR-FTIR)). The effect of photobleaching versus non-photobleaching photoinitiators on the initial light gradient on the resulting polymer film is examined. The inherent reactive difference between methacrylates and acrylates are combined with differences in oxygen inhibition to produce further control over the compositional gradient. The effect of combining mono-ene and di-enes methacrylates and acrylates is also examined. The presented work illustrates the utility of photopolymerization as a method to produce stratified films in a single reaction step using a light gradient and monomers of different reactivity.

Experimental

Materials

Monomers used in the pre-polymer formulations include 2-hydroxyethyl acrylate (HEA), 2-hydroxyethyl methacrylate (HEMA), 2-methoxyethyl acrylate (MOA), 2-(dimethylamino)ethyl acrylate (DMAEA), and 2-(dimethylamino)ethyl methacrylate (DMAEMA, see Figure 6.1 for chemical structures). Criteria for monomer selection included the presence of functional groups to facilitate identification via Fourier transform infrared spectroscopy and small size to minimize diffusional limitations. The monomers were purchased from Sigma Aldrich. Photoinitiators used include 2,2-dimethoxy-2-phenylacetophenone (DMPA) and 2,4,6-trimethylbenzoyl-diphenylphosphineoxide (TPO). Using DMPA and TPO allowed for experimentation with both traditional and photobleaching photoinitiators. The photoinitiators were provided by CIBA. Chemicals were used as received without further purification.

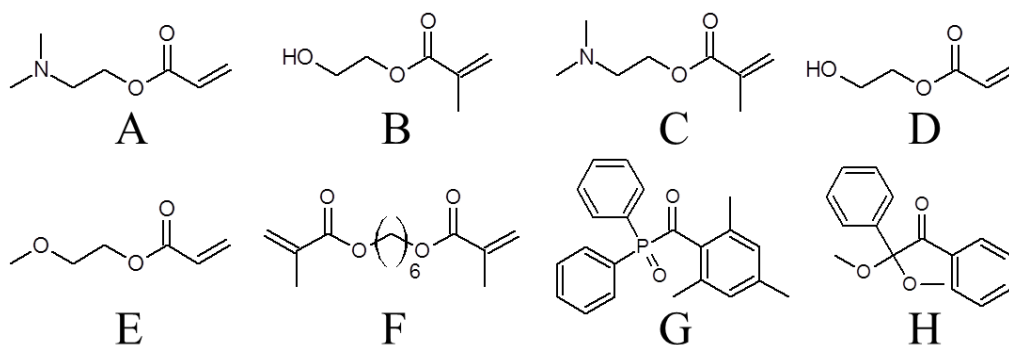


Figure 6.1. Chemical structures of monomers and photoinitiators used in this study including: (A) 2-(dimethylamino)ethyl acrylate, (B) 2-hydroxyethyl methacrylate, (C) 2-(dimethylamino)ethyl methacrylate, (D) 2-hydroxyethyl acrylate, (E) 2-methoxyethyl acrylate, (F) 1,6-hexanediol dimethacrylate, (G) 2,4,6-trimethylbenzoyl-diphenyl-phosphineoxide, and (H) 2,2-dimethoxy-2-phenylacetophenone.

Sample Preparation

Photopolymerization was initiated with an OnmiCure Series 1500 lamp equipped with a customized collimating lens. The UV lamp was filtered with the OnmiCure 365 nm filter and the light intensity was adjusted to 1 mW/cm². Polymer samples were produced as either drawn films or laminate films. Films were drawn using a drawdown bar to a thickness of approximately 200 micrometers then photopolymerized under a nitrogen atmosphere for approximately 15 minutes unless noted otherwise. Illumination continued until a tack free surface was achieved. To examine the impact of oxygen, films were polymerized in air for five minutes followed by nitrogen purge and illumination until a tack free surface was achieved. Laminate films were produced using an approximate 300 micrometer thick laminate model. The laminate mold consisted of glass slides treated with Rain-X, to facilitate sample removal. Illumination continued until complete through cure was achieved.

Fourier Transform Infrared Spectroscopy

Fourier transform infrared spectroscopy (FTIR) was utilized to determine chemical compositions. Monomers with hydroxyl (~3500 cm⁻¹), amine (~1150 cm⁻¹), or carbonyl (~1720 cm⁻¹) functional groups were selected that are readily distinguished via FTIR. The chemical compositions were determined via transmission FTIR and attenuated total reflectance-FTIR (ATR-FTIR) by taking the ratio of either the amine peak height to the hydroxyl peak height or the hydroxyl peak height to the carbonyl peak height, depending on the formulation. Transmission FTIR of a polymerized sample was used to determine the overall peak ratio. The surface composition ratio was found using ATR-FTIR.

Confocal Raman Microscopy

Raman spectra were collected using a custom confocal Raman microscope equipped with a 785 nm excitation laser from Kaiser Optical Systems, Inc. Spectra were

collected at the surface of the polymer film and every 4 micrometers thereafter until signal could no longer be accurately determined. The methacrylate peak height ($\sim 605 \text{ cm}^{-1}$) was divided by the carbonyl peak height ($\sim 1720 \text{ cm}^{-1}$) to determine the polymer film composition as a function of depth.

Results and Discussion

The temporal and spatial control inherent to photopolymerization can be utilized for the single step production of polymer films that exhibit a chemical concentration gradient (see Chapter 4). Specifically, monomer segregation has been observed in a co-photopolymerization of mono- and di-ene monomers in the presence of a reactive gradient. When created via light attenuation, this reactive gradient drives enrichment of the preferentially reacting di-ene in high light intensity regions. Production of stratified films via the manipulation of other types of kinetic differences should also be possible. To this end, co-polymerizations of monomers with different inherent reactivities and the combination of multiple kinetic differences are presented in this work to produce photo-induced stratification.

The chemical structure of a monomer can result in differences in reactivity towards the propagating radical during photopolymerization. For example, the stability of the intermediate radical species will determine the polymerization rate. The inherent reaction difference will affect monomer reaction in both neat and copolymerizations. Moreover, inherent reaction differences determine how monomers in a copolymerization will add to a polymerizing polymer. Reactivity ratios are used to quantify inherent monomer reactivity in a copolymerization by taking the ratio of the homo-propagation rate constant to the hetero-propagation rate constant.³⁸ A larger reactivity ratio indicates the preferred reactant in the copolymerization. For instance, the reactivity ratios for a copolymerization of methyl methacrylate and methyl acrylate are 2.2 and 0.4,³⁸ respectively, indicating that the methacrylate is the preferentially reacting monomer.

Thus, the reactivity ratios predict enrichment of methacrylate in the high light intensity regions from a co-photopolymerization of a methacrylate and an acrylate in the presence of a light gradient. To test this hypothesis, formulations containing a one to one weight ratio of 2-hydroxyethyl methacrylate (HEMA) to 2-(dimethylamino)ethyl acrylate (DMAEA) with varying amounts of 2,2-dimethoxy-2-phenylacetophenone (DMPA, photoinitiator) were polymerized. Films approximately 200 micrometers thick were drawn and cured under an inert atmosphere with a UV light filtered to 365 nm with a light intensity of 7 mW/cm^2 . Films were analyzed with FTIR and composition ratios were calculated by taking the carbon-nitrogen peak height divided by the hydroxyl peak height. The homogenous composition ratio, which is representative of the surface composition ratio in the absence of stratification, is determined from the transmission FTIR of the polymerized formulation. Infrared spectra of the near surface region were collected utilizing attenuated total reflectance (ATR-FTIR) to determine the surface composition ratio. The surface composition ratio is normalized to the homogenous composition ratio and plotted as a function of weight percent (wt%) photoinitiator, DMPA (Figure 6.2A). Surface composition ratios greater than and less than the homogenous composition ratio indicate methacrylate and acrylate surface enrichment respectively.

At low concentrations of photoinitiator (and thus minimal light attenuation), the surface composition ratio is approximately equal to the homogenous composition ratio, indicating that the polymer films are relatively homogenous. Upon further increases in the concentration of DMPA above 1 wt%, the surface composition ratio is significantly lower than the homogenous composition ratio correlating to an almost 50 percent methacrylate surface enrichment. Further increases in DMPA concentration results in decreased methacrylate surface enrichment, as indicated by the surface composition ratio again approaching the homogenous composition ratio. Loss of stratification upon increasing concentration of DMPA was also observed when producing stratified films

utilizing kinetic differences between mono- and di-ene monomers (see Chapter 4).

Decreases in stratification at high initiator concentrations can be attributed to increased polymerization rates and thus, decreased time available for monomer diffusion. These results demonstrate that inherent monomeric reactivity differences can be used to drive the enrichment of specific monomers to a polymer surface.

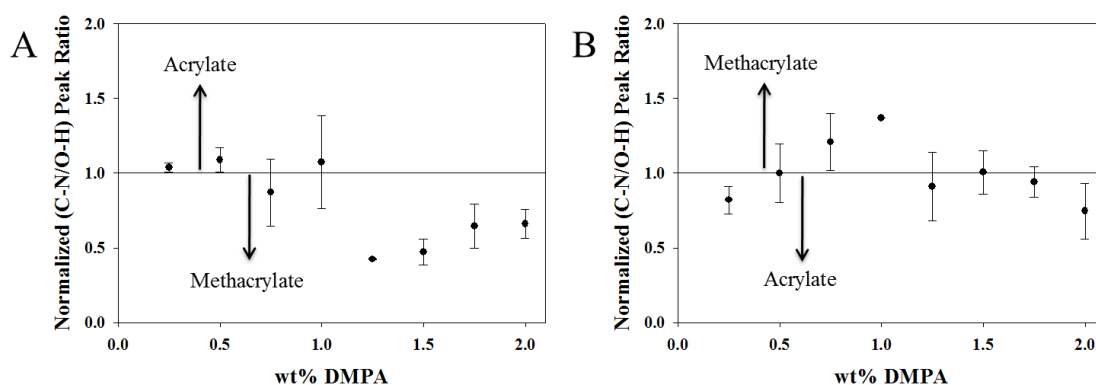


Figure 6.2. Normalized peak height ratios from the surface of polymers produced with a range of DMPA concentrations for a 1:1 weight ratio of (A) HEMA to DMAEA and (B) HEA to DMAEMA formulations using ATR-FTIR. Peak height ratios were normalized to the ratio determined using transmission FTIR of the same samples. 200 micrometer drawn films were polymerized with 365 nm light at 7 mW/cm². Error bars represent the standard deviation of a minimum of three replicate measurements.

To examine if stratification was a result of inherent monomer reactivity differences, as hypothesized, and not due to surface energy differences or other possible affects from the chemical differences the hydroxyl and amine functional groups were exchanged between the methacrylate and the acrylate. Formulations containing 2-hydroxyethyl acrylate (HEA) and 2-(dimethylamino)ethyl methacrylate (DMAEMA) were polymerized with varying amounts of DMPA and analyzed using the same techniques described above (Figure 6.2B). At low concentrations of DMPA the surface composition is approximately equivalent to the bulk composition. Increasing the DMPA

concentration results in an approximate 40 percent surface enrichment of methacrylate indicating the production of a stratified film. Above 1 wt%, additional DMPA results in a loss of stratification due to increased rates of polymerization with increasing DMPA concentration resulting in less time for monomer diffusion. Thus, the chemistry and surface energy in this system displays a similar trend as the previous system. Both copolymerization formulations produced a stratified film with a methacrylate enriched surface regardless of the functional group used for identification indicating that producing a stratified film with these systems is predominately controlled from the inherent reactivity differences between the monomers.

DMPA was chosen as the photoinitiator for these studies because it is non-photobleaching, allowing for relatively constant light attenuation during the photopolymerization. The ability to use a photobleaching photoinitiators facilitates the realization of stratified films in a wider range of systems by increasing the number of photoinitiator for formulating and possibly allowing for thicker systems to stratify while still achieving good through cure. To this end, copolymerization formulations were produced with a one to one weight ratio of HEMA to DMAEA with 2,4,6-trimethylbenzoyl-diphenyl-phosphineoxide (TPO) as the photobleaching photoinitiator. Approximately 200 micrometer drawn films were polymerized in an inert atmosphere (365 nm, 7 mW/cm².) The surface and homogenous composition ratios were determined as a function of weight percent photoinitiator (Figure 6.3A). At low levels of photoinitiator (< 0.5 wt% TPO) little to no variation of the surface composition is observed compared to the homogenous composition. Intermediate levels of photoinitiator (0.5 – 1.5 wt% TPO) result in substantial deviation of the surface composition illustrating an approximate methacrylate surface enrichment of 30 percent. At high levels of photoinitiator (>1.5 wt% TPO) the surface composition approaches that of the homogenous composition. This study illustrates that in addition to non-photobleaching

initiators, photobleaching initiators (i.e. TPO), can also be used to produce stratified films.

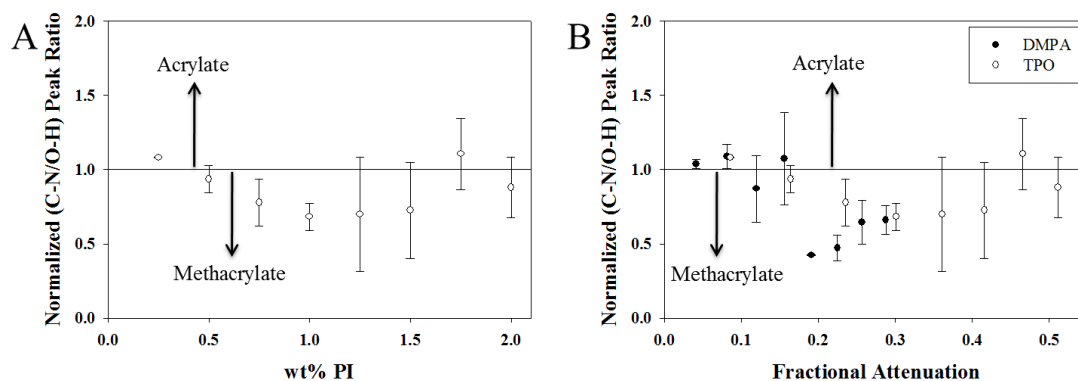


Figure 6.3. Normalized peak height ratios from the surface of polymers produced with various amounts of (A) TPO in a 1:1 weight ratio of HEMA to DMAEA formulation as determined by ATR-FTIR. (B) Comparison of the normalized peak height ratios observed from TPO (○) and DMPA (●). Peak height ratios were normalized by the C-N/O-H ratio from transmission FTIR of the same samples. 200 micrometer drawn films were polymerized with 365 nm light at 7 mW/cm². Error bars represent the standard deviation of a minimum of three replicate measurements.

While both DMPA and TPO give similar results, TPO allows stratification at lower concentrations. To more directly compare the two systems, the normalized peak ratio is plotted as a function of fractional light attenuation (Figure 6.3B) as defined as the fraction of light absorbed by the photoinitiator through the film. Examining the surface composition ratio as a function of fractional attenuation illustrates very low to no stratification at low levels of attenuation for both initiators, some stratification at moderate levels, and a decrease in stratification at high fractional attenuation. Interestingly, the fractional attenuation required to produce a stratified film for both DMPA and TPO is approximately 0.2 fractional attenuation. Thus, production of a stratified film requires a sufficient light gradient in order for non-uniform monomer

consumption to occur. As this differential monomer consumption occurs, concentration gradients develop and drive diffusion and counter-diffusion of the HEMA and DMAEA, respectively. Thus, the minimum required light attenuation most likely correlates to the threshold of sufficient reaction gradient required to produce enough diffusion to produce the stratified film. Further, these results demonstrate the importance and sensitivity of the light gradient during the production of photo-stratified films.

In order to produce a stratified film utilizing photopolymerization, both a sufficient light gradient and monomers with significant differences in kinetic rates must be present in the co-photopolymerization. Enhancing the reaction rate differences between monomers should enhance the degree of stratification observed after reaction completion. To this end, formulations for co-photopolymerization with multiple reactivity differences and driving forces could produce significantly greater stratification in films. One example of such a formulation is a co-photopolymerization of a methacrylate and acrylate formulation in the presence of atmospheric oxygen. Reactivity ratios indicate that the more stable tertiary methacrylate radical will form preferentially over the secondary acrylate radical. The increased stability of the methacrylate radical results in decreased reactivity with molecular oxygen, thereby decreasing the degree of oxygen inhibition of methacrylate polymerization as compared to acrylates. Thus, the kinetic difference of inherent reactivity may be used in combination with oxygen inhibition to generate films with increased enrichment of methacrylate at the surface. To test this hypothesis, formulations were produced with 2-methoxyethyl acrylate (MOA) and HEMA with varying amounts of DMPA as photoinitiator. Approximately 200 micrometer thick films were drawn and cured for five minutes in air and thus inhibited by oxygen. The films were then purged with nitrogen and illuminated until a tack free surface was obtained. The formation of peroxy radicals during polymerization in the presence of oxygen results in overlapping spectral features in the resulting ATR-FTIR spectrum. Therefore, alternate methods are required to analyze the enrichment of

monomer residues both at the surface and throughout the thickness of the film. Raman spectroscopy provides a means for the determination of composition because of the unique methacrylate vibrational band at ~605 wavenumbers.^{39,40} Additionally, Raman spectroscopy affords detection of the carbonyl group on the monomers. This allows for the calculation of a composition ratio to examine composition as a function of depth while mitigating signal loss with increasing depth. The carbonyl peak will vary with conversion,⁴¹ however the additional cure under nitrogen results in an approximately constant conversion through the depth profiled.⁴² As a result, the carbonyl peak is still an appropriate peak to facilitate determination of the composition. This technique was used to determine the composition of the oxygen-inhibited film with the largest hydroxyl to carbonyl peak ratio. The peak height of the methacrylate specific and carbonyl peaks were determined and used to calculate the methacrylate composition ratio as a function of depth (Figure 6.4). A high methacrylate composition ratio is observed at the surface of the film which then decreases and remains approximately constant in the bulk of the film at depths greater than 25 micrometers. The high surface methacrylate composition ratio corresponds to an approximate 60 percent surface enrichment of methacrylate. Thus, the combination of oxygen inhibition and reactivity differences resulted in a roughly 20 percent increase in the amount of methacrylate that is enriched at the surface of the film compared to films prepared in nitrogen (approximately 50 percent methacrylate surface enrichment).

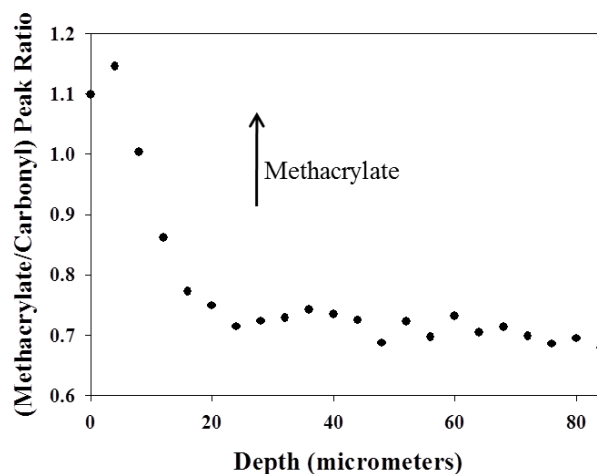


Figure 6.4. Methacrylate to carbonyl peak height ratio from confocal Raman spectroscopy depth profile. Polymer sample was produced from a 1:1 weight ratio of MOA to HEMA with a 1.25 wt% DMPA concentration polymerized in air. 200 micrometer drawn film were polymerized with 365 nm light at 1 mW/cm².

Previous work (see Chapter 4) illustrates the ability to produce films with a chemical composition gradient utilizing the kinetic difference between mono and di-ene monomers. Specifically, the photopolymerization of formulations containing 1,6-hexanediol dimethacrylate (HDDMA) and HEMA results in HDDMA surface enrichment of approximately 20 percent. Combining both the mono- and di-ene reactivity differences with inherent monomer reactivity differences is expected to further enhance kinetic distinction between monomers resulting in an enhanced composition gradient in the resulting polymer film. A pre-polymer formulation of HDDMA and HEA, for example, has significant kinetic differences that could facilitate HDDMA surface enrichment. The di-methacrylate would be favored kinetically because di-enes react faster than mono-enes and because methacrylates preferentially react over acrylates.

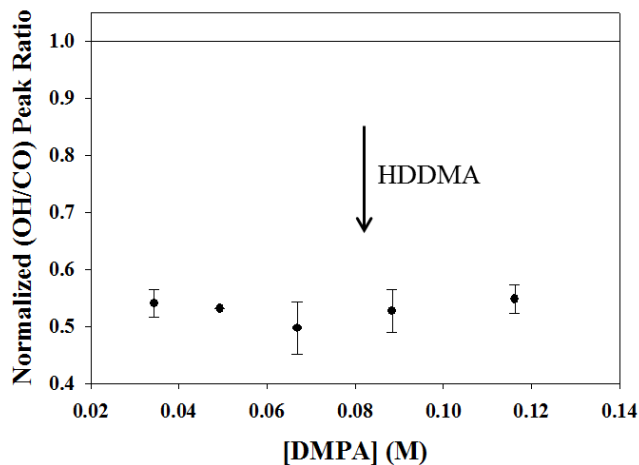


Figure 6.5. Normalized peak height ratio from the surface polymers produced using a 1:1 molar ratio of HDDMA to HEA with various amounts of DMPA using ATR-FTIR. 200 micrometer drawn film were polymerized with 365 nm light at 1 mW/cm². Error bars represent the standard deviation of a minimum of three replicate measurements.

To determine the level of stratification by combining the kinetic differences, films were produced from a 1:1 molar ratio of HEA:HDDMA with varying amounts of photoinitiator (DMPA). (Figure 6.5) All films produced exhibit a much lower composition ratio than the bulk, indicating HDDMA enrichment at the surface of the film. An approximate maximum enrichment of 50 percent HDDMA was achieved, compared to the only 20 percent maximum enrichment observed for systems with only one kinetic difference. By combining two kinetic differences, namely reactivity ratio and functionality, it is possible to substantially increase the amount of di-ene enriched at the surface. Additionally, the trend of decreased enrichment with increasing concentration of DMPA was observed in this system, similar to the reactivity ratio and HEMA:HDDMA systems.

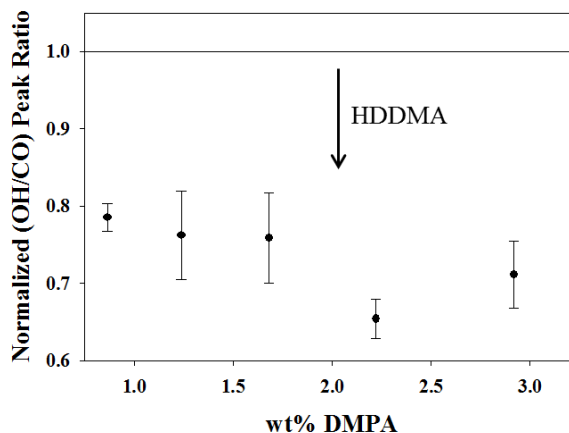


Figure 6.6. Normalized peak height ratios from the surface of polymer films of 1:1 molar ratio of HDDMA to HEMA with various amounts of DMPA using ATR-FTIR. 200 micrometer drawn films were polymerized with 365 nm light at 7 mW/cm². Error bars represent the standard deviation of a minimum of three replicate measurements.

Previous studies of the HEMA:HDDMA system (see Chapter 4) was accomplished utilizing films produced from laminate mold. To examine if the manner of production, mold versus drawn film, affects stratification, films were produced with a one to one molar ratio of HEMA to HDDMA with varying amounts of photoinitiator. The surface composition was determined with ATR and compared to the bulk transmission ratio for various concentrations of DMPA (Figure 6.6). All formulations exhibit ratios significantly lower than that for the bulk, indicating enrichment of HDDMA at the surface of the film. This production technique results in a maximum HDDMA enrichment of approximately 30 percent compared to the maximum HDDMA enrichment observed in the laminate films of only 20 percent. Both the kinetic differences and the physical manner in which films are produced are vital for producing a stratified film.

Conclusions

The ability to generate stratified polymer films in a single reaction step allows for production of polymer films with novel properties not available with currently

technologies. The ability to produce stratified films from co-photopolymerization formulations containing monomers with kinetic differences was examined in this work. Specifically, the inherent reactivity difference between methacrylate and acrylate monomers facilitated the production of stratified films. A co-photopolymerization of HEMA and DMAEA with various concentrations of photoinitiator, DMPA, resulted in an approximate 40 percent enrichment of the methacrylate monomer at the surface. To verify that stratification was not produced from surface energy interactions, the acrylate and methacrylate were switched for analogous monomers to HEA and DMAEMA. Despite the change in the respective monomer surface energy interactions, the co-photopolymerization still results in enrichment of methacrylate at the surface of the film. Consequently, methacrylate enrichment in both systems indicates the stratification is a result of the inherent monomer reactivity differences. Production of stratified films is also possible with both non-photobleaching and photobleaching photoinitiators. Varying the TPO concentration, a photobleaching photoinitiator, in the HEMA and DMAEA systems resulted in similar degrees of stratification as the DMPA formulations. Normalization of the DMPA and TPO films to fractional light attenuation results in an apparent minimum light attenuation needed to produce a stratified HEMA and MOA copolymer film illustrates the importance of the light gradient in producing stratified films. Increased degrees of stratification were observed by combining multiple kinetic differences to increase the reactive preference of a monomer in the co-photopolymerization. Combining the inherent reactivity difference between methacrylate and acrylate monomers with oxygen inhibition allows a stronger reactivity preference for the methacrylate. The increased reactivity preference results in an approximately 60 percent enrichment of methacrylate at the surface. Combination of monomer functionality with reactivity ratios was examined with a HEA and HDDMA formulation with various concentrations of DMPA. This system shows an approximate enrichment of 50 percent of the dimethacrylate monomer. Combining monomer functionality with reactivity ratios increases

stratification approximately 150 percent compared to utilizing monomer functionality alone. The increased control observed in a drawn film with the HEA and HDDMA system prompted a revisit of the previously examined system of HEMA and HDDMA. Drawn HEMA and HDDMA films resulted in an approximate 50 percent increase in HDDMA enrichment. The results discussed in this work illustrate and highlight the ability to generate stratified films from pre-polymer formulations containing monomers of different reactivity utilizing photopolymerization. Photo-enforced stratification facilitates the generation of polymer films with controllable surface properties in a single reaction step, an advantage that is unattainable with current polymerization techniques.

Notes

1. Sangermano, M., *et al.*, *Polymer* (2009) **50** (24), 5647
2. Nowicki, M., *et al.*, *Polymer* (2003) **44** (21), 6599
3. Okouchi, M., *et al.*, *Macromolecules* (2006) **39** (3), 1156
4. Noeske, M., *et al.*, *International Journal of Adhesion and Adhesives* (2004) **24** (2), 171
5. Liston, E. M., *et al.*, *Journal of Adhesion Science and Technology* (1993) **7** (10), 1091
6. Goddard, J. M., and Hotchkiss, J. H., *Progress in Polymer Science* (2007) **32** (7), 698
7. Ma, Z., *et al.*, *Colloids and Surfaces B: Biointerfaces* (2007) **60** (2), 137
8. Clapper, J. D., *et al.*, *Biomacromolecules* (2008) **9** (4), 1188
9. Wavhal, D. S., and Fisher, E. R., *Langmuir* (2002) **19** (1), 79
10. Statz, A. R., *et al.*, *Journal of the American Chemical Society* (2005) **127** (22), 7972
11. Huang, J., *et al.*, *Biomacromolecules* (2007) **8** (5), 1396
12. Cen, L., *et al.*, *Langmuir* (2003) **19** (24), 10295
13. Zhang, W., *et al.*, *Biomaterials* (2006) **27** (1), 44
14. Walheim, S., *et al.*, *Macromolecules* (1997) **30** (17), 4995
15. Chen, J., and Gardella, J. A., *Macromolecules* (1998) **31** (26), 9328
16. Ikejima, T., and Inoue, Y., *Macromol. Chem. Phys.* (2000) **201** (14), 1598
17. Le Minez, J.-J., and Schmitt, B., Wet-on-wet coating process. Peintures Corona S.A., United States, (1983)
18. Chen, W., and McCarthy, T. J., *Macromolecules* (1997) **30** (1), 78
19. Kubota, H., *J. Appl. Polym. Sci.* (1992) **46** (3), 383
20. Pan, B., *et al.*, *J. Polym. Sci. A Polym. Chem.* (2004) **42** (8), 1953
21. Zhu, J., *et al.*, *Macromol. Chem. Phys.* (2006) **207** (1), 75
22. Inagaki, N., *et al.*, *Journal of Polymer Science Part B: Polymer Physics* (2004) **42** (20), 3727
23. Vesel, A., *et al.*, *Surface and Interface Analysis* (2008) **40** (11), 1444
24. White, T. J., *et al.*, *Macromolecules* (2007) **40** (4), 1121

25. White, T. J., *et al.*, *Polymer* (2007) **48** (20), 5979
26. White, T. J., *et al.*, *Polymer* (2006) **47** (7), 2289
27. Penterman, R., *et al.*, *Nature* (2002) **417** (6884), 55
28. Vorflusev, V., and Kumar, S., *Science* (1999) **283** (5409), 1903
29. van Oosten, C. L., *et al.*, *Macromolecules* (2008) **41** (22), 8592
30. Tomlinson, W. J., *et al.*, *Appl. Opt.* (1976) **15** (2), 534
31. Andrzejewska, E., *Progress in Polymer Science* (2001) **26** (4), 605
32. Dube, M., *et al.*, *J. Polym. Sci. A Polym. Chem.* (1991) **29** (5), 703
33. Polic, A. L., *et al.*, *J. Polym. Sci. A Polym. Chem.* (1998) **36** (5), 813
34. Jansen, J. F. G. A., *et al.*, *Macromolecules* (2004) **37** (6), 2275
35. Kloosterboer, J. G., *et al.*, *Polym Mat: Sci Eng Proc ACS Div Polym Mater: Sci Eng* (1989) **60**, 122
36. Lee, T. Y., *et al.*, *Polymer* (2004) **45** (18), 6155
37. Jansen, J. F. G. A., *et al.*, *Macromolecules* (2003) **36** (11), 3861
38. Odian, G., *Principles of Polymerization*. 4 ed.; John Wiley & Sons: Hoboken, New Jersey, 2004
39. Zou, Y., *et al.*, *Journal of Biomedical Materials Research Part A* (2008) **86A** (4), 883
40. Zou, Y., *et al.*, *Journal of Biomedical Materials Research Part A* (2010) **94A** (1), 288
41. De Santis, A., *Polymer* (2005) **46** (14), 5001
42. Cai, Y., and Jessop, J. L. P., *Polymer* (2006) **47**, 6560

CHAPTER 7 INVESTIGATING THE BULK PROPERTIES AND
MULTIPLE PATHWAYS FOR PRODUCING COMPOSITION
GRADIENTS IN PHOTOPOLYMER FILMS

Abstract

The temporal and spatial control inherent to photopolymerization can be utilized to control the surface chemistry and properties in a single reaction step. Specifically, monomers with kinetic differences are photopolymerized in the presence of a light gradient to yield controlled surface composition. Herein, dynamic mechanical analysis, swelling studies, and stress release via heating are utilized to examine the bulk properties of stratified films which illustrate little variation with the degree of stratification. Stratified films produced from a co-photopolymerization of a methacrylate and an acrylamide exhibit adhesion only on the side acrylamide enriched side. Alternatives to a Norrish type one photoinitiation of a radical chain polymerization are also examined as methods to produce a stratified polymer film. Specifically, utilizing type two initiation resulted in a 40 percent enrichment of the monomer containing the co-initiator and thiol-ene polymerization resulted in an approximately 20 percent surface enrichment of the preferentially reacting ene monomer. Based on these results, generation of novel polymer films which are not currently accessible may be realized via controlling the surface properties in a single reaction step with photo-enforced stratification.

Introduction

The ability to control the surface and bulk properties independently could provide significant advantages in numerous materials such as adhesives,^{1,2} antifouling systems,^{3,4} and antimicrobial films.⁵⁻⁷ Independent control would allow for the tailoring of surface properties such as contact angle,⁸ hardness,^{9,10} biological response,^{11,12} and adhesion.^{1,2} Current techniques to achieve this level of control over the bulk and surface chemistry include changing or modifying the substrate,¹³ casting multiple films,^{14,15} precipitation of one component during polymerization,^{13,16,17} plasma modification,^{18,19} or surface grafting.²⁰⁻²² These methods afford control and/or modification of polymer surface chemistry but are not ideal due to lack of control, requiring additional processing steps, and/or may adversely affect final polymer properties.

Generating a controlled chemical concentration through a polymer film could allow for control over the surface chemistry and properties. Utilizing photopolymerization to produce a composition gradient through a polymer film via photo-enforced stratification requires a co-polymerization formulation containing monomers of different reactivity polymerized in the presence of a light gradient (Chapter 4 and 6). The light gradient results in higher polymerization rates in these regions of the film. Thus, the preferentially reacting monomer enriches the high light intensity surface of the film allowing for control over the surface chemical composition and therefore surface properties of the film. For instance, a co-photopolymerization of 2-hydroxyethyl methacrylate and 1,6-hexanediol dimethacrylate, mixed at a one to one mole ratio, with the photoinitiator 2,2-dimethoxy-2-phenylacetophenone was able to produce films with a 20 percent surface enrichment of 1,6-hexanediol dimethacrylate (Chapter 4). The stratified films exhibit increased contact angle and an increase in the hardness of the film. Thus, photo-enforced stratification allows for the generation of films with a chemical composition gradient which then allows for control over the surface properties of the film.

In addition to the number of functional groups, many other kinetic differences employing radical photopolymerization exist which could lead to the production of a stratified film. Inherent reactivity differences between monomer functional groups have been utilized in photo-enforced stratification to produce a chemical concentration gradient (Chapter 6). Additionally, it should be possible to utilize chemistries outside of the traditional Norrish type one photoinitiated radical chain growth photopolymerization such as Norrish type two photoinitiation or radical step growth polymerization. Norrish type two photoinitiation requires both a photoinitiator and a co-initiator.^{23,24} A tertiary amine species is typically utilized as the co-initiator which can be an additional chemical in the formulation²⁴ or attached to one of the polymerizing monomers.²⁵ Formulations utilizing a monomer that will also act as a co-initiator are expected to result in sufficient kinetic differences to allow for photo-enforced stratification to occur. Radical step growth photopolymerization, such as thiol-ene chemistry,^{26,27} could be another variant in reaction chemistry to produce stratified films via photo-enforced stratification. Thiol-ene chemistry affords numerous benefits for producing stratified films such as delayed gelation due to step growth mechanism, resulting in addition time for monomer diffusion, and a wide variety of reactivities between thiols and enes.

Producing polymers with controllable surface chemistries should be possible via co-photopolymerization of monomers with kinetic differences and the presence of a light gradient resulting from the concentration of photoinitiator utilized during the polymerization. As a result, the higher light intensity regions would experience increased rates of polymerization and thus the preferentially reacting monomer is enriched in these regions. Herein, stratified films are produced from co-photopolymerization of a mono- and di-ene to examine variation in bulk film properties with the degree of stratification. A formulation is developed which illustrates the ability to change film adhesion with photo-enforced stratification. X-ray photoelectron spectroscopy is examined as an instrumental method to quantify polymer surface compositions. Finally, Norrish type two

photoinitiation and thiol-ene photopolymerization are examined as alternative photopolymerization reaction mechanisms to produce stratified films. The presented work illustrates the single step production of a composition gradient in a polymer via copolymerization of monomers with different inherent reactivity polymerized in the presence of a light gradient.

Experimental

Chemicals

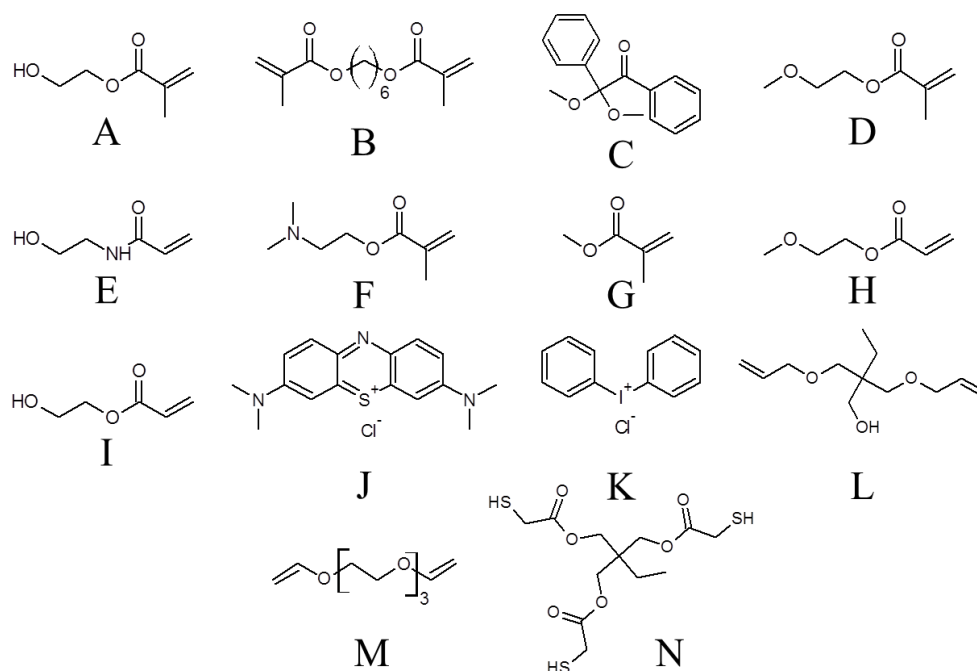


Figure 7.1. Chemical structures of (A) 2-hydroxyethyl methacrylate, (B) 1,6-hexanediol dimethacrylate, (C) 2,2-dimethoxy-2-phenylacetophenone, (D) 2-methoxyethyl methacrylate, (E) N-hydroxyethyl acrylamide, (F) 2-(dimethylamino)ethyl methacrylate, (G) methyl methacrylate, (H) 2-methoxyethyl acrylate, (I) 2-hydroxyethyl acrylate, (J) methylene blue, (K) diphenyliodonium chloride, (L) trimethylolpropane diallyl ether, (M) tri(ethylene glycol) divinyl ether, and (N) trimethylolpropane tris(2-mercaptoacetate).

Monomers studied included 2-hydroxyethyl methacrylate, 1,6-hexanediol dimethacrylate, 2-methoxyethyl methacrylate, N-hydroxyethyl acrylamide, 2-(dimethylamnio)ethyl methacrylate, methyl methacrylate, 2-methoxyethyl acrylate, 2-hydroxyethyl acrylate, (J) trimethylolpropane diallyl ether, tri(ethylene glycol) divinyl ether, and trimethylolpropane tris(2-mercaptoacetate). The monomers were purchased from Sigma Aldrich. Photoinitiators used included 2,2-dimethoxy-2-phenylacetophenone, methylene blue, and diphenyliodonium chloride. The 2,2-dimethoxy-2-phenylacetophenone was provided by CIBA while the others were purchased from Sigma Aldrich (see Figure 7.1 for chemical structures). Chemicals were used as received without further purification.

Polymer Film Sample Preparation

Laminate films were produced using an approximate 300 micrometer thick laminate mold. The laminate mold consisted of glass slides treated with Rain-X, to facilitate sample removal, separated by a 300 micrometer spacer. Illumination continued until complete through-cure was achieved.

Attenuated Total Reflectance – Fourier Transform Spectroscopy

Chemical analysis of the polymer surface for the thiol-ene systems was completed using a Thermo Fisher Nexus 670 Fourier Transform Infrared Spectrometer with a Horizontal Attenuated Total Reflector (ATR) attachment containing a ZeSn crystal with a 45 degree angle of incidence. The resulting IR spectra were then analyzed by determining hydroxyl (OH) and carbonyl (CO) peak height at approximately 3510 cm^{-1} and 1720 cm^{-1} , respectively. The OH peak height is then divided by the CO peak height for each side of a sample. The ratio for each side of the sample is then divided by each other with the high light intensity side (the side closest to the UV light) being divided by the low light

intensity side (the side furthest from the UV light) to determine if stratification has occurred.

X-ray Photoelectron Spectroscopy

XPS measurements were collected using a Kratos Axis Ultra Spectrometer with a monochromatic Al K α X-ray source as described elsewhere.^{28,29} Briefly, a 160 eV pass energy, 1 eV step size, 200 ms dwell time, and $\sim 700 \mu\text{m} \times 300 \mu\text{m}$ X-ray spot size were used for a survey scan (range = 1200 – -5 eV). All spectra were charge-calibrated with respect to the adventitious C 1s peak at 285.0 eV and were analyzed using CasaXPS. A linear background was used to subtract the inelastic background and the curves were fit using a Gaussian/Lorentzian (GL(30)) lineshape.

Adhesion Test

Polymer samples were placed between two glass slides. Pressure was applied to the glass slides over the location of the polymer sample and then the slides were gently pulled apart. The side of the polymer sample which sticks to the glass slide was noted allowing for differences in adhesive forces on the surfaces of the polymer to be qualitatively evaluated.

Dynamic Mechanical Analysis

A TA Instruments Q800 DMA was used to evaluate the tan delta of polymer samples in tensile mode. A sinusoidal strain of 0.05 percent was applied at 1 Hz through the temperature range of interest, thus allowing for the determination of the thermal transitions of the polymer. A minimum of two cycles was used to insure additional cure did not occur during DMA testing and thus final mechanical properties were measured.

Shrinkage Stress Relief via Heating

Polymer samples were placed into an oven set at 175 degrees Celsius. The samples were held at this temperature for a minimum of an hour. Upon removal of

samples from the oven, changes in the polymer shape were noted. Specifically, determination of the degree that the polymer samples curled was evaluated.

Swelling Studies

The initial mass of the polymer samples was recorded. The samples were then placed into water, ethanol, or ethyl acetate and allowed to soak. The mass was recorded as a function of time by removing the samples from the solvent, gently removing the excess solvent from the sample surface, and recording the mass.

Results and Discussion

Photo-enforced stratification has illustrated the ability to change surface chemistry and surface properties of a photopolymer film but the influence of stratification on bulk properties has yet to be examined. Changes in the bulk properties may result from stratification depending on how significant and how prevalent the stratification is in the film. The bulk properties of polymer films can be measured using dynamic mechanical analysis (DMA),³⁰ swelling studies,³¹ and shrinkage stress³² from photopolymerization.

To test the impact of stratification on phase characteristic, the mechanical properties of a one to one mole ratio of 2-hydroxyethyl methacrylate (HEMA) to 1,6-hexanediol dimethacrylate (HDDMA) polymer film was examined with DMA by comparing the glass transition temperature behavior as represented by tan delta of a neat HEMA film, a neat HDDMA film, a photo stratified film of a one to one mole ratio of HEMA to HDDMA, and a thermally cured film of a one to one mole ratio of HEMA to HDDMA (Figure 7.2). The photo stratified film was produced using 0.86 weight percent 2,2-dimethoxy-2-phenylacetophenone (DMPA) which produces a polymer film with approximately 20 percent surface enrichment of HDDMA (Chapter 4). The thermally cured film was used as a homogenous control. Neat HEMA exhibits a strong transition at 136 °C and neat HDDMA exhibits a very broad transition with a tan delta maximum at

approximately 20 °C. The thermally cured and stratified films both show evidence of the HEMA and HDDMA transitions; however, the stratified film exhibits a slightly stronger and more distinct HDDMA transition as evident from the approximate increase of 0.02 in the tan delta through the temperature region (~ -50 to 100 degrees Celsius) corresponding to the HDDMA thermal transition. These differences, even though slight, are reproducible. The photocured film exhibiting a slightly stronger HDDMA transition is consistent with surface enrichment of HDDMA. Additionally, neither of the co-polymer films show evidence of micro- phase separation (films were visually clear) indicating that monomer stratification results in a smooth composition transition. The DMA results show further evidence of the surface enrichment and changes in properties in surface regions.

The extent of polymer swelling can also be used to examine differences in polymer bulk properties. The ability for a polymer to swell in solvent is, in part, determined from the crosslink density. Enriching HDDMA in a region within the polymer will increase the crosslink density in those regions. Enrichment, however, also results in other areas of the film being enriched in the other monomer, HEMA, which would decrease the crosslink density. As a result, a chemical composition gradient could result in varying the overall degree the polymer film can swell. To test the polymer swelling properties, films produced from the HDDMA and HEMA formulations with varying degrees of stratification with a thermally polymerized control were submerged into water, ethanol, or ethyl acetate and the mass was recorded at various time intervals. No difference in the degree of swelling was observed for any of the films tested in any of the solvents tested. These results indicate that locally changing the crosslink density in this system does not affect the overall ability for the polymer to swell. Varying the chemical composition through the depth via photo-enforced stratification without affecting polymer swelling could allow for the design of hydrogels with chemical gradients.

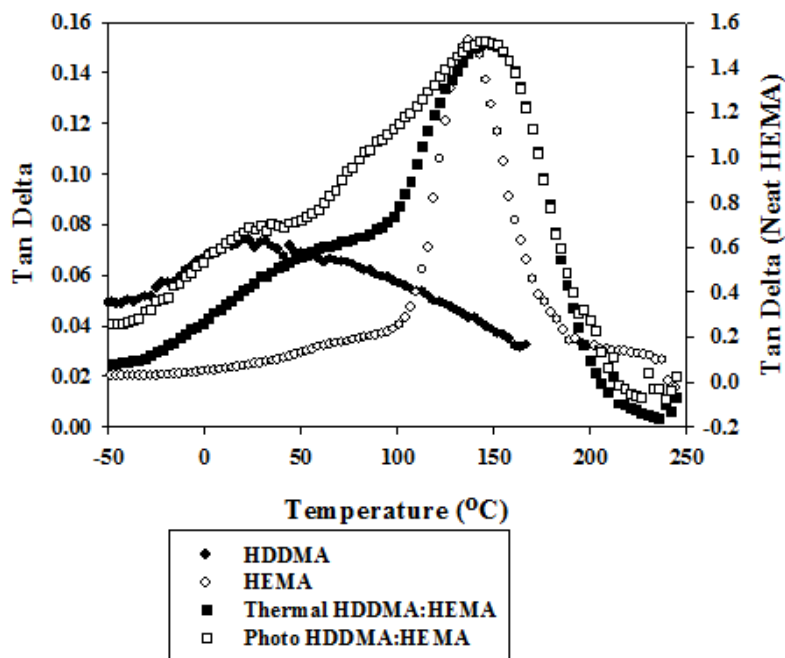


Figure 7.2. Dynamic mechanical analysis tan delta temperature sweep of neat HEMA (\circ), neat HDDMA (\bullet), thermally polymerized one to one molar ratio of HEMA to HDDMA (\blacksquare), and photopolymerized one to one molar ratio of HEMA to HDDMA that exhibits photo-enforced stratification (\square). Films were polymerized in a 300 micron laminate mold with 365 nm light at 1 mW/cm².

The gradient in crosslink density discussed in the swelling studies could also result in a stress gradient within the polymer film with more shrinkage stress occurring in the higher crosslinked regions of the film. Exceeding the glass transition temperature of the polymer allows for the network to reorganize and relieve some of the shrinkage stress generated during photopolymerization.³³ To measure the effect of shrinkage stress in the higher crosslinked regions, HDDMA:HEMA co-photopolymerized films with varying degrees of stratification were placed in a 175 degrees Celsius oven (above the glass transition temperature) for one hour. All of the films tested curled toward the HDDMA enriched side. The film curls as a result of more stress being relieved on the opposite side of the HDDMA enriched side via heating due to the increased mobility from decreased

crosslinked density. However, the amount of film curl did not correlate with the degree of stratification possibly due to conversion or modulus differences also present through the thickness of the film. Non-uniform stress relief is another illustration of how stratification could affect the bulk properties of a film.

The HEMA:HDDMA system illustrates the ability to produce films with a chemical concentration gradient utilizing photo-enforced stratification (Chapter 4). Changes in the surface chemical composition result in changing the surface properties with only small changes in bulk properties. The ability to change the surface properties without greatly affecting the bulk properties will reduce the complexity in designing functional polymer film with desired surface properties since the surface properties seem to be relatively independent of the bulk properties.

Differential reactivity rate of mono- and di-ene monomers is not the only driving force capable of producing stratified films where the changes in surface chemistry also change surface properties. Monomers with inherent differences in reactivity, specifically methacrylate and acrylate monomers, have exhibited the ability to generate stratified films for which preferentially reacting monomer, methacrylate in these formulations, is enriched in the high light intensity regions of the film (Chapter 6). These differences in inherent reactivity in a co-polymerization can be expressed as reactivity ratios defined as the ratio of the homo-polymerization rate coefficient to the hetero-polymerization rate coefficient.^{34,35} The monomers with the higher reactivity ratio in the co-polymerization will preferentially react. These reactivity ratios predict that the methacrylate monomer would preferential react in a co-photopolymerization of methacrylate and acrylamide.

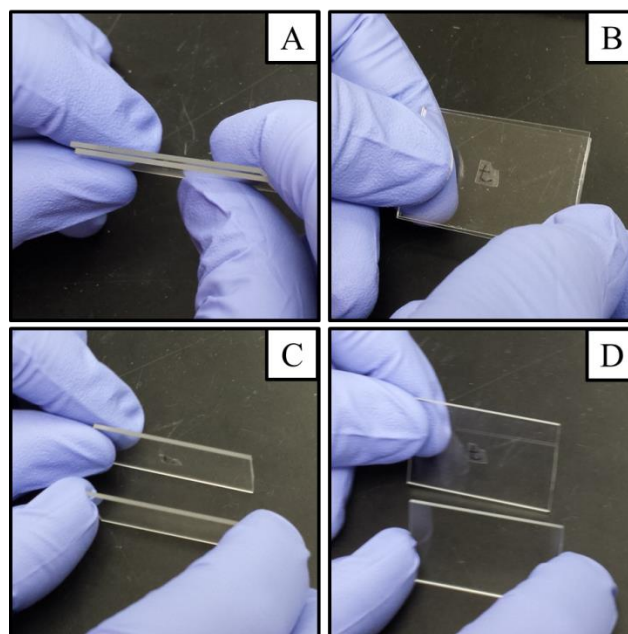


Figure 7.3. Images of one to one mole ratio 2-methoxyethyl methacrylate and N-hydroxyethyl acrylamide polymerized (A and B) in a laminate mold. The high light intensity side of the film is labeled with a t. (C and D) Pulling the laminate mold apart results in the low light intensity side of the film adhering to the glass slide.

To test the hypothesis that this co-photopolymerization could result in a stratified film with different surface properties, formulations containing 2-methoxyethyl methacrylate and N-hydroxyethyl acrylamide, in a one to one mole ratio, were polymerized with various concentrations of DMPA in a laminate mold using 365 nm light with an intensity of 1 mW/cm^2 . Based on the inherent reactivity difference, the production of stratified films should result in surface enrichment of the methacrylate. The produced films proved difficult to analyze with ATR probably due to the very high degree of hydrogen bonding present which affects the infrared band desired to be analyzed.³⁶⁻³⁹ However, stratified films were produced as evident via differential surface adhesion properties (Figure 7.3). These surface adhesion property differences are evident by placing a stratified film between two glass slides and pressing the glass slide together (Figures 7.3A and B). When the glass slides are pulled apart the film consistently sticks

to the low light intensity side of the polymer film (Figures 7.3C and D). The differences in surface adhesion occur because the low light intensity side has a higher concentration of the acrylamide which acts as an adhesion promoter due to all the hydrogen bonding. These results illustrate the ability to modify adhesion in a film and thus increase the number of surface properties which can be tuned via photo-enforced stratification.

The difficulties in analyzing the methacrylate and acrylamide copolymerization films with ATR illustrate the need for other techniques to analyze the surface of the polymer films. An attractive technique for surface analysis is x-ray photoelectron spectroscopy (XPS). XPS is an analytical technique that interrogates the surface of the sample by exposing the surface to x-rays resulting in the ejection of core photoelectrons.⁴⁰ The kinetic energy of the ejected electron is indicative of a particular atom thereby allowing identification of chemical or electronic state of the elements in the film and therefore the composition of the film surface.

XPS was used to examine film surface composition utilizing a simple copolymerization of methyl methacrylate (MMA) and 2-(dimethylamino)ethyl acrylate (DMAEA) produced from a low, 0.1 weight percent, and high, 4 weight percent, concentration of photoinitiator, DMPA. Thus, the low concentration of photoinitiator would result in a small light gradient which is likely insufficient for photo-enforced stratification in contrast to the high concentration on initiator which has a much greater light gradient. As seen with previous systems (Chapter 6), photo-enforced stratification would result in a surface enrichment of the methacrylate and therefore result in a decrease in the nitrogen signal detected with XPS as the nitrogen is only in the acrylate structure. XPS was used to examine nitrogen (Figure 7.4A) and carbon (Figure 7.4B) 1S signals for both the low (Figure 7.4A and B spectrum 1) and the high (Figure 7.4A and B spectrum 2) concentration of photoinitiator. The nitrogen peak area can be divided by the carbon peak area to yield a ratio which allows for the surface composition to be analyzed. The ratios are equal to 0.144 and 0.055 for the low and high concentration of photoinitiator,

respectively, indicating the presence of approximately 3 times more nitrogen species at the surface of the low photoinitiator concentration film. The decreased nitrogen at the surface of the higher photoinitiator concentration system is a direct result of photo-enforced stratification enriching the surface with methacrylate and thus reducing the nitrogen signal from the acrylate. XPS is a viable technique for examining the surface composition of polymer films and could be used for formulations where it is difficult to use ATR or Raman spectroscopy.

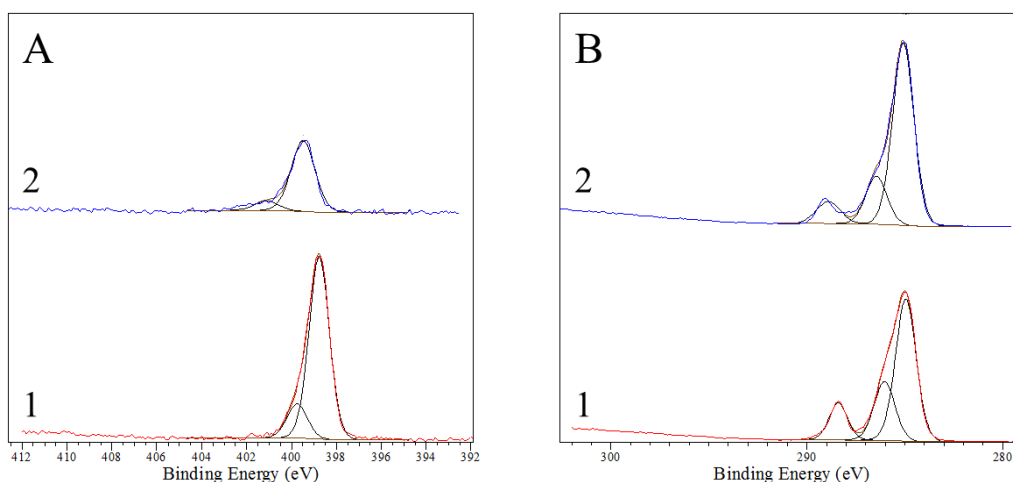


Figure 7.4. XPS spectral regions for (A) N 1s and (B) C 1s of polymer composed of a 1:1 mass ratio of methyl methacrylate to 2-(dimethylamino)ethyl acrylate polymerized with (1) 0.1 and (2) 4 wt% photoinitiator.

The systems studied so far have all utilized Norrish type one photoinitiation in which the photoinitiator absorbs a photon and cleaves to produce radicals. Other strategies exist for initiating photopolymerization such as Norrish type two photoinitiation which requires an initiator, commonly a dye, and a co-initiator, commonly a tertiary amine. An advantage to using a Norrish type two process is that visible light can be used to initiate photopolymerization rather than needing UV light as for typical

Norrish type one processes. Type two photoinitiation is a process in which a dye absorbs light which then abstracts a hydrogen atom from the co-initiator to generate a radical that can subsequently initiate polymerization. In order to produce a composition gradient via photopolymerization with a Norrish type two photoinitiator, a light gradient will induce a reaction gradient in the film as the upper regions of the film polymerize faster due to the increased rates of initiation. This causes a change in the chemical potential of the tertiary amine species driving its diffusion to the surface. If the tertiary amine is attached to one of the monomers in the copolymerization, that monomer would thereby be enriched at the surface in the event of photo-enforced stratification.

To test type two photoinitiation as a driving force for photo-enforced stratification, a series of three systems of monomers and photoinitiators were studied. The first system (DMAEA:HEA) consists of an amine containing monomer (DMAEA) and a dye for the photoinitiator (methylene blue (MB)) which only allows for type two initiation in the polymerization (Initiation Type 2). The initiating light was a full spectrum white light. The second system also employs an amine contacting monomer (DMAEA:HEA), but DMPA is used as the photoinitiator so that type two photoinitiation is still possible but is not the primary method of initiation (Initiation Type 1A). UV light was used to cure this system. The third and final system (MOA:HEA) did not employ an amine containing monomer or a dye as the initiator thereby eliminating the possibility of type two photoinitiation leaving only type one photoinitiation (Initiation Type 1B). Again, UV light was used to cure this system. All the films were polymerized as a laminate and ATR spectra were collected for each surface of the film. The hydroxyl to carbonyl peak height was determined from the ATR spectra using the ratio of top to bottom composition to examine the degree of stratification (Table 1). When type two photoinitiation is the only initiating mechanism then an approximate forty percent surface enrichment of the tertiary amine monomer, DMAEA, is observed. This indicates that type two photoinitiation is a strong driving force for stratification. If the tertiary amine is not

in the system, then less than 5 percent monomer enrichment is observed when polymerizing two acrylates indicating virtually no photo-enforced stratification. If type one photoinitiation is the primary initiation method but type two photoinitiation is still possible, then a small amount of stratification is observed as illustrated from the approximately 10 percent surface enrichment of the tertiary amine monomer (DMAEA). These results indicate that Norrish type two photoinitiation processes are capable of producing a chemical gradient in a polymer film even if it is not the only photoinitiation process present in the formulation. The ability to generate stratified photopolymer films using visible light allows for photo-enforced stratification to be utilized in systems where the use of UV light could have a negative affect such as the photopolymerization of dental resins.

Table 7.1. Percent surface enrichment of the three different initiation systems in photopolymers. All monomers are at a 1:1 molar ratio.

Initiation Type	Photoinitiator	Monomers	Surface Enrichment
2	0.05 wt% MB w/0.25 wt% DPI	DMAEA:HEA	~ 40%
1A	1 wt% DMPA	DMAEA:HEA	~ 10%
1B	1 wt% DMPA	MOA:HEA	>5%

Finally, another promising photopolymerization method has been explored with great potential for stratification. All previous examples have utilized radical chain growth photopolymerization. Thiol-ene photopolymerization utilizes a radical step growth photopolymerization which has several distinct advantages including: 1) a significant range of reactivities and 2) vitrification at much higher conversions. The large reactive differences allow for larger differences in monomer consumption resulting in increased monomer diffusion during co-photopolymerization in the presence of a light gradient.

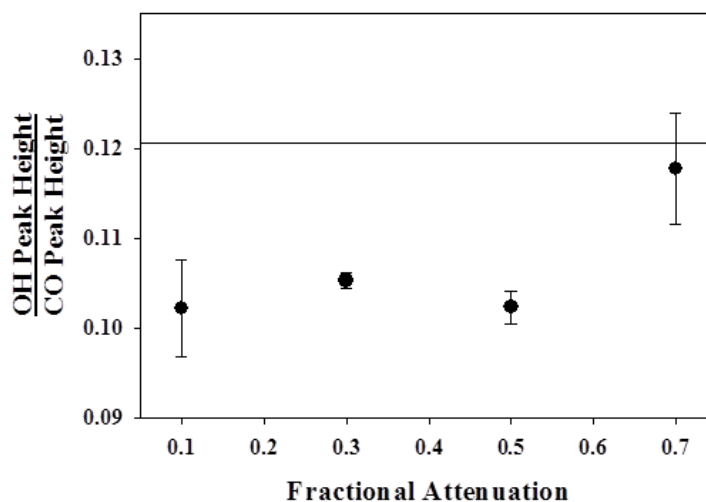


Figure 7.5. Surface composition ratio of thiol-ene films produced from a two to one to one molar ratio of trimethylopropane tris(2-mecaptoacetate) to tri(ethylene glycol) divinyl ether to trimethlopropane diallyl ether as a function of fractional attenuation of light from DMPA. 8 mil thick films were polymerized on a glass slide in an inert atmosphere with 365 nm light at 1 mW/cm². Composition ratios were determined via ATR. Error bars represent the standard deviation of a minimum of three replicate measurements.

Additionally, the delayed vitrification affords additional time for monomer diffusion to occur during the photopolymerization. Thus, the combination of increased reactivity differences and increased monomer diffusion time may result in a range in stratification. The reactivity difference between allyl and vinyl ethers toward a thiol was examined to potentially produce stratified films. The vinyl ether is more reactive than the allyl ether in thiol-ene polymerization, and therefore surface enrichment of the vinyl ether should result. Thiol-ene formulations consisted of a 2:1:1 molar ratio of trimethylopropane tris(2-mecaptoacetate) to tri(ethylene glycol) divinyl ether and trimethlopropane diallyl ether with various concentrations of DMPA. Film surfaces were analyzed with ATR to determine the surface composition defined by the ratio of the OH to CO peak height. The surface composition was plotted as a function of light attenuation (Figure 7.5). The solid line indicates the transmission IR spectrum and the polymerized

formulation giving the overall ratio of OH to CO peaks for the bulk formulation. Deviations from this line indicate a stratified film. The 0.1, 0.3, and 0.5 fractional light attenuation formulations all exhibit surface compositions of approximately 0.10 indicating surface enrichment of the vinyl ether. Increasing the concentration DMPA to yield a 0.7 fractional light attenuation resulted in the surface composition being approximately equal to the bulk composition indicating a loss of vinyl ether from the surface. The lower fractional attenuation films show an approximate 20 percent enrichment of the vinyl ether at the surface of the film. The observed monomer enrichment illustrates the ability and potential for thiol-ene systems to undergo photo-enforced stratification.

Conclusions

The single step production of a chemical composition gradient in a polymer film allows production of novel properties in polymer films which are not currently available with current technologies. Co-photopolymerization of monomers with kinetic differences in the presence of a light gradient was utilized to produce stratified films and the bulk and surface properties were examined. Photo-cured HDDMA:HEMA stratified films exhibit slight increases in the thermal transitions associated with HDDMA due to the higher concentration of HDDMA at the surface. Additionally, releasing the shrinkage stress by heating the film above its glass transition temperature results in the films curling toward the HDDMA enrich side. These results illustrate only small changes in the bulk properties with chemical composition gradients. Adhesion modification was illustrated with a 1:1 molar ratio of MOMA:HEAA by producing a polymer film with only one side being able to stick to glass. XPS can be utilized to determine polymer film surface composition and is a viable analytical substitute for formulations that are not easily analyzed with ATR or Raman spectroscopy. Type two photoinitiation was shown to produce stratified films when a monomer in the formulation contained a functional group

capable of acting as a co-initiator. Finally, Thiol-ene photopolymers produced from a 2:1:1 molar ratio of trimethylolpropane diallyl ether to tri(ethylene glycol) divinyl ether and trimethylpropane tris(2-mercaptoacetate) resulting in an approximately a 20 percent surface enrichment of the tri(ethylene glycol) divinyl ether monomer. The results presented in this work illustrate numerous chemistries which allow for the production of a polymer film with a chemical concentration gradient from a single reaction step via photopolymerization. Further study of these chemistries and the resulting bulk and surface chemistries will result in the ability to produce polymer films with novel properties which are currently inaccessible.

Notes

1. Noeske, M., et al., International Journal of Adhesion and Adhesives (2004) **24** (2), 171
2. Liston, E. M., et al., Journal of Adhesion Science and Technology (1993) **7** (10), 1091
3. Wavhal, D. S., and Fisher, E. R., Langmuir (2002) **19** (1), 79
4. Statz, A. R., et al., Journal of the American Chemical Society (2005) **127** (22), 7972
5. Huang, J., et al., Biomacromolecules (2007) **8** (5), 1396
6. Cen, L., et al., Langmuir (2003) **19** (24), 10295
7. Zhang, W., et al., Biomaterials (2006) **27** (1), 44
8. Okouchi, M., et al., Macromolecules (2006) **39** (3), 1156
9. Sangermano, M., et al., Polymer (2009) **50** (24), 5647
10. Nowicki, M., et al., Polymer (2003) **44** (21), 6599
11. Goddard, J. M., and Hotchkiss, J. H., Progress in Polymer Science (2007) **32** (7), 698
12. Ma, Z., et al., Colloids and Surfaces B: Biointerfaces (2007) **60** (2), 137
13. Walheim, S., et al., Macromolecules (1997) **30** (17), 4995
14. Le Minez, J.-J., and Schmitt, B., Wet-on-wet coating process. Peintures Corona S.A., United States, (1983)
15. Chen, W., and McCarthy, T. J., Macromolecules (1997) **30** (1), 78
16. Chen, J., and Gardella, J. A., Macromolecules (1998) **31** (26), 9328
17. Ikejima, T., and Inoue, Y., Macromol. Chem. Phys. (2000) **201** (14), 1598
18. Inagaki, N., et al., Journal of Polymer Science Part B: Polymer Physics (2004) **42** (20), 3727
19. Vesel, A., et al., Surface and Interface Analysis (2008) **40** (11), 1444
20. Kubota, H., J. Appl. Polym. Sci. (1992) **46** (3), 383
21. Pan, B., et al., J. Polym. Sci. A Polym. Chem. (2004) **42** (8), 1953
22. Zhu, J., et al., Macromol. Chem. Phys. (2006) **207** (1), 75
23. Padon, K. S., and Scranton, A. B., J. Polym. Sci. A Polym. Chem. (2000) **38** (11), 2057

24. Van Landuyt, K. L., et al., *Biomaterials* (2007) **28** (26), 3757
25. Corrales, T., et al., *J. Photochem. Photobiol. A-Chem.* (2003) **159** (2), 103
26. Hoyle, C. E., and Bowman, C. N., *Angew. Chem.-Int. Edit.* (2010) **49** (9), 1540
27. Hoyle, C. E., et al., *Chem. Soc. Rev.* (2010) **39** (4), 1355
28. Usher, C. R., et al., *Langmuir* (2007) **23** (13), 7039
29. Volkert, A. A., et al., *ACS Nano* (2011) **5** (6), 4570
30. Forney, B. S., and Guymon, C. A., *Macromol. Rapid Commun.* (2011) **32** (9-10), 765
31. Lester, C. L., et al., *Chemistry of Materials* (2003) **15** (17), 3376
32. Owusu-Adom, K., et al., *Macromolecules* (2009) **42** (9), 3275
33. Kahar, N., et al., *Polymer* (1978) **19** (2), 136
34. Odian, G., *Principles of Polymerization*. 4 ed.; John Wiley & Sons: Hoboken, New Jersey, 2004
35. Jansen, J. F. G. A., et al., *Macromolecules* (2004) **37** (6), 2275
36. Skrovanek, D. J., et al., *Macromolecules* (1985) **18** (9), 1676
37. Huggins, C. M., and Pimentel, G. C., *The Journal of Physical Chemistry* (1956) **60** (12), 1615
38. Witkowski, A., *The Journal of Chemical Physics* (1967) **47** (9), 3645
39. Dong, J., et al., *Macromolecules* (1997) **30** (4), 1111
40. Kolasinski, K. W., *Surface Science: Foundations of Catalysis and Nanoscience*. Second ed.; John Wiley & Sons, Ltd: 2008

CHAPTER 8 CONCLUSIONS AND RECOMMENDATIONS

In this thesis, control of the surface chemistry and properties has been achieved using photopolymerization in a single step. The inherent temporal and spatial control of photopolymerization allows generation of controlled, non-uniform polymerization conditions which can be utilized to spatially control the composition of a polymer film produced from a co-photopolymerization of monomers of unequal reactivity. The preferentially reacting monomer is enriched in regions of the film where the polymerization rates are greater. Moreover, developing an understanding of kinetic and diffusional effects controlled by the formulation chemistry and processing conditions on the resulting stratification has been critical for successful production of stratified photopolymer films.

The differences observed in the rate of polymerization between a mono-ene and a di-ene monomer was hypothesized to afford production of a stratified film via photopolymerization. Moreover, di-ene monomers are known to polymerize at a greater rate than an analogous mono-ene monomers which should result in enrichment of the di-ene monomer in the high light intensity regions of the film. To test this hypothesis, co-photopolymerization formulations of 2-hydroxyethyl methacrylate (HEMA) with 1,6-hexanediol dimethacrylate (HDDMA) initiated with various amounts of 2,2-dimethoxy-2-phenylacetophenone (DMPA) was used to examine the kinetic difference between mono- and di-ene monomers in Chapter 4. Photopolymerization of 300 micrometer thick films utilizing 365 nm light with an intensity of 1 mW/cm^2 produced films with an approximately 20 percent surface enrichment of the faster reacting HDDMA. Processing parameters such as the concentration of photoinitiator, film thickness, light intensity, and constant versus pulsed illumination were examined to determine important parameters for the production of stratified films. Specifically, increasing the photoinitiator concentration in the pre-polymer formulations results in decreased degrees of monomer surface

enrichment. Increasing the film thickness results in increasing the difference in the light intensities at the top and bottom of the polymerizing film which results in additional monomer surface enrichment. Similar to increasing the DMPA concentration, increasing the initiating light intensity causes increases in the observed rates of polymerization and decreases in the amount of stratification. Finally, pulsed illumination reduces monomer enrichment for all formulations tested. These results illustrate the important balance between kinetic differences and diffusion. Specifically, stratification requires the presence of a light gradient and sufficient time for monomer diffusion. Additionally, production of a stratified film affords control over the resulting surface properties. Increasing the surface concentration with HDDMA, the crosslinking and more hydrophobic monomer, increases the hardness of the film and the water contact angle by five degrees.

The production of a chemical concentration gradient in a polymer film via photopolymerization requires both non-uniform polymerization rates through the depth of the film and monomer diffusion. Moreover, the HDDMA (di-ene)/ HEMA (mono-ene) co-photopolymerization was further examined through the production of a mathematical model based on the principles of kinetics and diffusion in Chapter 5. The core of the model is a mass balance which was solved using coupled differential equations for the kinetics and diffusion as a function of depth and time utilizing a modified Euler method. The rate of polymerization, monomer consumption, monomer diffusion, and chemical composition are all critical to the production of a stratified film and was readily examined with the model. Specifically, the modeled rate of polymerization shows increased rates of polymerization at the surface of the film, due to the light gradient, which results in greater monomer consumption in these high light intensity regions of the film. Due to the higher rates of monomer consumption at the surface, the model predicts a net diffusion of the di-ene monomer to the surface and an equimolar counter diffusion of the mono-ene into the bulk. As a result, the final predicted film has a 10 percent enrichment of the di-

ene monomer at the surface of the polymer film. Moreover, the model qualitatively agrees with the expected trends for polymerization rate, monomer consumption, and monomer diffusion. Additionally, the model qualitatively correlates with the experimentally observed chemical composition in which the di-ene is enriched at the surface of the polymer film.

The kinetic difference between mono-ene and di-ene monomers illustrates the ability to produce photopolymer films with differences in surface composition and properties. Chapter 6 tested the hypothesis that pre-polymer formulations with other kinetic differences would be capable of producing a polymer film with a chemical concentration gradient via photopolymerization. Specifically, inherent monomer reactivity between a methacrylate and an acrylate, as quantified by reactivity ratios, produced films with the preferentially reacting methacrylate enriching the high light intensity regions of the film. Additionally, the hypothesis that films with large amounts of stratification are possible by utilizing pre-polymer formulations with multiple kinetic differences synergistically working together to generate substantial reaction differences between monomers in the co-photopolymerization was evaluated. The synergic kinetic difference combination of oxygen inhibition with inherent monomer reactivity was studied with a co-photopolymerization of a methacrylate and an acrylate leading to substantial reaction preference of the methacrylate resulted in an approximate 50 percent increase in methacrylate surface enrichment compared to stratified films produced utilizing inherent monomer reactivity alone. Another example of synergistic combinations examined was mono- vs di-ene with inherent monomer reactivity as studied by a co-photopolymerization of a di-methacrylate and a mono-acrylate. This system exhibits a 150 percent increase in di-ene monomer surface enrichment compared to films produced with mono- vs di-ene kinetic differences alone. Additionally, both photobleaching and non-photobleaching photoinitiators produce similar stratified films.

A brief examination of bulk properties, type two photoinitiation, and thiol-ene chemistry was also described in Chapter 7. Bulk polymer properties were examined in the HEMA:HDDMA co-photopolymerization via dynamic mechanical analysis (DMA), swelling studies, and heating polymer films above the glass transition temperature. DMA results illustrate increases in an HDDMA phase transitions due to the increased HDDMA phase as a result of stratification. Stratification appears to have little effect on the bulk polymer properties especially when compared to the large changes observed in the surface properties as a result of the chemical gradient allowing for simplified formulation development of stratified films. Using a monomer in the co-photopolymerization that acts as a co-initiator for type two photoinitiation films also enhance enrichment of the co-initiator monomer in the high light intensity regions of the film. Finally, thiol-ene chemistry yields films with the preferentially reacting ene monomer enriching at the high light intensity regions of the film from a co-photopolymerization of a thiol with two different ene monomers. Thus, thiol-ene chemistry is a viable and promising mechanism of producing a stratified film. The results from the type two photoinitiation and thiol-ene chemistry illustrate the ability to produce stratified films from mechanisms other than radical chain photopolymerization initiated via type one photoinitiation, thereby greatly increasing the flexibility of formulations capable of producing a stratified film.

The presented body of work illustrates production of stratified films with controllable surface chemistries and properties in a single reaction step utilizing the inherent temporal and spatial control of photopolymerization. While this work establishes concepts and general criteria for the production of a stratified film via photopolymerization, there are still significant questions and opportunities. Building off of the current body of work, further research into advanced model development, production of a light gradient with a secondary chromophore, and exploration into thiol-ene chemistry would greatly enhance the understanding and applicability of photo-enforced stratification.

For example, additions to the model described in Chapter 5 will help increase the predictive power of the model and as a result, valuable experimental time could be saved by narrowing in on experimental parameters and monomer formulations to predict the highest degrees of monomer enrichment possible. Initial and immediately implementable model improvements include fractional free volume during the polymerization and heat of polymerization. Fractional free volume is a way to express how freely material can move within the system.¹ Goodner, et al. has eloquently illustrated methods in which fractional free volume and heat of polymerization can be utilized to adjust kinetic and diffusive parameters during the course of a polymerization. Specifically, fractional free volume and heat of polymerization allows changes to the propagation rate coefficient, termination rate coefficient, and the diffusion coefficient. As a result, kinetic features like autoacceleration and diffusive features like vitrification could be more accurately predicted by the model. Additionally, fractional free volume would allow for modeling the addition of inert solvent into the formulations and the possible effects on the final stratification achieved in the polymer.

Completion of a reaction-diffusion model to predict photo-enforced stratification, as outlined above, would also serve as a great starting point for modeling other pre-polymer formulations of interest. For example, modifying the model to predict other radical chain photopolymerizations such as the acrylate methacrylate co-photopolymerization described in Chapter 6 could be accomplished by modifying the kinetic differences in the model. This would require a more rigorous mass balance, specifically on the radical species with the presence of multiple radical types, to capture the kinetics but should be possible given the framework of the current model. Modeled systems would not be limited to radical chain photopolymerizations. Thiol-ene kinetics equations can also be modeled² which should allow for the kinetic behavior of thiol-enes to predict stratification as observed in experimental results.

As stated previously, the work presented utilized the photoinitiator to create the light gradient required for photo-enforced stratification to occur. As a result, increasing the light gradient also increased the rate of polymerization resulting in less time for monomer diffusion to occur which, in turn, decreased the amount of stratification. Decoupling these effects would result in increased control over the final polymer composition. A straightforward method of decoupling these effects would be the addition of a secondary chromophore to produce the light gradient. Chromophores of interest include photostabilizers and non-reactive chromophores. The inclusion of a photostabilizer as the chromophore could lead to stratified coatings for outdoor applications and would also make stratified coatings formulations more realistic for industrial applications. However, the addition of a photostabilizer would add complexity to the photopolymerization reaction which would require further study to be able to produce stratified films utilizing these additives.³⁻⁵

Non-reactive dyes, for the purposes of this study, would be chemicals which do not form radicals and do not directly react with radicals in high yields. For instance, utilizing dyes to form the light gradient would be instructive in real world applications where the addition of a dye is desired for coloration. Readily available, well studied dyes with absorption spectra that cover the majority of wavelengths⁶ used to initiate photopolymerization such as laser dyes could be used. Another well studied chromophore with potentially interesting properties for photo-enforced stratification is azobenzene which goes through a cis-trans isomerization. Ground state azobenzene is primarily in the trans state but will isomerize to the cis state when illuminated with UV light. The cis state will return to the ground state given sufficient time or upon heating or illumination with visible light.^{7,8} Rather than adding azobenzene alone, a symmetric, di-functional monomer could be synthesized which has the azobenzene moiety at the center.⁹⁻¹¹ Thus, utilizing the synthesized monomer in a co-photopolymerization of a mono-methacrylate (Chapter 4) should result in a polymer film enriched with the azo monomer. Films of

similar nature have illustrated non-uniform stress at the side of the film enriched with the crosslinking monomer. However, molecular volume reduction has been illustrated to occur as a result of the isomerization and with sufficient loading of azobenzene functional group can result in polymer actuation.^{8,11} In this formulation the crosslinking monomer would be in the shorter cis conformation during polymerization and could then revert back to the longer trans conformation post polymerization as a means of reducing polymerized induced shrinkage stress.

Finally, thiol-ene chemistry has many mechanistic advantages for producing a stratified film via photopolymerization (Chapters 1 and 7). Briefly, thiol-ene polymerizations have a wide range of monomer reactivities to utilize in the production of a stratified film. They also exhibit delayed in the gel point conversion allowing additional time for monomer diffusion to produce a stratified film. The presented work demonstrates the production of a stratified film from a single formulation of a thiol monomer with two different ene monomers. Numerous other ene monomer combinations exist allowing for the resulting stratification. Of particular interest would be ternary system of thiol-ene-methacrylate due to the unique reaction kinetics observed due to the methacrylate reacting almost exclusively via homopolymerization.¹² Moreover, there are other thiol monomers which could be studied in combination with a constant ene monomer. These combinatorial studies will help further elucidate the kinetic requirements for the production of a stratified film. Additionally, thiol-ene formulations containing four monomers should be studied. Such formulations, while greatly increased in complexity, could result in a high degree of control and wide range of the polymer film properties.

The work presented generates a fundamental understanding of utilizing photopolymerization for the production of polymers with a composition gradient. Completion of the suggested work will result in a versatile toolbox for generating formulations and processing techniques which can produce films with controllable

surface chemistries and properties. Moreover, polymers will be able to be produced in a single step process with unprecedented control of surface chemistry and properties independent from the bulk chemistry and properties allowing for the generation of many novel properties in various applications. Additionally, the production cost of films with this degree of control over the surface chemistry and properties in a single step is very attractive from an industrial production perspective as the reduction of processing steps and time will result in significant financial advantages.

Notes

1. Goodner, M. D., and Bowman, C. N., *Chemical Engineering Science* (2002) **57** (5), 887
2. Cramer, N. B., *et al.*, *Macromolecules* (2003) **36** (12), 4631
3. Cho, J.-D., *et al.*, *Macromol. Res.* (2007) **15** (6), 560
4. Schrof, W., *et al.*, *Progress in Organic Coatings* (1999) **35** (1-4), 197
5. Decker, C., *et al.*, *J. Polym. Sci. A Polym. Chem.* (1991) **29** (5), 739
6. Duarte, F. J., and Foster, D. R., Lasers, Dye. In *The Optics Encyclopedia*, Wiley-VCH Verlag GmbH & Co. KGaA(2007)
7. Wei-Guang Diao, E., *The Journal of Physical Chemistry A* (2004) **108** (6), 950
8. Merino, E., and Ribagorda, M., *Beilstein Journal of Organic Chemistry* (2012) **8**, 1071
9. Launay, J.-P., *et al.*, *Inorganic Chemistry* (1991) **30**, 1033
10. Brown, E. V., and Granneman, G. R., *Journal of American Chemical Society* (1975) **97**, 621
11. Yu, Y., *et al.*, *Nature* (2003) **425**, 145
12. Lee, T. Y., *et al.*, *Macromolecules* (2007) **40** (5), 1466

APPENDIX A MATLAB MODEL OF PHOTO-ENFORCED STRATIFICATION FOR MONO- VS DI-ENE SYSTEMS

Description

The modeling code described in Chapter 5 is shown in detail below. The code is written and evaluated using MatLab and the associated proper programming language. As such, the information per line and the indentation of each line is intentional to ease visualization and reproduction. Additionally, italicized text is not part of the model code itself but rather comments about the code to aid the reader. Finally, the units for a given variable will be listed using [=] followed by the units. This appendix serves as a resource for modeling photopolymerization reactions with specific emphasis on modeling the production of a stratified film from photopolymerization.

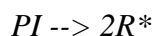
Background Information

The model is generated from differential equations which describe the kinetics of photopolymerization and diffusion in a polymerizing system. A modified Euler method is used to solve for the differential equations. Good background is provided in the following paper: Goodner, M. D., and Bowman, C. N., Chemical Engineering Science (2002) 57 (5), 887. Additionally, the user should be familiar with MatLab code prior to using the model.

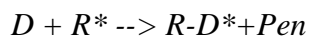
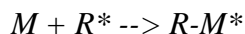
MatLab Code

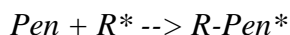
Chemical Reactions

Initiation

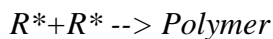


Propagation





Termination



Diffusion

Fick diffusion accounting for equal molar counter diffusion is utilized in this model.

VERY IMPORTANT

*Convergence Criteria: For this model to work you need to satisfy $0.5 < ((D*dt)/(dz^2))$ where D is your diffusion coefficient, dt is your time step, and dz is your depth step. If this criteria is not met the model will not work.*

clear all clears all data and variables from MatLab

Time Variance

dt = 0.01; incremental illumination time step [=] seconds

Tt = 150; total illumination time [=] seconds

a = 0:dt:Tt; arbitrary array describing the time steps used allowing for calculation loops to be utilized with the proper step size and variable value

Depth Variance

dz = 0.0005; incremental thickness of layers [=] cm

Tz = 0.0300; total film thickness [=] cm

b = 0:dz:Tz; arbitrary array describing the depth steps used allowing for calculation loops to be utilized with the proper step size and variable value

Constants

kpM = 18; rate constant for propagation of mono-ene

kpD = 18; rate constant for propagation of di-ene

kpPen = 180; rate constant for propagation of pendant reaction

kt = 415; rate constant for overall termination reaction

epsilon = 150; molecular absorbance of the photoinitiator in log base 10

Io = 1; light intensity [=] mW/cm²

$\text{DiffCoeffM} = 4.5 \times 10^{-6}$; *diffusion coefficient Mono-Ene [=] cm²/s*

$\text{DiffCoeffD} = 4.5 \times 10^{-6}$; *diffusion coefficient Di-Ene [=] cm²/s*

$E_{\text{prime}} = 327744.016$ *this value is calculated from (Avogadro's Number)*(Planck's constant)*(frequency of initiating light)*

Initial Values of Variables

$M_0 = 4.1$; *initial concentration of mono-ene [=] moles/L*

$D_0 = 8.2$; *initial concentration of di-ene [=] moles/L*

$\text{Pen}_0 = 0$; *initial concentration of pendant group [=] moles/L*

$\text{PI}_0 = 0.04$; *initial concentration of photo initiator [=] moles/L*

Pre-allocation of Variables - this makes the calculation run faster

$M = \text{zeros}(\text{length}(b), \text{length}(a))$; *creates Mono-ene concentration matrix*

$D = \text{zeros}(\text{length}(b), \text{length}(a))$; *creates Di-ene concentration matrix*

$\text{Pen} = \text{zeros}(\text{length}(b), \text{length}(a))$; *creates Pendant concentration matrix*

$R = \text{zeros}(\text{length}(b), \text{length}(a))$; *creates Radical concentration matrix*

$\text{PI} = \text{zeros}(\text{length}(b), \text{length}(a))$; *creates Photoinitiator concentration matrix*

$R_i = \text{zeros}(\text{length}(b), \text{length}(a))$; *creates Ri matrix*

$R_pM = \text{zeros}(\text{length}(b), \text{length}(a))$; *creates RpM matrix*

$R_pD = \text{zeros}(\text{length}(b), \text{length}(a))$; *creates RpD matrix*

$R_p\text{Pen} = \text{zeros}(\text{length}(b), \text{length}(a))$; *creates RpPen matrix*

$R_t = \text{zeros}(\text{length}(b), \text{length}(a))$; *creates Rt matrix*

$M_{\text{prime}} = \text{zeros}(\text{length}(b), \text{length}(a))$; *creates first derivate of M matrix*

$D_{\text{prime}} = \text{zeros}(\text{length}(b), \text{length}(a))$; *creates first derivate of D matrix*

$M_{\text{flux}} = \text{zeros}(\text{length}(b), \text{length}(a))$; *creates mono-ene flux matrix*

$D_{\text{flux}} = \text{zeros}(\text{length}(b), \text{length}(a))$; *creates di-ene flux matrix*

$M_{\text{diff}} = \text{zeros}(\text{length}(b), \text{length}(a))$; *creates mono-ene diffusion matrix*

$D_{\text{diff}} = \text{zeros}(\text{length}(b), \text{length}(a))$; *creates di-ene diffusion matrix*

$M_{\text{Diff}} = \text{zeros}(\text{length}(b), \text{length}(a))$; *creates mono-ene net diffusion matrix*

DDiff = zeros(length(b),length(a)); *creates di-ene net diffusion matrix*

Photo-Enforced Stratification Model Calculations

Initial Inputs - populates the pre-allocated matrixes with the initial values defined earlier

M(:,1) = M0; *initial total concentration of Mono-ene group [=] moles/L*

D(:,1) = D0; *initial total concentration of Di-ene group [=] moles/L*

Pen(:,1) = Pen0; *initial total concentration of Pendant group [=] moles/L*

R(:,1) = 0; *initial total concentration of radical [=] moles/L*

PI(:,1) = PI0; *initial concentration of photo initiator [=] moles/L*

The model itself is an all-encompassing time loop with embedded depth loops.

Specifically, the model calculates the desired variables for all depths and then advances one step in time and again calculates all the depth steps again. Thus, the differential equations are explicitly solved at each time step using either the initial inputs (first cycle only) or the results from the previous time cycle. In so doing, the model solves for the coupled polymerization rate and diffusion rate utilizing a modified Euler technique.

for t = 1:length(a);

POLYMERIZATION

Initiation

for z = 1:length(b);

$R_i(z,t) = (((\epsilon \cdot I_0 \cdot 10^{(-\epsilon \cdot PI_0 \cdot (z-1) \cdot dz))} \cdot PI(z,t)) / E_{prime}) \cdot dt$;

initiation rate as a function of depth

end

Propagation

for z = 1:length(b);

$R_pM(z,t) = (k_pM \cdot M(z,t) \cdot R(z,t)) \cdot dt$; *mono-ene propagation rate*

$R_pD(z,t) = (k_pD \cdot D(z,t) \cdot R(z,t)) \cdot dt$; *di-ene propagation rate*

$R_pPen(z,t) = (k_pPen \cdot Pen(z,t) \cdot R(z,t)) \cdot dt$; *pendent propagation rate*

end

Termination

for z = 1:length(b);

$$Rt(z,t) = ((kt.*R(z,t).^2)).*dt; \textit{ termination rate}$$

end

DIFFUSION

for z = 2:length(b)-1;

first derivatives of mono- and di-ene mole

note: the z loop excludes the top and bottom due to the boundary condition stating you cannot have things diffuse out of or into the laminate system.

$$Mprime(z,t) = (((-1/2).*M(z-1,t)+(1/2).*M(z+1,t))./dz);$$

$$Dprime(z,t) = (((-1/2).*D(z-1,t)+(1/2).*D(z+1,t))./dz);$$

end

for z = 1:length(b); *flux of mobile species*

$$Mflux(z,t) = DiffCoeffM.*Mprime(z,t);$$

$$Dflux(z,t) = DiffCoeffD.*Dprime(z,t);$$

end

Calculating the actual diffusion of the mobile species

note: The ends have to be treated differently than the center points.

The equations used have the same order of accuracy.

$$Mdiff(1,t) = ((((-3/2).*Mflux(1,t)+2.*Mflux(2,t)+(-1/2).*Mflux(3,t))./dz).*dt);$$

$$Ddiff(1,t) = ((((-3/2).*Dflux(1,t)+2.*Dflux(2,t)+(-1/2).*Dflux(3,t))./dz).*dt);$$

for z = 2:length(b)-1;

$$Mdiff(z,t) = ((((-1/2).*Mflux(z-1,t)+(1/2).*Mflux(z+1,t))./dz).*dt);$$

$$Ddiff(z,t) = ((((-1/2).*Dflux(z-1,t)+(1/2).*Dflux(z+1,t))./dz).*dt);$$

end

$$Mdiff(length(b),t) = (((3/2).*Mflux(length(b),t)-2.*Mflux(length(b)-1,t)+(1/2).*Mflux(length(b)-2,t))./dz).*dt);$$

$Ddiff(length(b),t) = (((3/2). *Dflux(length(b),t)-2.*Dflux(length(b)-1,t)+(1/2). *Dflux(length(b)-2,t))./dz). *dt);$

for z = 1:length(b); *this calculates equimolar counter diffusion – think of the calculated diffusion as vectors, this step is then just a sum of vectors*

$MDiff(z,t) = Mdiff(z,t)-Ddiff(z,t);$

$DDiff(z,t) = Ddiff(z,t)-Mdiff(z,t);$

end

Overall Mass Balances

d[]/dt = Diffusion - Reaction

for z = 1:length(b)

$PI(z,t+1) = PI(z,t)-Ri(z,t);$

$R(z,t+1) = R(z,t)+2.*Ri(z,t)-2.*Rt(z,t);$

$M(z,t+1) = M(z,t)-RpM(z,t)+MDiff(z,t);$

$D(z,t+1) = D(z,t)-2.*RpD(z,t)+DDiff(z,t);$

$Pen(z,t+1) = Pen(z,t)+RpD(z,t)-RpPen(z,t);$

end

end

You will now find matrix outputs with describe the variables used in the calculations as a function of depth (rows) and time (columns).

BIBLIOGRAPHY

- Adrus, N. and M. Ulbricht. "Rheological Studies on Pnipaam Hydrogel Synthesis Via in Situ Polymerization and on Resulting Viscoelastic Properties." *Reactive & Functional Polymers* 73, no. 1 (2013): 141-148.
- Aimetti, A. A., A. J. Machen and K. S. Anseth. "Poly(Ethylene Glycol) Hydrogels Formed by Thiol-Ene Photopolymerization for Enzyme-Responsive Protein Delivery." *Biomaterials* 30, no. 30 (2009): 6048-6054.
- Allcock, Harry R., Frederick W. Lampe and James E. Mark. *Contemporary Polymer Chemistry*. Third ed. Upper Saddle River, New Jersey: Pearson Education, Inc., 2003.
- Alvarez-Blanco, S, S. Manolache and F. Denes. "A Novel Plasma-Enhanced Way for Surface-Functionalization of Polymeric Substrates." *Polym Bull* 47, (2001): 329-236.
- An, Y. J. and J. A. Hubbell. "Intraarterial Protein Delivery Via Intimately-Adherent Bilayer Hydrogels." *Journal of Controlled Release* 64, no. 1-3 (2000): 205-215.
- Andrzejewska, Ewa. "Photopolymerization Kinetics of Multifunctional Monomers." *Progress in Polymer Science* 26, no. 4 (2001): 605-665.
- Anseth, K. S., K. J. Anderson and C. N. Bowman. "Radical Concentrations, Environments, and Reactivities During Crosslinking Polymerizations." *Macromolecular Chemistry and Physics* 197, no. 3 (1996): 833-848.
- Atkins, P. and J. De Paula. *Atkins' Physical Chemistry*. 8th ed. New York, NY: W. H. Freeman and Company, 2006.
- Bal, T., B. Kepsutlu and S. Kizilel. "Characterization of Protein Release from Poly(Ethylene Glycol) Hydrogels with Crosslink Density Gradients." *Journal of Biomedical Materials Research Part A* 102, no. 2 (2014): 487-495.
- Barachevskii, V. A. "Photopolymerizable Recording Media for Three-Dimensional Holographic Optical Memory." *High Energy Chemistry* 40, no. 3 (2006): 131-141.
- Berchtold, Kathryn A., Theodore W. Randolph and Christopher N. Bowman. "Propagation and Termination Kinetics of Cross-Linking Photopolymerizations Studied Using Electron Paramagnetic Resonance Spectroscopy in Conjunction with near Ir Spectroscopy." *Macromolecules* 38, no. 16 (2005): 6954-6964.
- Brandrup, J., E. H. Immergut and E. A. Grulke, eds. *Polymer Handbook*. Hoboken, NJ: John Wiley & Sons, 1999.
- Brown, Ellis V and G. Richard Granneman. "Cis-Trans Isomerism in the Pyridyl Analogs of Azobenzene. A Kinetic and Molecular Orbital Analysis." *Journal of American Chemical Society* 97, (1975): 621-627.
- Brown, William H. and Christopher S. Foote. *Organic Chemistry*. 2nd ed.: Fort Worth: Saunders College Pub, 1998.

- Bryant, S. J. and K. S. Anseth. "Hydrogel Properties Influence Ecm Production by Chondrocytes Photoencapsulated in Poly(Ethylene Glycol) Hydrogels." *Journal of Biomedical Materials Research* 59, no. 1 (2002): 63-72.
- Bunning, T. J., L. V. Natarajan, V. P. Tondiglia and R. L. Sutherland. "Holographic Polymer-Dispersed Liquid Crystals (H-Pdlcs)1." *Annual Review of Materials Science* 30, no. 1 (2000): 83-115.
- Cai, Ying and Julie L. P. Jessop. "Decreased Oxygen Inhibition in Photopolymerized Acrylate/Epoxide Hybrid Polymer Coatings as Demonstrated by Raman Spectroscopy." *Polymer* 47, (2006): 6560-6566.
- Carioscia, Jacquelyn A., Hui Lu, Jeffrey W. Stanbury and Christopher N. Bowman. "Thiol-Ene Oligomers as Dental Restorative Materials." *Dental Materials* 21, no. 12 (2005): 1137-1143.
- Cen, Lian, K. G. Neoh and E. T. Kang. "Surface Functionalization Technique for Conferring Antibacterial Properties to Polymeric and Cellulosic Surfaces." *Langmuir* 19, no. 24 (2003): 10295-10303.
- Chan, C.-M., T.-M. Ko and H. Hiraoka. "Polymer Surface Modification by Plasmas and Photons." *Surface Science Reports* 24, (1996): 1-54.
- Chan, Justin W., Hui Zhou, Charles E. Hoyle and Andrew B. Lowe. "Photopolymerization of Thiol-Alkynes: Polysulfide Networks." *Chemistry of Materials* 21, no. 8 (2009): 1579-1585.
- Chen, Jiaying and Joseph A. Gardella. "Solvent Effects on the Surface Composition of Poly(Dimethylsiloxane)-Co-Polystyrene/Polystyrene Blends." *Macromolecules* 31, no. 26 (1998): 9328-9336.
- Chen, Wei and Thomas J. McCarthy. "Layer-by-Layer Deposition: A Tool for Polymer Surface Modification." *Macromolecules* 30, no. 1 (1997): 78-86.
- Cho, Jung-Dae, Sung-Hwa Kim, In-Cheol Chang, Kwon-Seok Kim and Jin-Who Hong. "Photostabilization and Cure Kinetics of Uv-Curable Optical Resins Containing Photostabilizers." *Macromolecular Research* 15, no. 6 (2007): 560-564.
- Clapper, J. D., L. Sievens-Figueroa and C. A. Guymon. "Photopolymerization in Polymer Templating." *Chemistry of Materials* 20, no. 3 (2008): 768-781.
- Clapper, Jason D., Megan E. Pearce, C. Allan Guymon and Aliasger K. Salem. "Biotinylated Biodegradable Nanotemplated Hydrogel Networks for Cell Interactive Applications." *Biomacromolecules* 9, no. 4 (2008): 1188-1194.
- Cook, Clinton J. and C. Allan Guymon. "Photo-Enforced Stratification of Polymeric Materials." USA: The University of Iowa Research Foundation, 2011.
- Corrales, T., F. Catalina, C. Peinado and N. S. Allen. "Free Radical Macrophotoinitiators: An Overview on Recent Advances." *Journal of Photochemistry and Photobiology a-Chemistry* 159, no. 2 (2003): 103-114.

- Cramer, Neil B. and Christopher N. Bowman. "Kinetics of Thiol–Ene and Thiol–Acrylate Photopolymerizations with Real-Time Fourier Transform Infrared." *Journal of Polymer Science Part A: Polymer Chemistry* 39, no. 19 (2001): 3311-3319.
- Cramer, Neil B., Tanner Davies, Allison K. O'Brien and Christopher N. Bowman. "Mechanism and Modeling of a Thiol–Ene Photopolymerization." *Macromolecules* 36, no. 12 (2003): 4631-4636.
- Cramer, Neil B., Sirish K. Reddy, Hui Lu, Tsali Cross, Rishi Raj and Christopher N. Bowman. "Thiol-Ene Photopolymerization of Polymer-Derived Ceramic Precursors." *Journal of Polymer Science Part A: Polymer Chemistry* 42, no. 7 (2004): 1752-1757.
- Cramer, Neil B., J. Paul Scott and Christopher N. Bowman. "Photopolymerizations of Thiol–Ene Polymers without Photoinitiators." *Macromolecules* 35, no. 14 (2002): 5361-5365.
- Crank, John. *The Mathematics of Diffusion*. New York: Oxford University Press, 1975.
- De Santis, Alberto. "Photo-Polymerisation Effects on the Carbonyl Co Bands of Composite Resins Measured by Micro-Raman Spectroscopy." *Polymer* 46, no. 14 (2005): 5001-5004.
- Decker, C., K. Moussa and T. Bendaikha. "Photodegradation of Uv-Cured Coatings Ii. Polyurethane–Acrylate Networks." *Journal of Polymer Science Part A: Polymer Chemistry* 29, no. 5 (1991): 739-747.
- Decker, Christian and Aubrey D. Jenkins. "Kinetic Approach of Oxygen Inhibition in Ultraviolet- and Laser-Induced Polymerizations." *Macromolecules* 18, no. 6 (1985): 1241-1244.
- Denes, Ferencz S. and Sorin Manolache. "Macromolecular Plasma-Chemistry: An Emerging Field of Polymer Science." *Progress in Polymer Science* 29, (2004): 815-885.
- Dong, Jian, Yukihiko Ozaki and Kenichi Nakashima. "Infrared, Raman, and near-Infrared Spectroscopic Evidence for the Coexistence of Various Hydrogen-Bond Forms in Poly(Acrylic Acid)." *Macromolecules* 30, no. 4 (1997): 1111-1117.
- Duarte, Francisco J. and David R. Foster. "Lasers, Dye." In *The Optics Encyclopedia*: Wiley-VCH Verlag GmbH & Co. KGaA, 2007.
- Dube, M., R. Amin Sanayei, A. Penlidis, K. F. O'Driscoll and P. M. Reilly. "A Microcomputer Program for Estimation of Copolymerization Reactivity Ratios." *Journal of Polymer Science Part A: Polymer Chemistry* 29, no. 5 (1991): 703-708.
- Elabd, Yossef A., Marco Giacinti Baschetti and Timothy A. Barbari. "Time-Resolved Fourier Transform Infrared/Attenuated Total Reflection Spectroscopy for the Measurement of Molecular Diffusion in Polymers." *Journal of Polymer Science Part B: Polymer Physics* 41, no. 22 (2003): 2794-2807.

- Elliott, J. E., L. G. Lovell and C. N. Bowman. "Primary Cyclization in the Polymerization of Bis-Gma and Tegdma: A Modeling Approach to Understanding the Cure of Dental Resins." *Dental Materials* 17, no. 3 (2001): 221-229.
- Forney, B. S., C. Baguenard and C. A. Guymon. "Effects of Controlling Polymer Nanostructure Using Photopolymerization within Lyotropic Liquid Crystalline Templates." *Chemistry of Materials* 25, no. 15 (2013): 2950-2960.
- Forney, B. S. and C. A. Guymon. "Fast Deswelling Kinetics of Nanostructured Poly(N-Isopropylacrylamide) Photopolymerized in a Lyotropic Liquid Crystal Template." *Macromolecular Rapid Communications* 32, no. 9-10 (2011): 765-769.
- Fouassier, Jean-Pierre. *Photoinitiation, Photopolymerization, and Photocuring*. Munchen, Germany: Ludwig Auer GmbH, Donauworth, 1995.
- Gleeson, Michael R. and John T Sheridan. "A Review of the Modelling of Free-Radical Photopolymerization in the Formation of Holographic Gratings." *Journal of Optics A: Pure and Applied Optics* 11, (2009): 024008.
- Goddard, J. M. and J. H. Hotchkiss. "Polymer Surface Modification for the Attachment of Bioactive Compounds." *Progress in Polymer Science* 32, no. 7 (2007): 698-725.
- Goodner, Michael D. and Christopher N. Bowman. "Modeling and Experimental Investigation of Light Intensity and Initiator Effects on Solvent-Free Photopolymerizations." In *Solvent-Free Polymerizations and Processes*, 220-231 SE - 14: American Chemical Society, 1999.
- Goodner, Michael D. and Christopher N. Bowman. "Modeling Primary Radical Termination and Its Effects on Autoacceleration in Photopolymerization Kinetics." *Macromolecules* 32, no. 20 (1999): 6552-6559.
- Goodner, Michael D. and Christopher N. Bowman. "Development of a Comprehensive Free Radical Photopolymerization Model Incorporating Heat and Mass Transfer Effects in Thick Films." *Chemical Engineering Science* 57, no. 5 (2002): 887-900.
- Goodner, Michael D., Hyun R. Lee and Christopher N. Bowman. "Method for Determining the Kinetic Parameters in Diffusion-Controlled Free-Radical Homopolymerizations." *Industrial & Engineering Chemistry Research* 36, no. 4 (1997): 1247-1252.
- Gou, Lijing, Blaine Opheim and Alec B. Scranton. "The Effect of Oxygen in Free Radical Photopolymerization." *Recent Research Developments in Polymer Science*, (2004): 125-141.
- Gou, Lijing, Blaine Opheim and Alec B. Scranton. "Methods to Overcome Oxygen Inhibition in Free Radical Photopolymerizations." *Photochemistry and UV Curing: New Trends*, (2006): 301-310.
- Herlihy, S. "The Influence of Uv Light Absorption and Oxygen Inhibition on Photo-Dsc Results." *RadTech Europe 99 Conference Proceedings, 8-10 November 1999*, (1999): 489-495.

- Hinkelmann, F., O. F. Olaj, I. Schnoll-Bitai and G. Zifferer. "A Linearization Procedure for Determining Radical Reactivity Ratios in Restricted Penultimate Copolymerization Systems, 2." *Macromolecular Rapid Communications* 29, no. 9 (2008): 695-712.
- Hoyle, C. E. and C. N. Bowman. "Thiol-Ene Click Chemistry." *Angewandte Chemie-International Edition* 49, no. 9 (2010): 1540-1573.
- Hoyle, C. E., A. B. Lowe and C. N. Bowman. "Thiol-Click Chemistry: A Multifaceted Toolbox for Small Molecule and Polymer Synthesis." *Chemical Society Reviews* 39, no. 4 (2010): 1355-1387.
- Hoyle, Charles E., Tai Yeon Lee and Todd Roper. "Thiol-Enes: Chemistry of the Past with Promise for the Future." *Journal of Polymer Science Part A: Polymer Chemistry* 42, no. 21 (2004): 5301-5338.
- Huang, Jinyu, Hironobu Murata, Richard R. Koepsel, Alan J. Russell and Krzysztof Matyjaszewski. "Antibacterial Polypropylene Via Surface-Initiated Atom Transfer Radical Polymerization." *Biomacromolecules* 8, no. 5 (2007): 1396-1399.
- Huggins, Charles M. and George C. Pimentel. "Systematics of the Infrared Spectral Properties of Hydrogen Bonding Systems: Frequency Shift, Half Width and Intensity." *The Journal of Physical Chemistry* 60, no. 12 (1956): 1615-1619.
- Ikejima, T. and Y. Inoue. "Experimental Approaches to Generate Compositional Gradients in the Fully Biodegradable Polymer Blend System Based on Poly(3-Hydroxybutyric Acid)." *Macromolecular Chemistry and Physics* 201, no. 14 (2000): 1598-1604.
- Ikemura, Kunio and Takeshi Endo. "A Review of the Development of Radical Photopolymerization Initiators Used for Designing Light-Curing Dental Adhesives and Resin Composites." *Dental Materials Journal* 29, no. 5 (2010): 481-501.
- Inagaki, Norihiro, Kazuo Narushim, Norio Tsuchida and Kohji Miyazaki. "Surface Characterization of Plasma-Modified Poly(Ethylene Terephthalate) Film Surfaces." *Journal of Polymer Science Part B: Polymer Physics* 42, no. 20 (2004): 3727-3740.
- Jansen, Johan F. G. A., Aylvin A. Dias, Marko Dorschu and Betty Coussens. "Fast Monomers: Factors Affecting the Inherent Reactivity of Acrylate Monomers in Photoinitiated Acrylate Polymerization." *Macromolecules* 36, no. 11 (2003): 3861-3873.
- Jansen, Johan F. G. A., Erwin E. J. E. Houben, Peter H. G. Tummens, Dietrich Wienke and John Hoffmann. "Real-Time Infrared Determination of Photoinitiated Copolymerization Reactivity Ratios: Application of the Hilbert Transform and Critical Evaluation of Data Analysis Techniques." *Macromolecules* 37, no. 6 (2004): 2275-2286.
- Kahar, N., R. A. Duckett and I. M. Ward. "Stress Optical Studies of Oriented Poly(Methyl Methacrylate)." *Polymer* 19, no. 2 (1978): 136-144.

- Kato, Koichi, Emiko Uchida, En-Tang Kang, Yoshikimi Uyama and Yoshito Ikada. "Polymer Surface with Graft Chains." *Progress in Polymer Science* 28, (2003): 209-259.
- Kenning, Nicole Stephenson, Beth A. Ficek, Cindy C. Hoppe and Alec B. Scranton. "Spatial and Temporal Evolution of the Photoinitiation Rate for Thick Polymer Systems Illuminated by Polychromatic Light: Selection of Efficient Photoinitiators for Led or Mercury Lamps." *Polymer International* 57, no. 10 (2008): 1134-1140.
- Kim, Soon Ki and C. Allan Guymon. "Photopolymerization Behavior in Nanocomposites Formed with Thiol–Acrylate and Polymerizable Organoclays." *Journal of Polymer Science Part A: Polymer Chemistry* 49, no. 2 (2011): 465-475.
- Kloosterboer, J. G., G. F. C. M. Lijten and C. P. G. Zegers. "Formation of Densely Crosslinked Polymer Glasses by Photopolymerization." *Polym Mat: Sci Eng Proc ACS Div Polym Mater: Sci Eng* 60, (1989): 122-127.
- Kolasinski, Kurt W. *Surface Science: Foundations of Catalysis and Nanoscience*. Second ed.: John Wiley & Sons, Ltd, 2008.
- Kubota, H. and A. Fukuda. "Photopolymerization Synthesis of Poly(N-Isopropylacrylamide) Hydrogels." *Journal of Applied Polymer Science* 65, no. 7 (1997): 1313-1318.
- Kubota, Hitoshi. "Factors Influencing Vapor-Phase Photografting of Styrene/Acrylonitrile Monomer Mixtures on Polymer Films." *Journal of Applied Polymer Science* 46, no. 3 (1992): 383-388.
- Launay, Jean-Pierre, Myriam Tourrel-Pagis, Jean-Francois Lipskier, Valerie Marvaud and Christian Joachim. "Control of Intramolecular Electron Transfer by a Chemical Reaction. The 4,4'-Azopyridine/1,2-Bis(4-Pyridyl)Hydrazine System." *Inorganic Chemistry* 30, (1991): 1033-1038.
- Le Minez, Jean-Jacques and Bernard Schmitt. "Wet-on-Wet Coating Process." United States: Peintures Corona S.A., 1983.
- Lee, E., K. Kim, M. Choi, Y. Lee, J. W. Park and B. Kim. "Development of Smart Delivery System for Ascorbic Acid Using Ph-Responsive P(Maa-Co-Egma) Hydrogel Microparticles." *Drug Delivery* 17, no. 8 (2010): 573-580.
- Lee, Sang-Hyuck, No-Cheol Park, Hyunseok Yang, Kyoung-Su Park and Young-Pil Park. "Optical Design of a Single-Sided Microholographic Data-Storage System Using a Diffractive Optical Element and a Blue Laser." *Journal of Optics* 13, no. 5 (2011): 055403.
- Lee, T.Y., C.A. Guymon, E. Sonny Jönsson and C.E. Hoyle. "The Effect of Monomer Structure on Oxygen Inhibition of (Meth)Acrylates Photopolymerization." *Polymer* 45, no. 18 (2004): 6155-6162.
- Lee, Tai Yeon, Zachary Smith, Sirish K. Reddy, Neil B. Cramer and Christopher N. Bowman. "Thiol–Allyl Ether–Methacrylate Ternary Systems. Polymerization Mechanism." *Macromolecules* 40, no. 5 (2007): 1466-1472.

- Leewis, C. M., A. M. de Jong, L. J. van Ijzendoorn and D. J. Broer. "Reaction-Diffusion Model for the Preparation of Polymer Gratings by Patterned Ultraviolet Illumination." *Journal of Applied Physics* 95, no. 8 (2004): 4125-4139.
- Leewis, C. M., A. M. de Jong, L. J. van Ijzendoorn and D. J. Broer. "Simulations with a Dynamic Reaction-Diffusion Model of the Polymer Grating Preparation by Patterned Ultraviolet Illumination." *Journal of Applied Physics* 95, no. 12 (2004): 8352-8356.
- Leewis, C. M., D. P. L. Simons, A. M. de Jong, D. J. Broer and M. J. A. de Voigt. "Pixe Monitoring of Diffusion During Photo-Polymerization." *Nuclear Instruments and Methods in Physics Research Section B: Beam Interactions with Materials and Atoms* 161-163, (2000): 651-655.
- Leewis, C.M., P.H.A. Mutsaers, A.M. de Jong, L.J. van IJzendoorn, D.J. Broer and M.J.A. de Voigt. "Monomer Diffusion Assisted Preparation of Polymer Gratings: A Nuclear Microprobe Study." *Nuclear Instruments and Methods in Physics Research Section B: Beam Interactions with Materials and Atoms 7th International Conference on Nuclear Microprobe Technology and Applications* 181, no. 1-4 (2001): 367-371.
- Leewis, Christian M., Arthur M. de Jong, Leo J. van IJzendoorn and Dirk J. Broer. "Simulations with a Dynamic Reaction-Diffusion Model of the Polymer Grating Preparation by Patterned Ultraviolet Illumination." *Journal of Applied Physics* 95, no. 12 (2004): 8352-8356.
- Leewis, Christian M., Arthur M. de Jong, Leo J. van IJzendoorn and Dirk J. Broer. "Reaction-Diffusion Model for the Preparation of Polymer Gratings by Patterned Ultraviolet Illumination." *Journal of Applied Physics* 95, no. 8 (2004): 4125-4139.
- Leewis, Christian M., Peter H.A. Mutsaers, Arthur M. de Jong, Leo J. van IJzendoorn, Martien J.A. de Voigt, Min Q. Ren, Frank Watt and Dirk J. Broer. "The Mutual Diffusion Coefficient for (Meth)Acrylate Monomers as Determined with a Nuclear Microprobe." *Journal of Chemical Physics* 120, no. 4 (2004): 1820-1825.
- Lester, Christopher L., Shannon M. Smith, Colleen D. Colson and C. Allan Guymon. "Physical Properties of Hydrogels Synthesized from Lyotropic Liquid Crystalline Templates." *Chemistry of Materials* 15, no. 17 (2003): 3376-3384.
- Li, Xin, Mengmeng Wang, Lei Wang, Xiujuan Shi, Yajun Xu, Bo Song and Hong Chen. "Block Copolymer Modified Surfaces for Conjugation of Biomacromolecules with Control of Quantity and Activity." *Langmuir* 29, no. 4 (2012): 1122-1128.
- Liston, E. M., L. Martinu and M. R. Wertheimer. "Plasma Surface Modification of Polymers for Improved Adhesion: A Critical Review." *Journal of Adhesion Science and Technology* 7, no. 10 (1993): 1091-1127.
- Lovestead, Tara M., Allison K. O'Brien and Christopher N. Bowman. "Models of Multivinyl Free Radical Photopolymerization Kinetics." *Journal of Photochemistry and Photobiology A: Chemistry* 159, no. 2 (2003): 135-143.

- Lu, Hui, Jacquelyn A. Carioscia, Jeffery W. Stansbury and Christopher N. Bowman. "Investigations of Step-Growth Thiol-Ene Polymerizations for Novel Dental Restoratives." *Dental Materials* 21, no. 12 (2005): 1129-1136.
- Ma, Zuwei, Zhengwei Mao and Changyou Gao. "Surface Modification and Property Analysis of Biomedical Polymers Used for Tissue Engineering." *Colloids and Surfaces B: Biointerfaces* 60, no. 2 (2007): 137-157.
- Mann, B. K., A. S. Gobin, A. T. Tsai, R. H. Schmedlen and J. L. West. "Smooth Muscle Cell Growth in Photopolymerized Hydrogels with Cell Adhesive and Proteolytically Degradable Domains: Synthetic Ecm Analogs for Tissue Engineering." *Biomaterials* 22, no. 22 (2001): 3045-3051.
- Maruo, Shoji, Osamu Nakamura and Satoshi Kawata. "Three-Dimensional Microfabrication with Two-Photon-Absorbed Photopolymerization." *Optics Letters* 22, no. 2 (1997): 132-134.
- McQuillan, A. J. "Probing Solid-Solution Interfacial Chemistry with Atr-Ir Spectroscopy of Particle Films." *Advanced Materials* 13, no. 12-13 (2001): 1034-1038.
- Merino, Estíbaliz and María Ribagorda. "Control over Molecular Motion Using the Cis-Trans Photoisomerization of the Azo Group." *Beilstein Journal of Organic Chemistry* 8, (2012): 1071-1090.
- Nguyen, K. T. and J. L. West. "Photopolymerizable Hydrogels for Tissue Engineering Applications." *Biomaterials* 23, no. 22 (2002): 4307-4314.
- Noeske, Michael, Jost Degenhardt, Silke Strudthoff and Uwe Lommatzsch. "Plasma Jet Treatment of Five Polymers at Atmospheric Pressure: Surface Modifications and the Relevance for Adhesion." *International Journal of Adhesion and Adhesives* 24, no. 2 (2004): 171-177.
- Nowicki, Marek, Asta Richter, Bodo Wolf and Halina Kaczmarek. "Nanoscale Mechanical Properties of Polymers Irradiated by Uv." *Polymer* 44, no. 21 (2003): 6599-6606.
- O'Brien, Allison K. and Christopher N. Bowman. "Modeling Thermal and Optical Effects on Photopolymerization Systems." *Macromolecules* 36, no. 20 (2003): 7777-7782.
- O'Brien, Allison K. and Christopher N. Bowman. "Impact of Oxygen on Photopolymerization Kinetics and Polymer Structure." *Macromolecules* 39, no. 7 (2006): 2501-2506.
- O'Brien, Allison K. and Christopher N. Bowman. "Modeling the Effect of Oxygen on Photopolymerization Kinetics." *Macromolecular Theory and Simulations* 15, no. 2 (2006): 176-182.
- O'Brien, Allison K., Neil B. Cramer and Christopher N. Bowman. "Oxygen Inhibition in Thiol-Acrylate Photopolymerizations." *Journal of Polymer Science Part A: Polymer Chemistry* 44, no. 6 (2006): 2007-2014.
- Odian, George. *Principles of Polymerization*. 4 ed. Hoboken, New Jersey: John Wiley & Sons, 2004.

- Okouchi, Motohiro, Yoshinao Yamaji and Kiyoshi Yamauchi. "Contact Angle of Poly(Alkyl Methacrylate)s and Effects of the Alkyl Group." *Macromolecules* 39, no. 3 (2006): 1156-1159.
- Oral, E. and N. A. Peppas. "Dynamic Studies of Molecular Imprinting Polymerizations." *Polymer* 45, no. 18 (2004): 6163-6173.
- Owusu-Adom, K., J. Schall and C. A. Guymon. "Photopolymerization Behavior of Thiol-Acrylate Monomers in Clay Nanocomposites." *Macromolecules* 42, no. 9 (2009): 3275-3284.
- Padon, Kathryn Sirovatka and Alec B. Scranton. "A Mechanistic Investigation of a Three-Component Radical Photoinitiator System Comprising Methylene Blue, N-Methyldiethanolamine, and Diphenyliodonium Chloride." *Journal of Polymer Science Part A: Polymer Chemistry* 38, no. 11 (2000): 2057-2066.
- Pan, Bo, Kalyanaraman Viswanathan, Charles E. Hoyle and Robert B. Moore. "Photoinitiated Grafting of Maleic Anhydride onto Polypropylene." *Journal of Polymer Science Part A: Polymer Chemistry* 42, no. 8 (2004): 1953-1962.
- Penterman, Roel, Stephen I. Klink, Henk de Koning, Giovanni Nisato and Dirk J. Broer. "Single-Substrate Liquid-Crystal Displays by Photo-Enforced Stratification." *Nature* 417, no. 6884 (2002): 55.
- Polic, A. L., T. A. Duever and A. Penlidis. "Case Studies and Literature Review on the Estimation of Copolymerization Reactivity Ratios." *Journal of Polymer Science Part A: Polymer Chemistry* 36, no. 5 (1998): 813-822.
- Qian, T. Z., J. H. Kim, S. Kumar and P. L. Taylor. "Phase-Separated Composite Films: Experiment and Theory." *Physical Review E* 61, no. 4 (2000): 4007-4010.
- Qie, Lili and Marc A. Dubé. "Manipulation of Chain Transfer Agent and Cross-Linker Concentration to Modify Latex Micro-Structure for Pressure-Sensitive Adhesives." *European Polymer Journal* 46, no. 6 (2010): 1225-1236.
- Reddy, S. K., N. B. Cramer, M. Kalvaitas, T. Y. Lee and C. N. Bowman. "Mechanistic Modelling and Network Properties of Ternary Thiol-Vinyl Photopolymerizations." *Australian Journal of Chemistry* 59, no. 8 (2006): 586-593.
- Rosen, Stephen L. *Fundamental Principles of Polymeric Materials*. Second ed. New York, New York: John Wiley & Sons, Inc., 1993.
- Sangermano, M., M. Messori, M. Martin Galleco, G. Rizza and B. Voit. "Scratch Resistant Tough Nanocomposite Epoxy Coatings Based on Hyperbranched Polyesters." *Polymer* 50, no. 24 (2009): 5647-5652.
- Sawhney, A. S., C. P. Pathak and J. A. Hubbell. "Bioerodible Hydrogels Based on Photopolymerized Poly(Ethylene Glycol)-Co-Poly(Alpha-Hydroxy Acid) Diacrylate Macromers." *Macromolecules* 26, no. 4 (1993): 581-587.

- Schrof, W., E. Beck, R. Königer, W. Reich and R. Schwalm. "Depth Profiling of Uv Cured Coatings Containing Photostabilizers by Confocal Raman Microscopy." *Progress in Organic Coatings* 35, no. 1-4 (1999): 197-204.
- Sheridan, J T, J V Kelly, M R Gleeson, C E Close and F T O'Neill. "Optimized Holographic Data Storage: Diffusion and Randomization." *Journal of Optics A: Pure and Applied Optics* 8, no. 3 (2006): 236.
- Skeist, Irving. "Copolymerization: The Composition Distribution Curve." *Journal of the American Chemical Society* 68, no. 9 (1946): 1781-1784.
- Skrovanek, Daniel J., Stephen E. Howe, Paul C. Painter and Michael M. Coleman. "Hydrogen Bonding in Polymers: Infrared Temperature Studies of an Amorphous Polyamide." *Macromolecules* 18, no. 9 (1985): 1676-1683.
- Smith, Derrick M., Christopher Y. Li and Timothy J. Bunning. "Light-Directed Mesoscale Phase Separation Via Holographic Polymerization." *Journal of Polymer Science Part B: Polymer Physics* 52, no. 3 (2014): 232-250.
- Standard, ASTM. "Astm Standard D3363." In *Standard Test Method for Film Hardness by Pencil Test*. West Conshohocken, PA: ASTM International, 2005 (2011).
- Statz, Andrea R., Robert J. Meagher, Annelise E. Barron and Phillip B. Messersmith. "New Peptidomimetic Polymers for Antifouling Surfaces." *Journal of the American Chemical Society* 127, no. 22 (2005): 7972-7973.
- Staudinger, H. and J. Schneiders. *Ann. Chim.* 541, no. 151 (1939).
- Stevens, Malcolm P. *Polymer Chemistry: An Introduction*. Third ed. New York, New York: Oxford University Press, 1999.
- Straub, M., L. H. Nguyen, A. Fazlic and M. Gu. "Complex-Shaped Three-Dimensional Microstructures and Photonic Crystals Generated in a Polysiloxane Polymer by Two-Photon Microstereolithography." *Optical Materials* 27, no. 3 (2004): 359-364.
- Sullivan, Amy C., Matthew W. Grabowski and Robert R. McLeod. "Three-Dimensional Direct-Write Lithography into Photopolymer." *Applied Optics* 46, no. 3 (2007): 295-301.
- Sutherland, R. L., L. V. Natarajan, V. P. Tondiglia and T. J. Bunning. "Bragg Gratings in an Acrylate Polymer Consisting of Periodic Polymer-Dispersed Liquid-Crystal Planes." *Chemistry of Materials* 5, no. 10 (1993): 1533-1538.
- Tomlinson, W. J., E. A. Chandross, H. P. Weber and G. D. Aumiller. "Multicomponent Photopolymer Systems for Volume Phase Holograms and Grating Devices." *Applied Optics* 15, no. 2 (1976): 534-541.
- Tummers, Peter H.G., Erwin J.E. Houben, Johan F.G.A. Jansen and Dietrich Wienke. "Evaluation of Advanced Data Analysis Techniques on Time Resolved Ft-Ir Spectroscopy Data of Photo-Copolymerization Reactions." *Vibrational Spectroscopy* 43, no. 1 (2007): 116-124.

- Usher, Courtney R., Jonas Baltrusaitis and Vicki H. Grassian. "Spatially Resolved Product Formation in the Reaction of Formic Acid with Calcium Carbonate (1014): The Role of Step Density and Adsorbed Water-Assisted Ion Mobility." *Langmuir* 23, no. 13 (2007): 7039-7045.
- van der Zande, Bianca M. I., Jan Steenbakkens, Johan Lub, Christian M. Leewis and Dirk J. Broer. "Mass Transport Phenomena During Lithographic Polymerization of Nematic Monomers Monitored with Interferometry." *Journal of Applied Physics* 97, no. 12 (2005): 123519.
- Van Landuyt, Kirsten L., Johan Snauwaert, Jan De Munck, Marleen Peumans, Yasuhiro Yoshida, André Poitevin, Eduardo Coutinho, Kazuomi Suzuki, Paul Lambrechts and Bart Van Meerbeek. "Systematic Review of the Chemical Composition of Contemporary Dental Adhesives." *Biomaterials* 28, no. 26 (2007): 3757-3785.
- van Nostrum, C. F., R. J. M. Nolte, D. J. Broer, T. Fuhrmann and J. H. Wendorff. "Photoinduced Opposite Diffusion of Nematic and Isotropic Monomers During Patterned Photopolymerization." *Chemistry of Materials* 10, no. 1 (1998): 135-145.
- van Oosten, Casper L., Daniel Corbett, Dylan Davies, Mark Warner, Cees W. M. Bastiaansen and Dirk J. Broer. "Bending Dynamics and Directionality Reversal in Liquid Crystal Network Photoactuators." *Macromolecules* 41, no. 22 (2008): 8592-8596.
- Vesel, Alenka, Ita Junkar, Uros Cvelbar, Janez Kovac and Miran Mozetic. "Surface Modification of Polyester by Oxygen- and Nitrogen-Plasma Treatment." *Surface and Interface Analysis* 40, no. 11 (2008): 1444-1453.
- Volkert, A. A. and A. J. Haes. "Advancements in Nanosensors Using Plastic Antibodies." *Analyst* 139, no. 1 (2014): 21-31.
- Volkert, Anna A., Varuni Subramaniam, Michael R. Ivanov, Amanda M. Goodman and Amanda J. Haes. "Salt-Mediated Self-Assembly of Thioctic Acid on Gold Nanoparticles." *ACS Nano* 5, no. 6 (2011): 4570-4580.
- Vorflusev, Valery and Satyendra Kumar. "Phase-Separated Composite Films for Liquid Crystal Displays." *Science* 283, no. 5409 (1999): 1903.
- Walheim, Stefan, Martin Böltau, Jürgen Mlynek, Georg Krausch and Ullrich Steiner. "Structure Formation Via Polymer Demixing in Spin-Cast Films." *Macromolecules* 30, no. 17 (1997): 4995-5003.
- Wavhal, Dattatray S. and Ellen R. Fisher. "Membrane Surface Modification by Plasma-Induced Polymerization of Acrylamide for Improved Surface Properties and Reduced Protein Fouling." *Langmuir* 19, no. 1 (2002): 79-85.
- Wei-Guang Diao, Eric. "A New Trans-to-Cis Photoisomerization Mechanism of Azobenzene on the S1(N,Π*) Surface." *The Journal of Physical Chemistry A* 108, no. 6 (2004): 950-956.
- Wei, Huanyu, Qin Li, Moriam Ojelade, Samy Madbouly, Joshua U. Otaigbe and Charles E. Hoyle. "Thiol-Ene Free-Radical and Vinyl Ether Cationic Hybrid Photopolymerization." *Macromolecules* 40, no. 24 (2007): 8788-8793.

- White, Timothy J., William B. Liechty, Lalgudi V. Natarajan, Vincent P. Tondiglia, Timothy J. Bunning and C. Allan Guymon. "The Influence of N-Vinyl-2-Pyrrolidinone in Polymerization of Holographic Polymer Dispersed Liquid Crystals (Hpdlds)." *Polymer* 47, no. 7 (2006): 2289-2298.
- White, Timothy J., Lalgudi V. Natarajan, Vincent P. Tondiglia, Pamela F. Lloyd, Timothy J. Bunning and C. Allan Guymon. "Holographic Polymer Dispersed Liquid Crystals (Hpdlds) Containing Triallyl Isocyanurate Monomer." *Polymer* 48, no. 20 (2007): 5979-5987.
- White, Timothy J., Lalgudi V. Natarajan, Vincent P. Tondiglia, Pamela F. Lloyd, Timothy J. Bunning and C. Allan Guymon. "Monomer Functionality Effects in the Formation of Thiol-Ene Holographic Polymer Dispersed Liquid Crystals." *Macromolecules* 40, no. 4 (2007): 1121-1127.
- Witkowski, Andrzej. "Infrared Spectra of the Hydrogen-Bonded Carboxylic Acids." *The Journal of Chemical Physics* 47, no. 9 (1967): 3645-3648.
- Yu, Y. K., X. Y. Wang and P. L. Taylor. "Theory of Domain Boundary Effects in a Phase-Separated Mixture of Polymer and Liquid Crystal." *Journal of Chemical Physics* 104, no. 7 (1996): 2725-2731.
- Yu, Yanlei, Manoto Nakano and Tomiki Ikeda. "Photomechanics: Directed Bending of a Polymer Film by Light." *Nature* 425, (2003): 145.
- Zhang, Jian and Michael B. Sponsler. "Switchable Liquid Crystalline Photopolymer Media for Holography." *Journal of the American Chemical Society* 114, no. 4 (1992): 1506-1507.
- Zhang, Wei, Paul K. Chu, Junhui Ji, Yihe Zhang, Xuanyong Liu, Ricky K. Y. Fu, Peter C. T. Ha and Qi Yan. "Plasma Surface Modification of Poly Vinyl Chloride for Improvement of Antibacterial Properties." *Biomaterials* 27, no. 1 (2006): 44-51.
- Zhu, Jianwu, Jianping Deng, Shoumei Cheng and Wantai Yang. "A Facile Method for Grafting Polymerisation of Acrylonitrile onto Ldpe Film with High Grafting Efficiency." *Macromolecular Chemistry and Physics* 207, no. 1 (2006): 75-80.
- Zou, Yuan, Steven R. Armstrong and Julie L. P. Jessop. "Apparent Conversion of Adhesive Resin in the Hybrid Layer, Part 1: Identification of an Internal Reference for Raman Spectroscopy and the Effects of Water Storage." *Journal of Biomedical Materials Research Part A* 86A, no. 4 (2008): 883-891.
- Zou, Yuan, Steven R. Armstrong and Julie L. P. Jessop. "Quantitative Analysis of Adhesive Resin in the Hybrid Layer Using Raman Spectroscopy." *Journal of Biomedical Materials Research Part A* 94A, no. 1 (2010): 288-297.